UNIVERSITÀ DEGLI STUDI DI TRIESTE

XXX CICLO DEL DOTTORATO DI RICERCA IN AMBIENTE E VITA

Istituto Nazionale di Oceanografia e di Geofisica Sperimentale - OGS

CARBON CYCLE IN MARINE SYSTEMS UNDER DIFFERENT ANTHROPOGENIC PRESSURE

Settore scientifico-disciplinare: **BIO/07**

DOTTORANDA
DOTT.SSA FEDERICA RELITTI

COORDINATORE
PROF. GIORGIO ALBERTI

SUPERVISORE DI TESI
DOTT.SSA PAOLA DEL NEGRO

CO-SUPERVISORE DI TESI
DOTT.SSA CINZIA DE VITTOR

ANNO ACCADEMICO 2016/2017

Contents

ABSTRACT

During the past two centuries, human activities have greatly modified the exchange of carbon and nutrients between land, atmosphere, freshwater bodies, coastal zones and open ocean. This PhD thesis focuses on different aspects of carbon cycle, considering three case study for the evaluation of the effects of anthropogenic pressure and of the natural evolution of carbon cycle.

The first case study focuses on anthropogenic impacts on contaminated coastal areas. These environments connect terrestrial and oceanic systems, and are highly subjected to anthropogenic pressure. An example of a contaminated coastal area is the Mar Piccolo of Taranto (Ionian Sea) and the results of two published papers are reported. The evaluation of nutrients and carbon fluxes at sediment-water interface showed that the multi-contamination of both inorganic and organic pollutants in the sediments is potentially transferable to the water column and to the aquatic trophic chain. On the other hand, the analysis of a long time series of chemical-physical characteristics of the water column has highlighted that the implementation of sewage treatment plants has positively affected the trophic status of the Mar Piccolo from being relatively eutrophic to moderately oligotrophic.

The increase of atmospheric CO_2 concentration has been recognised as one of the main causes of climate change, and carbon capture and storage technology (CCS) is expected to play a key role among mitigation strategies by reducing CO_2 emissions into atmosphere from fossil fuel combustion. Although leakages from storage sites are not expected, the environmental impacts related to potential CO_2 seepages are a major issue for the acceptance of this approach. The second case study here presented aims to the evaluation of phytoplankton stable carbon isotopes as a tool for effective early warning of CO_2 leakage from CCS, since different carbon sources have specific $\delta^{13}C$ values. Two culture experiments were conducted under controlled conditions for monitoring $\delta^{13}C$ changes in the diatom *Thalassiosira rotula*. The isotopic composition of microalgae grown in natural seawater (NAT) was compared to that of diatoms grown in an artificial seawater (ASW) characterised by strongly ^{13}C-depleted dissolved inorganic carbon values. The uptake of inorganic carbon in ASW resulted in a rapid and significant change in microalgae $\delta^{13}C$ values, whereas in NAT phytoplankton $\delta^{13}C$ did not show important deviations from the starting value, confirming the effectiveness of phytoplankton $\delta^{13}C$ as a tool for detecting different CO_2 sources.

The third case study aims at a better understanding of carbon cycle, as the rate of changes not only depends on human activities, but also on natural biogeochemical processes. Marine dissolved organic matter plays a crucial role in oceanic carbon storage, and the extent of its contribution on carbon sequestration depends on its bioavailability. In this study, a plug-flow bioreactor approach has been tested in order to evaluate dissolved organic carbon (DOC), nitrogen (DON) and phosphorus (DOP) availability for microbial community in the Gulf of Trieste (Northern Adriatic Sea) and the parallel nutrient uptake. The bioreactor approach confirmed to be useful for bioavailable DOC assessment, but further research is needed for confirming its effectiveness for defining DON and DOP bioavailability and nutrients utilisation.

RIASSUNTO

A partire dalla rivoluzione industriale, le attività umane hanno profondamente alterato i naturali scambi di carbonio e nutrienti tra i comparti ambientali. I tre casi studio riportati in questa tesi di dottorato hanno come obiettivo l'approfondimento di diversi aspetti del ciclo del carbonio, al fine di valutarne la naturale evoluzione e gli effetti dell'impatto antropico.
Il primo caso studio è inerente alla valutazione degli impatti antropici in aree costiere. Tali aree costituiscono zone di transizione tra ambiente terrestre e marino, e sono soggette a una forte pressione antropica. Si riportano i risultati pubblicati in due articoli di ricerca relativi a indagini svolte nell'area costiera contaminata del Mar Piccolo di Taranto (Mar Ionio). L'analisi dei flussi di carbonio e nutrienti all'interfaccia acqua-sedimento ha evidenziato che la contaminazione dei sedimenti da parte di composti sia organici che inorganici è potenzialmente trasferibile alla colonna d'acqua e alla catena trofica. Tuttavia, l'analisi della serie storica dei parametri chimico-fisici della colonna d'acqua ha evidenziato l'efficacia dei trattamenti di purificazione delle acque reflue. Lo stato trofico del Mar Piccolo è infatti passato da una condizione relativamente eutrofica a una moderatamente oligotrofica.
L'aumento della concentrazione di CO_2 in atmosfera è stato riconosciuto come una delle principali cause del cambiamento climatico, e le tecniche di confinamento geologico di CO_2 (CCS) rientrano tra le più promettenti strategie per ridurne le emissioni in atmosfera. Tuttavia, sebbene un'adeguata progettazione di tali siti di stoccaggio non preveda rilascio di CO_2, eventuali fuoriuscite potrebbero avere importanti ripercussioni ambientali. Dal momento che diverse fonti di CO_2 hanno una differente composizione isotopica, il secondo caso studio si propone di valutare se il $\delta^{13}C$ del fitoplancton possa costituire uno strumento utile all'identificazione precoce di fuoriuscite di CO_2 da CCS. La composizione isotopica della diatomea *Thalassiosira rotula* è stata determinata in due diversi mezzi di coltura tramite due esperimenti in condizioni controllate. I valori di $\delta^{13}C$ delle microalghe cresciute in acqua naturale (NAT) sono stati confrontati con quelli delle diatomee cresciute in acqua artificiale (ASW), caratterizzata da valori di carbonio inorganico disciolto fortemente impoveriti in ^{13}C. L'utilizzo del carbonio inorganico in ASW è risultato in un rapido e significativo cambiamento dei valori di $\delta^{13}C$, confermando l'efficacia dell'analisi della composizione isotopica del fitoplancton come strumento utile a identificare diverse fonti di CO_2.
Obiettivo del terzo caso studio è l'approfondimento delle conoscenze del ciclo del carbonio, in quanto le variazioni a cui questo è soggetto non dipendono solo dall'impatto antropico ma anche dai naturali processi biogeochimici. La sostanza organica disciolta (DOM) ricopre un ruolo chiave nel sequestro oceanico del carbonio. L'efficacia del sequestro all'interno del pool di DOM è funzione della biodisponibilità della sostanza organica. Nello studio presentato, la biodisponibilità di DOM per la comunità microbica nel Golfo di Trieste (Nord Adriatico) è stata analizzata tramite un bioreattore a flusso controllato, valutando la degradazione di carbonio (DOC), azoto (DON) e fosforo (DOP) organici disciolti e l'utilizzo di nutrienti. Il bioreattore è risultato idoneo per la valutazione della biodisponibilità del DOC. Tuttavia, sono necessari ulteriori approfondimenti per stabilirne l'efficacia anche nella stima della biodisponibilità di DON e DOP e dell'utilizzo di nutrienti.

CHAPTER 1

1. Introduction

During the past two centuries, human activities have greatly modified the exchange of carbon and nutrients between land, atmosphere, freshwater bodies, coastal zones and open ocean (Regnier et al. 2013). Industrialisation, energy production, land use change, population growth, pollution and production of new materials have resulted in strong and often irreversible alterations of natural element cycling. The rapid and widespread changes due to human perturbations will persist and intensify in the future, and have already been sufficient to produce a stratigraphic signature in sediments and ice, distinct from that of the Holocene epoch, that has suggested the definition of a new epoch, the Anthropocene (Waters et al. 2016).

Human activities have considerably altered the global carbon cycle, especially by significantly increasing carbon dioxide concentration (CO_2) in atmosphere (Sarmiento & Gruber 2002). Oceans play a key role in the global carbon budget in the regulation of atmospheric CO_2 concentration, but the responses to human perturbations in a long-time scale are not already fully understood (Libes 2009). Given the present trends, atmospheric CO_2 concentration seems destined to increase throughout the next century (Falkowski et al. 2000). The understanding of the consequences of human pressure in the alteration of carbon cycle is critical for establishing effective policies for the prevention of ecosystem damages and for the establishment of recovery actions. Changes in carbon cycle are not only completely depending on anthropogenic pressure, but also on natural biogeochemical processes (Falkowski et al. 2000). It is however difficult to differentiate between natural and anthropogenic drivers, especially in coastal environments. Thus, major uncertainties still remain in our understanding of natural and undisturbed carbon cycle (Bauer et al. 2013), hence the need of more research effort in this field for predicting, and hopefully mitigating, future impacts of anthropogenic pressure (Sarmiento & Gruber 2002).

1.1. Anthropogenic impacts in marine coastal areas

Despite occupying only 7-10% of global ocean area, coastal regions are one of the most biogeochemically active environments in the biosphere and represent a crucial link between land, open ocean, and atmosphere (Bauer et al. 2013; Gattuso et al. 1998; Borges et al. 2005; Liu et al. 2010). Coastal zones offer a wide variety of valuable habitats and ecosystem services that have always

attracted humans and human activities. Today, approximately half of the human population lives within 200 km from a coastline, and this trend is likely to double by 2025 (Creel 2003). The intensive concentration of population and excessive exploitation of natural resources determine massive pressure on coastal ecosystems, leading to biodiversity loss, habitat destruction, pollution, eutrophication and alteration of natural cycles. One recent estimate found that at least 40% of the global oceans are heavily affected by human activities (IOC/UNESCO et al. 2011). These changes are threatening marine ecosystems resilience, and thus its capacity to provide ecosystem services. Carbon fluxes within and between coastal systems and their alteration by climate and anthropogenic changes are substantial. It is therefore of primary importance to safeguard coastal ecosystem diversity and complexity and, on the other hand, there is a urgent need to understand their natural functioning in order to allow better interpretation of changes and to establish mitigation and preventing strategies for their protection (Bauer et al. 2013; Falkowski et al. 2000).

One of the worldwide largest issues caused by the increase of anthropogenic inputs is eutrophication, especially in areas with limited water exchange, as estuaries, salt marshes and lagoons (Kralj et al. 2016 and references therein). Indeed, increased terrestrial export of nutrients and carbon by rivers due to agricultural activities and land-use change has led to excess primary production and organic carbon accumulation in estuarine and shelf waters and sediments. The enhanced microbial degradation activity can lead to a change in sediment status by lowering oxygen levels in bottom waters, and eventually resulting in anoxic conditions (De Vittor et al. 2012). Many other biogeochemical cycles are controlled by oxygen, and the change of redox status could enhance release of contaminants eventually accumulated in sediments because of human activities (e.g., mercury, iron, sulfur) (Santos-Escheandia et al. 2009; Covelli et al. 2011; Emili et al. 2011; De Vittor et al. 2012). Ecosystem status is hence a balance between respiration of riverine organic matter and in situ autotrophic production stimulated by nutrient inputs. Anthropogenic nutrient supply could therefore alter the CO_2 sink–source balance of coastal systems (Jiang et al. 2008; Reigner et al. 2013; Gruber 2015) by the shift from net autotrophic to net heterotrophic conditions, with still poorly understood implication in the global carbon budget (Bauer et al. 2013).

1.2. Global anthropogenic impact on carbon cycle

A valuable indicator of global carbon cycle is represented by atmospheric CO_2 concentration, as this relatively small reservoir acts as a conveyor for the exchange of carbon between terrestrial and marine ecosystems. Because atmospheric CO_2 exchanges rapidly with oceans and terrestrial systems, it is expected to react sensitively to changes in the global carbon cycle (Sarmiento & Gruber 2006).

Biogeochemical analysis of ice cores has allowed the reconstruction of past atmospheric CO_2 concentration, revealing oscillations between 180 ppmv and 280 ppmv during the 100,000-year cycles of glacial-interglacial transitions (Falkowski et al. 2000). Atmospheric CO_2 concentration has increased over 40% since the beginning of industrial revolution, and now exceeds 400 ppmv (407.27 ppmv on 23rd December 2017; see the Keeling Curve at http://keelingcurve.ucsd.edu/). The alteration of CO_2 concentration by human activities has been 10 and possibly 100 times faster than any other time (Falkowski et al. 2000; Doney & Schimel, 2007), and it is superimposing over natural variations, resulting in climate changes by enhanced greenhouse effect (IPCC, 2007, 2013; Libes 2009; Sarmiento & Gruber 2002; Sarmiento & Gruber 2006). Oceans play a key role in regulating atmospheric CO_2 concentrations and currently take up about 25% of annual anthropogenic carbon emissions to the atmosphere (Heinze et al. 2015, Le Quéré et al. 2014; Le Quéré et al. 2009, 2010; McKinley et al. 2011). Since the beginning of the 19th century, the oceans are estimated to have taken up about 50% of fossil fuel emissions and about 30% of anthropogenic emissions, thus significantly reducing the accumulation of atmospheric CO_2 (Jiao et al. 2015). This effect mitigates human-driven climate change but, on the other hand, oceans are experiencing significant variations. The increase in atmospheric temperature has increased heat transfer towards oceans, leading to stronger thermal stratification, and contributing to the global sea level rise because of ice melting (IPCC, 2013). Moreover, higher sea temperatures have the potential to produce more intense storms and to increase evaporation that could even lead to alteration in the global water circulation (Libes 2009). Increasing concentrations of atmospheric CO_2 have also influenced the chemistry of ocean waters, leading to a growing inventory of inorganic carbon. Indeed, when CO_2 dissolves in seawater it reacts forming carbonic acid (H_2CO_3), a weak acid that then partially dissociates lowering ocean pH and altering carbonate chemistry balance. From a mean global pH of about 8.2 at the pre-industrial time, pH has decreased by about 0.1 (Royal Society, 2005) and with continuing combustion of fossil fuels may fall another 0.25 units by the end of the century (Orr et al. 2005). Acidification has been recognised as one of the main problems related to the increase of atmospheric CO_2 because of the consequences on marine organisms. Of particular concern is the impact of acidification on biocalcification and burial rates of sedimentary carbon (Libes 2009). By now, there is good evidence that corals, gastropods, and calcifying microalgae will suffer from ocean acidification (Kroeker et al. 2010) because of inhibition of shell formation. Moreover, lower pH could favour dissolution and desorption of metals that once mobilized can accumulate in marine organisms inhibiting growth or even causing death. Planktonic and benthic communities could be altered in composition and metabolic activity (Lichtschlag et al. 2015 and references therein; Noble et al. 2012; Jones et al. 2015), and photosynthetic activity might be altered by lower pH levels as well (Jones et al. 2015; Tait et al. 2015 and references therein).

Although we do not fully understand the global carbon cycle and how it is modified by human pressure, there is common agreement on the need of limiting CO_2 emissions and of establishing mitigation actions. The only method that can guarantee to mitigate the expected increase in CO_2 concentration is the reduction of fossil fuel combustion. Several different methods have been studied in order to reduce CO_2 levels in atmosphere, and, among these, carbon capture and storage technology (CCS) is one of the most promising mitigation strategies studied so far (De Coninck & Benson 2014; IPCC 2005) by trapping and storing carbon dioxide either on-shore or off-shore. However, research is still needed in order to gain deeper insights on the long-term effects of these approaches, especially because CO_2 leakages from storage sites would severely affect the surrounding environment (Blackford et al. 2015; Jones et al. 2015; Noble et al. 2012).

1.3. Ocean carbon sequestration and relevance of organic matter

Investigation of natural variability might offer new insights into how marine carbon cycle responds to changes in the Earth climate. Oceans represent the single largest biologically active reservoir in the global carbon cycle. Total dissolved carbon in oceans is 50 times that of the atmosphere and therefore it exerts a controlling influence on the other reservoirs (Falkwoski et al. 2000; Libes 2009). The key role of oceans in global carbon cycle is driven by two independent processes, the solubility pump and the biological carbon pump. The solubility pump depends on physical processes associated with gas solubility and water circulation. As all atmospheric gases, CO_2 dissolves in water, and solubility increases with decreasing seawater temperature. It follows that the cold waters sinking to depths during deep water formation at high latitudes are CO_2-rich relative to average oceanic surface water. The efficiency of this pump is therefore controlled by oceanic water circulation, the effect of temperature on solubility and the chemical reactions that CO_2 undergoes in seawater. Once CO_2 dissolves in water, it forms a weak acid that reacts with carbonate and water to form bicarbonate, the most abundant species among dissolved inorganic carbon (DIC). Ocean buffer capacity therefore depends on the presence of cations, which in turn is related to the relatively slow weathering of rocks. The rate of anthropogenic CO_2 emissions is significantly greater than the supply of mineral cations, thus the ability of oceans to absorb CO_2 will decrease as CO_2 atmospheric concentration increases (Falkowski et al. 2000) and will be also negatively influenced by water circulation modification due to global warming. About one-third of the surface-to-depth gradient of dissolved carbon is generated by solubility pump, and the other two-thirds are related to the biological carbon pump (Passow & Carlson 2012; Turner 2015). The biological pump is the set of processes by which photosynthetically produced organic matter in the ocean sinks to depth, and includes the carbonate pump and the soft-

tissue pump (Passow & Carlson 2012; Turner 2015). The carbonate pump is associated with the precipitation of $CaCO_3$ by calcifying plankton (mainly coccolithophores and foraminifera) in surface water, and the following settling of carbonate particles across the water column, and their burial in sediments (Volk and Hoffert, 1985). The soft-tissue pump is driven by photosynthetic fixation of CO_2 into organic matter, which is exported to deep regions by gravitational sinking of particulate organic matter (POM) and by mixing and advection of dissolved organic matter (DOM) and zooplankton migration. During vertical migration, much of POM is remineralized, and the re-solubilised carbon is removed from interactions with atmosphere until it is trapped below the termocline (i.e. for less than a thousand of years). Some particles can be buried in sediments and therefore effectively be removed from atmosphere interactions over much longer time scales. IPCC (2007) stipulated that long-term sequestration of carbon requires the removal from atmosphere for over 100 years, and this criterion is generally met after carbon is transported below 1000 m (Primeau 2005). The biological pump is relatively inefficient as only about 5-25% of primary production is exported from the euphotic zone (De La Rocha & Passow 2007 and references therein) for a long-term storage. The majority of primary production is consumed or respired in water column, with approximately 15% being processed by bacteria and the rest by micro- (30-70%) and meso- (20-35%) zooplankton (Turner 2015 and references therein). The relevance of microbial processes in the biological pump has recently prompted the definition of another carbon ocean pump: the microbial carbon pump (Legendre et al. 2015). Heterotrophic bacteria are the main responsible of degradation of dissolved organic matter (DOM). Despite dissolved organic carbon (DOC) accounts for about 2% of total oceanic carbon, it is one of the major active reservoirs of the global carbon cycle as it represents the largest pool of reduced carbon in ocean (Hansell et al. 2009). Approximately 95% of DOM is not available as food for many marine organisms, constituting the refractory fraction of DOM (RDOM), with a turnover time of centuries to millennia (Hansell & Carlson 2015, and references therein). Spatial and temporal variations in DOM production and removal affect the long-term carbon storage (Santinelli et al. 2010; Hansell 2013; Hansell & Carlson 2015), RDOM then plays a critical role in carbon sequestration and changes in its lability could influence the global carbon cycle (Hansell & Carlson 2015) and the whole marine ecosystem (Santinelli et al. 2013). The origin of RDOM in the ocean and the processes and mechanisms of its production, utilisation and degradation are still largely unknown (Legendre et al. 2015), and it is therefore hard to foresee how it would be affected by CO_2 increase and related climate change. Biological responses to increasing temperature, ocean stratification, nutrient availability and ocean acidification are frequently taxa-and ecosystem-specific, thus the results of synergistic effects are challenging to predict (Passow & Carlson 2012; Turner 2015;

Legendre et al. 2015). A better understanding of the efficiency and dynamics of the present biological pump is therefore critical for predicting future effects of global warming on the ocean.

2. Objectives and dissertation structure

Carbon cycle is driven by complex and dynamic processes involving the whole Earth system. Despite carbon cycle has been studies for long, still knowledge gaps exist, both on the natural evolution and in the response to anthropogenic pressure.
This PhD thesis focuses on different aspects of carbon cycle, considering three case study presented in four research papers:

- The first case study aims to define anthropogenic pressure on a contaminated coastal system, the Mar Piccolo of Taranto (Ionian Sea). The effects of anthropogenic activities in this area have been investigated in two research papers published in the journal Environmental Science and Pollution Research.
  - Carbon and nutrient fluxes at the sediment water interface were evaluated, as these processes are strongly related to contaminant cycling. **Chapter 2** – De Vittor C, Relitti F, Kralj M, Covelli S, Emili A. Oxygen, carbon, and nutrient exchanges at the sediment–water interface in the Mar Piccolo of Taranto (Ionian Sea, southern Italy), doi: 10.1007/s11356-015-4999-0.
  - The effectiveness of treatment plants and of the relocation of the sewage discharges was evaluated in order to identify improvement of water quality, as the Mar Piccolo of Taranto has experienced severe eutrophication events. **Chapter 3** – Kralj M, De Vittor C, Comici C, Relitti F, Auriemma R, Alabiso G, Del Negro P. Recent evolution of the physical-chemical characteristics of a Site of National Interest – the Mar Piccolo of Taranto (Ionian Sea) – and changes over the last 20 years, doi: 10.1007/s11356-015-5198-8.

- The second case study purpose is the identification of a useful tool for the evaluation of CO_2 leakages from carbon storage sites (CCS). In **Chapter 4** the results of two diatom culture experiments are reported with the aim of evaluating changes in phytoplankton isotopic composition in relation to the uptake of different CO_2 source (natural and anthropogenic). The study has been submitted for publication to Environmental Science and Pollution Research, and it is still under review. Relitti F, Ogrinc N, Giani M, Cerino F, De Vittor C, Urbini L, Krajnc B, Del Negro P. Stable carbon isotopes in phytoplankton as a tool to monitor CO_2 leakages at Carbon Capture and Storage sites.

- The third case study aims to evaluate dissolved organic matter bioavailability in seawater, as this information would give important insights on long-term carbon storage. **Chapter 5** reports the results of different experiments for defining the effectiveness of plug-flow bioreactors for the assessment of bioavailable dissolved organic carbon, and to verify its functionality for the evaluation of dissolved organic nitrogen and phosphorus degradation and inorganic nutrient uptake. A paper describing these results is in preparation for submission. Relitti F, De Vittor C, Del Negro P. Assessment of biodegradable dissolved organic matter (BDOM) and nutrients utilization in coastal seawater using a plug-flow bioreactor.

References

Bauer JE, Cai WJ, Raymond PA, Bianchi TS, Hopkinson CS, Reigner PAG (2013) The changing carbon cycle of the coastal ocean. Nature 504:61–70. doi:10.1038/nature12857.

Blackford J, Bull JM, Cevatoglu M, Connelly D, Hauton C, James RH, Lichtschlag A, Stahl H, Widdicombe S, Wright IC (2015) Marine baseline and monitoring strategies for carbon dioxide capture and storage (CCS). Int J Greenh Gas Control 38:221–229. doi:10.1016/j.ijggc.2014.10.004.

Borges AV, Delille B, Frankignoulle M (2005) Budgeting sinks and sources of CO_2 in the coastal ocean: diversity of ecosystems counts. Geophys Res Lett 32:L14601.

Covelli S, Emili A, Acquavita A, Koron N, Faganeli J (2011) Benthic biogeochemical cycling of mercury in two contaminated northern Adriatic coastal lagoons. Cont Shelf Res 31:1777–1789.

Creel, L (2003) Ripple effects: population and coastal regions (pp. 1-7). Washington, DC: Population Reference Bureau.

De Coninck H, Benson SM (2014) Carbon dioxide capture and storage: issues and prospects. Annu Rev Environ Resour 39:243–270. doi:10.1146/annurev-environ-032112-095222.

De La Rocha C, Passow U (2007) Factors influencing the sinking of POM and the efficiency of the global carbon pump. Deep Sea Res II 54:639–658.

De Vittor C, Faganeli J, Emili A, Covelli S, Predonzani S, Acquavita A (2012) Benthic fluxes of oxygen, carbon and nutrients in the Marano and Grado lagoon (Northern Adriatic sea, Italy). Estuar Coast Shelf Sci 113:57–70.

Doney SC, Schimel DS (2007) Carbon and climate system coupling on timescales from the Precambrian to the Anthropocene, Annu Rev Environ Resour 32:31–66.

Emili A, Koron N, Covelli S, Faganeli J, Acquavita A, Predonzani S, De Vittor C (2011) Does anoxia affect mercury cycling at the sediment–water interface in the Gulf of Trieste (northern Adriatic Sea)? Incubation experiments using benthic flux chambers. Appl Geochem 26:194–204.

Falkowski P, Scholes RJ, Boyle E, Canadell J, Canfield D, Elser J, Gruber N, Hibbard K, Högberg P, Linder S, Mackenzie FT, Moore III B, Pedersen T, Rosenthal Y, Seitzinger S, Smetacek V, Steffen W (2000) The global carbon cycle: a test of our knowledge of earth as a system. Science 290:291–296. doi:10.1126/science.290.5490.291.

Gattuso JP, Frankignoulle M, Wollast R (1998) Carbon and carbonate metabolism in coastal aquatic ecosystems. Annu Rev Ecol Syst 29:405-434.

Gruber N (2015) Carbon at the coastal interface. Nature 517:148–149.

Hansell DA, Carlson CA, Repeta DJ, Schlitzer R (2009) Dissolved organic matter in the ocean: a controversy stimulates new insights. Oceanography 22:202–211.

Hansell DA (2013) Recalcitrant Dissolved Organic Carbon Fractions. Annu Rev Mar Sci 5:421–45. doi:10.1146/annurev-marine-120710-100757.

Hansell DA, Carlson CA (2015) Biogeochemistry of marine dissolved organic matter. 2nd Ed. Elsevier Science, USA.

Heinze C, Meyer S, Goris N, Anderson L, Steinfeldt R, Chang N, Le Quéré C, Bakker DCE (2015) The ocean carbon sink – impacts, vulnerabilities and challenges. Earth Syst Dynam 6:327–358. doi:10.5194/esd-6-327-2015.

IOC/UNESCO, FAO, UNDP (2011) A Blueprint for Ocean and Coastal Sustainability.

IPCC (2005) IPCC special report on carbon dioxide capture and storage. Prepared by Working Group III of the Intergovernmental Panel on Climate Change [Metz B, Davidson O, de Coninck HC, Loos M, Meyer LA (eds.)]. Cambridge University Press, Cambridge, United Kingdom and New York, NY, USA.

IPCC (2007) Climate change 2007: the physical science basis. In: Solomon, S., Qin, D., Manning, M., Chen, Z., Marquis, M., Avery, K.B., Tignor, M., Miller, H.L. (Eds.), Contribution of Working Group I to the Fourth Assessment Report of the Intergovernmental Panel on Climate Change. Cambridge University Press, New York, 996 pp.

IPCC (2013) Climate change 2013: the physical science basis. In: Solomon, S., Quin, D., Manning, M., Chen, Z., Marquis, M., Averyt, K.B., Tignor, M., Miller, H.L. (Eds.), Contribution of Working Group I to the Fifth Assessment Report of the Intergovernmental Panel on Climate Change. Cambridge University Press, New York, 1535 pp.

Jiang LQ, Cai WJ, Wanninkhof R, Wang Y, Lüger H (2008) Air–sea CO_2 fluxes on the U.S. South Atlantic Bight: spatial and seasonal variability. J Geophys Res 13:C07019.

Jiao N-Z, Chen D-K, Luo Y-M, Huang X-P, Zhang R, Zhang H-B, Jiang Z-J, Zhang F (2015) Climate change and anthropogenic impacts on marine ecosystems and countermeasures in China. Advances in Climate Change Research 6:118–125.

Jones DG, Beaubien SE, Blackford JC, Foekema EM, Lions J, De Vittor C, West JM, Widdicombe S, Hauton C, Queirós AM (2015) Developments since 2005 in understanding potential environmental impacts of CO2 leakage from geological storage. Int J Greenh Gas Control 40:350–377. doi:10.1016/j.ijggc.2015.05.032.

Kralj M, De Vittor C, Comici C, Relitti F, Auriemma R, Alabiso G, Del Negro P (2016) Recent evolution of the physical–chemical characteristics of a Site of National Interest –the Mar Piccolo of Taranto (Ionian Sea) – and changes over the last 20 years. Environ Sci Pollut Res Int 23:12675–12690. doi:10.1007/s11356-015-5198-8.

Kroeker KJ, Kordas RL, Crim RN, Singh GG (2010) Meta-analysis reveals negative yet variable effects of ocean acidification on marine organisms. Ecol Lett 13:1419–1434.

Le Quéré C, Raupach MR, Canadell JG, Marland G, Bopp L, Ciais P, Conway TJ, Doney SC, Feely RA, Foster P, Friedlingstein P, Gurney K, Houghton RA, House JI, Huntingford C, Levy PE, Lomas MR, Majkut J, Metzl N, Ometto JP, Peters GP, Prentice IC, Randerson JT, Running SW, Sarmiento JL, Schuster U, Sitch S, Takahashi T, Viovy N, van der Werf GR, Woodward FI (2009) Trends in the sources and sinks of carbon dioxide. Nat Geosci 2:831–836. doi:10.1038/ngeo689.

Le Quéré C, Takahashi T, Buitenhuis ET, Rödenbeck C, Sutherland SC (2010) Impact of climate change and variability on the global oceanic sink of CO_2. Global Biogeochem Cycles 24:GB4007.

Le Quéré C, Moriarty R, Andrew RM, Peters GP, Ciais P, Friedlingstein P, Jones SD, Sitch S, Tans P, Arneth A, Boden TA, Bopp L, Bozec Y, Canadell JG, Chevallier F, Cosca CE, Harris I, Hoppema M, Houghton RA, House JI, Jain A, Johannessen T, Kato E, Keeling RF, Kitidis V, Goldewijk KK, Koven C, Landa CS, Landschützer P, Lenton A, Lima ID, Marland G, Mathis T, Metzl N, Nojiri Y, Olsen A, Ono T, Peters W, Pfeil B, Poulter B, Raupach MR, Regnier P, Rödenbeck C, Saito S, Salisbury JE, Schuster U, Schwinger J, Séférian R, Segschneider J, Steinho T, Stocker BD, Sutton AJ, Takahashi T, Tilbrook B, van der Werf GR, Viovy N, Wang YP, Wanninkhof R, Wiltshire A, Zeng N (2014) Global carbon budget 2014. Earth Syst

Sci Data Discuss 7:521–610. doi: 10.5194/essdd-7-521-2014.

Legendre L, Rivkin RB, Weinbauer MG, Guidi L, Uitz J (2015) The microbial carbon pump concept: potential biogeochemical significance in the globally changing ocean. Prog Oceanogr 134:432–450. doi:10.1016/j.pocean.2015.01.008.

Libes SM (2009) Introduction to marine biogeochemistry. Academic press, 2nd Ed., 928pp.

Lichtschlag A, James RH, Stahl H, Connelly D (2015) Effect of a controlled sub-seabed release of CO_2 on the biogeochemistry of shallow marine sediments, their pore waters, and the overlying water column. Int J Greenh Gas Control 38:80–92. doi: 10.1016/j.ijggc.2014.10.008.

Liu K-K, Atkinson L, Quiñones R, Talaue-McManus L (2010) Biogeochemistry of continental margins in a global context, in: Liu K-K, Atkinson L, Quiñones R, Talaue- McManus L (Eds.), Carbon and Nutrient Fluxes in Continental Margins: A Global Synthesis IGBP Book Series, Berlin, Springer, pp. 3–24.

McKinley GA, Fay AR, Takahashi T, Metzl N (2011) Convergence of atmospheric and North Atlantic carbon dioxide trends on multidecadal timescales, Nat Geosci 4:606–610. doi:10.1038/Ngeo1193.

Noble RRP, Stalker L, Wakelin SA, Pejcic B, Leybourne MI, Hortle AL, Michael K (2012) Biological monitoring for carbon capture and storage – A review and potential future developments. Int J Greenh Gas Control 10:520–535. doi:10.1016/j.ijggc.2012.07.022.

Orr JC, Fabry VJ, Aumont O, Bopp L, Doney SC, Feely RA, Gnanadesikan A, Gruber N, Ishida A, Joos F, Key RM, Lindsay K, Maier-Reimer E, Matear R, Monfray P, Mouchet A, Najjar RG, Plattner G-K, Rodgers KB, Sabine CL, Sarmiento JL, Schlitzer R, Slater RD, Totterdell IJ, Weirig M-F, Yamanaka Y, Yool A (2005) Anthropogenic ocean acidification over the twenty-first century and its impact on calcifying organisms. Nature 437:681–686.

Passow U, Carlson CA (2012) The biological pump in a high CO_2 world. Mar Ecol Prog Ser 470:249–271. doi:10.3354/meps09985.

Primeau F (2005) Characterizing transport between the surface mixed-layer and the ocean interior with a forward and adjoint global ocean transport model. J Phys Oceanogr 35:545–564.

Regnier P, Friedlingstein P, Ciais P, Mackenzie FT, Gruber N, Janssens IA, Laruelle GG, Lauerwald R, Luyssaert S, Andersson AJ, Arndt S, Arnosti C, Borges AV, Dale AW, Gallego-Sala A, Goddéris Y, Goossens N, Hartmann J, Heinze C, Ilyina T, Joos F, LaRowe DE, Leifeld J, Meysman FJR, Munhoven G, Raymond PA, Spahni R, Suntharalingam P, Thullner M (2013) Anthropogenic perturbation of the carbon fluxes from land to ocean. Nat Geosci 6:597–607. doi:10.1038/NGEO1830.

Royal Society (2005) Ocean acidification due to increasing carbon dioxide. Clyvedon Press, Cardiff, UK, Policy Document 12/05, 68 pp.

Santinelli C, Nannicini L, Seritti A (2010) DOC dynamics in the meso and bathy pelagic layers of the Mediterranean Sea. Deep Sea Res II 57: 1446–1459. doi:10.1016/j.dsr2.2010.02.014

Santinelli C, Hansell DA, d'Alcalà MR (2013) Influence of stratification on marine dissolved organic carbon (DOC) dynamics: The Mediterranean Sea case. Prog Oceanogr 119:68–77. doi:10.1016/j.pocean.2013.06.001

Santos-Escheandia J, Prego R, Cobelo-García A, Millward GE (2009) Porewater geochemistry in a Galician Ria (NW Iberian Peninsula): implications for benthic fluxes of dissolved trace elements (Co, Cu, Ni, Pb, V, Zn). Mar Chem 117:77–87

Sarmiento JL, Gruber N (2002) Sinks for anthropogenic carbon. Phys today 55:30–36.

Sarmiento JL, Gruber N (2006) Ocean biogeochemical dynamics. Princeton University Press, 528pp.

Tait K, Stahl H, Taylor P,Widdicombe S (2015) Rapid response of the active microbial community to CO_2 exposure from a controlled sub-seabed CO_2 leak in Ardmucknish Bay (Oban, Scotland). Int J Greenh Gas Control 38:171–181. doi:10.1016/j.ijggc.2014.11.021

Turner JT (2015) Zooplankton fecal pellets, marine snow, phytodetritus and the ocean's biological pump. Prog Oceanogr 130:205–248. doi:10.1016/j.pocean.2014.08.005

Volk T, Hoffert MI (1985) Ocean carbon pumps: Analysis of relative strengths and efficiencies in ocean-driven atmospheric CO_2 changes. Geophysical Monograph Series 32:99–110.

Waters CN, Zalasiewicz J, Summerhayes C, Barnosky AD, Poirier C, Gałuszka A, Cearreta A, Edgeworth M, Ellis EC, Ellis M, Jeandel C, Leinfelder R, McNeill JR, Richter D deB, Steffen W, Syvitski J, Vidas D, Wagreich M, Williams M, Zhisheng A, Grinevald J, Odada E, Oreskes N, Wolfe AP (2016) The anthropocene is functionally and stratigraphically distinct from the Holocene. Science 351:aad2622. doi:10.1126/science.aad2622.

CHAPTER 2

Oxygen, carbon, and nutrient exchanges at the sediment–water interface in the Mar Piccolo of Taranto (Ionian Sea, southern Italy)

Cinzia De Vittor[1*], Federica Relitti[1,3], Martina Kralj[1], Stefano Covelli[2,4], Andrea Emili[2]

[1] Oceanography Division, OGS (Istituto Nazionale di Oceanografia e di Geofisica Sperimentale), Trieste, Italy

[2] Department of Mathematics and Geosciences, University of Trieste, Trieste, Italy

[3] Department of Life Science, University of Trieste, Trieste, Italy

[4] Co.N.I.S.Ma. Consorzio Nazionale Interuniversitario per le Scienze del Mare

[*]**Corresponding author: Cinzia De Vittor**

OGS (Istituto Nazionale di Oceanografia e di Geofisica Sperimentale), Oceanography Division

Via A. Piccard 54, 34151 Trieste, Italy

Tel.: +39 040 2249723

email: cdevittor@inogs.it

Published in Environmental Science and Pollution Research

DOI 10.1007/s11356-015-4999-0

Environ Sci Pollut Res (2016) 23:12566–12581
DOI 10.1007/s11356-015-4999-0

Oxygen, carbon, and nutrient exchanges at the sediment–water interface in the Mar Piccolo of Taranto (Ionian Sea, southern Italy)

Cinzia De Vittor[1] · **Federica Relitti**[1,3] · **Martina Kralj**[1] · **Stefano Covelli**[2,4] · **Andrea Emili**[2]

Received: 2 April 2015 / Accepted: 30 June 2015 / Published online: 9 July 2015

Abstract In the shallow environment, the nutrient and carbon exchanges at the sediment–water interface contribute significantly to determine the trophic status of the whole water column. The intensity of the allochthonous input in a coastal environment subjected to strong anthropogenic pressures determines an increase in the benthic oxygen demand leading to depressed oxygen levels in the bottom waters. Anoxic conditions resulting from organic enrichment can enhance the exchange of nutrients between sediments and the overlying water. In the present study, carbon and nutrient fluxes at the sediment–water interface were measured at two experimental sites, one highly and one moderately contaminated, as reference point. In situ benthic flux measurements of dissolved species (O_2, DIC, DOC, N-NO_3^-, N-NO_2^-, N-NH_4^+, P-PO_4^{3-}, Si-Si$(OH)_4$, H_2S) were conducted using benthic chambers. Furthermore, undisturbed sediment cores were collected for analyses of total and organic C, total N, and biopolymeric carbon (carbohydrates, proteins, and lipids) as well as of dissolved species in porewaters and supernatant in order to calculate the diffusive fluxes. The sediments were characterized by suboxic to anoxic conditions with redox values more negative in the highly contaminated site, which was also characterized by higher biopolymeric carbon content (most of all lipids), lower C/N ratios and generally higher diffusive fluxes, which could result in a higher release of contaminants. A great difference was observed between diffusive and in situ benthic fluxes suggesting the enhancing of fluxes by bioturbation and the occurrence of biogeochemically important processes at the sediment–water interface. The multi-contamination of both inorganic and organic pollutants, in the sediments of the Mar Piccolo of Taranto (declared SIN in 1998), potentially transferable to the water column and to the aquatic trophic chain, is of serious concern for its ecological relevance, also considering the widespread fishing and mussel farming activities in the area.

Keywords Benthic fluxes · Nutrients · Sediment–water interface · DOC · DIC · Mar Piccolo of Taranto

Responsible editor: Philippe Garrigues

✉ Cinzia De Vittor
cdevittor@ogs.trieste.it

[1] OGS (Istituto Nazionale di Oceanografia e di Geofisica Sperimentale), Sezione Oceanografia, Via A. Piccard 54, 34151 Trieste, Italy

[2] Dipartimento di Matematica e Geoscienze, Università degli Studi di Trieste, Via Weiss 2, 34128 Trieste, Italy

[3] Dipartimento di Scienze della Vita, Università degli Studi di Trieste, Via Licio Giorgieri 5, 34128 Trieste, Italy

[4] Co.N.I.S.Ma. Consorzio Nazionale Interuniversitario per le Scienze del Mare, Piazzale Flaminio 9, 00196 Roma, Italy

Introduction

In shallow coastal ecosystems, nutrient regeneration at the sediment–water interface (SWI) plays a significant role in maintaining high primary production in the water column via benthic–pelagic coupling (Hyun et al. 2013). In fact, in systems receiving sufficient light to maintain a phytobenthic community, benthic microalgae have an important role as filter in the flux of dissolved nutrients by transforming, storing, and removing nutrients from the overlaying water (Sundbäck et al. 2000; Grenz et al. 2000; McGlathery et al. 2007). Thus, the autotrophic metabolism influences fluxes at the SWI by the uptake and temporary retention of nutrients, burial of recalcitrant organic matter and indirectly by oxygenating surface sediment (McGlathery et al. 2001). Sediments can

therefore constitute either a source or a sink of nutrients, becoming the main factor in controlling the trophic level in aquatic systems (Spagnoli and Bergamini 1997). Benthic–pelagic coupling works in both directions, as the release of nutrients from sediments enhances primary production in the water column, and the organic matter produced in pelagic system sinks to the surface sediment providing labile substrate to be regenerated (Grenz et al. 2000). It has been reported (Kelly and Nixon 1984) that up to 80 % of annual carbon and nitrogen deposition may be remineralized and returned to the overlying water, thus supporting primary pelagic production.

Coastal areas are often subjected to a severe exposition to urban, industrial, and agricultural wastewaters that influence the volume and quality of water inputs. Rivers are the greatest contributors to coastal areas of organic materials, nutrients, heavy metals, and sediments, usually untreated and unfiltered (Dunn et al. 2013 and references therein; Ortega et al. 2008). This organic material is extremely reactive and induces higher rates of microbial processes, sometimes resulting in eutrophication of the receiving water body. The enhanced microbial activity can lead to a change in sediment status from oxic to hypoxic or even anoxic, and reduces oxygen levels in bottom waters (De Vittor et al. 2012). Hypoxia is a global key stressor affecting a huge portion of coastal zones and the persistence of these episodes could result in changes in ecosystem functioning (Emili et al. 2011), especially in the increase of nutrient and dissolved organic carbon exchange between sediments and water column (De Vittor et al. 2012; Dunn et al. 2013).

Establishing the magnitude of benthic exchanges, especially in conditions of hypoxia/anoxia, is important because dissolved oxygen is a key regulator for many biogeochemical cycles, such as sulfur, nitrogen, and heavy metals; therefore, changes in sediment redox status could enhance the release of contaminants (e.g., mercury, iron, sulfur) (Santos-Escheandia et al. 2009; Covelli et al. 2011; Emili et al. 2011; De Vittor et al. 2012). Hence, the study of nutrient and carbon fluxes at the SWI is fundamental to define the functionality of coastal ecosystems and to provide indications for managing conservation and development land uses.

The present study has been conducted with the aim of evaluating benthic metabolism, and carbon and nutrient exchange at the SWI of the Mar Piccolo of Taranto (Southern Italy), an example of a marine ecosystem contaminated by waste waters. As these processes are strongly related to contaminant cycling, the study was associated with simultaneous measurements of major and trace element fluxes using the same benthic chambers (Emili et al. 2015). In situ benthic chamber experiments were performed in two experimental sites, one highly and one moderately contaminated, as reference point. In parallel, sediments as well as supernatant and porewaters were characterized.

Methods

Study area

As part of the Taranto Gulf, Mar Piccolo is a semi-enclosed basin located in the north area of the town. Its surface area accounts for approximately 21 km^2. It is divided into two inlets (called first and second inlet), and it is connected to Mar Grande and the Taranto Gulf (Ionian Sea) by two channels linked to the first inlet where the maximum depth of 13 m is achieved. Summer water stratification is usually detected due to its morphology and low water exchange. Hypoxic conditions at the bottom are often noticed as a consequence of oxygen consumption by microbial degradation of significant inputs of organic matter from wastewater discharges, mussel farming, and agricultural soil drainage which also supplies an excess of nutrients to the system (Spada et al. 2012). The sediments are made up of fine sands and muds with traces of shell fragments (Pastore 1993). In general, the benthic system of the Mar Piccolo is net heterotrophic. Microphytobenthic abundances are quite low in respect to other shallow environments, and diatoms are the most abundant group although their percentage decreases in relation to pollution (Rubino et al. 2015). The southeastern area of the second inlet is the most densely colonized by macroalgae, while in the first inlet a much lower areal coverage is present (Cibic et al. 2015). Macrobenthic community is generally dominated by polychaetes and molluscs, followed by crustaceans and other taxa (mainly anthozoans, sipunculids, and nemertines) (Franzo et al. 2015).

High sulfide concentration is present in bottom sediments throughout the year as a result of organic matter anaerobic degradation (Cardellicchio et al. 2006). Besides, this coastal environment has suffered from severe anthropogenic pressures (remarkably an iron and steel factory, a petroleum refinery, and the Italian Navy shipyard and arsenal), and it was declared a “Contaminated Site of National Interest (SIN)” in 1998.

A more exhaustive description of the study area is reported by Cardellicchio et al. (2015).

The study of biogeochemical fluxes at the SWI of the Mar Piccolo was carried out in June 2013 at two sites both at about 11-m depth (Fig. 1). Station 1E (sampled on June 12) is approximately located at the center of the first inlet. The second station (1I, sampled on June 14) is placed just in front of the Navy Arsenal, and it can be considered as the most contaminated by anthropogenic activities (Spada et al. 2012; Emili et al. 2015). The physical and chemical features of the two stations are described by Kralj et al. (2015) and environmental characteristics of bottom waters at the beginning of each sampling are reported in Table 1.

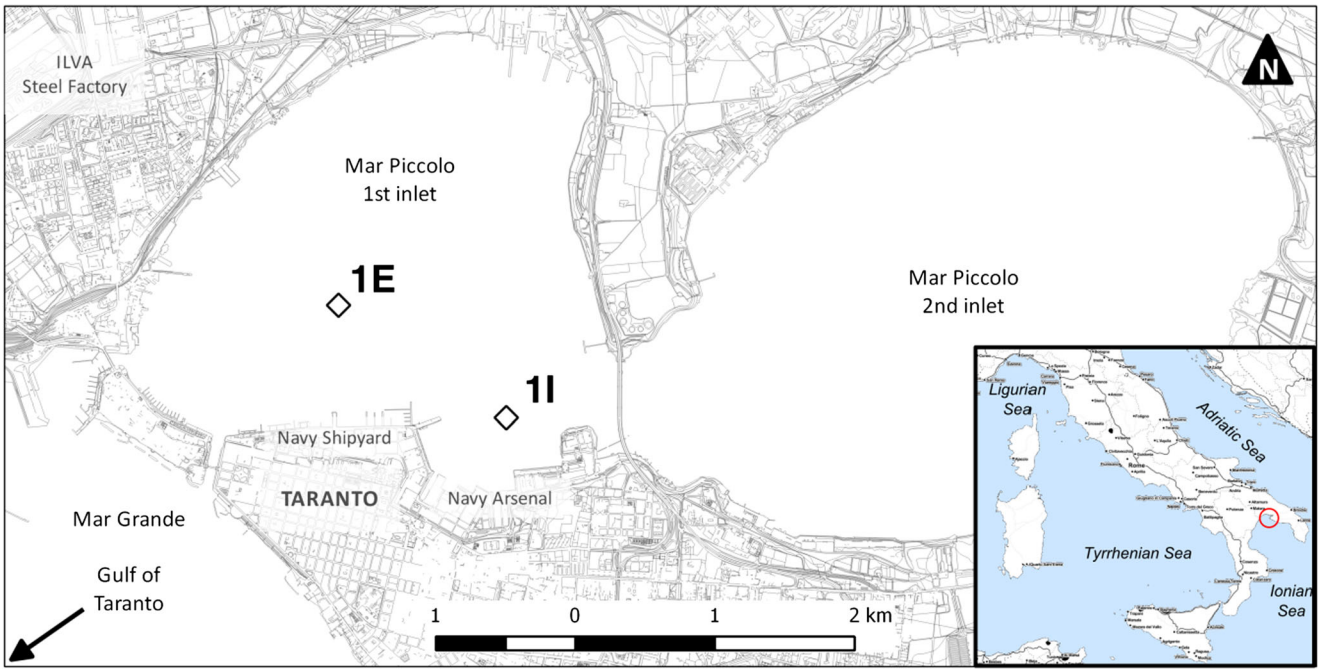

Fig. 1 Study area. Experimental stations 1E and 1I in the Mar Piccolo of Taranto (basemap courtesy of SIT Regione Puglia, 2014)

Sediment sampling and porewater collection

Undisturbed sediment cores, two for each sampling site (1E and 1I), were collected by divers pushing a Plexiglas tube (16-cm i.d; 30-cm length) into the sediment. Cores were stored at dark into refrigerate containers and carefully transported to the laboratory minimizing disturbance at the SWI. Upon return to the laboratory, within 2 h after core collection, the sediment cores were immediately extruded and sectioned into slices (0–1, 1–2, 2–3.5, 3.5–5, and 5–7 cm) in a N_2-filled chamber and redox potential was measured at each slice. Measurement of Eh was performed at room temperature directly into the N_2-filled chamber. After calibration, electrode was rinsed and an initial reading was made in the overlying seawater ~1 cm above the sediment surface after the reaching of a stable value (several minutes). Then, the overlying water was sampled with a syringe and the electrode was pushed in 0.5-cm depth into the surface sediment where a further reading was taken after several minutes. The sediment core was sliced and the operation repeated after each slicing. The redox electrode was rinsed with distilled water and dried between measurements. Porewaters were extracted from each sediment slice by centrifugation at in situ temperature. Samples were subsequently recovered in an inert atmosphere, filtered through Millipore Millex HA 0.45 μm pore size cellulose acetate filters and finally collected in acid-precleaned vials, which were stored frozen until analysis. Porewater samples and supernatant were analyzed for inorganic nutrients (nitrite, nitrate, ammonium, phosphate, and silicate), dissolved organic carbon (DOC), dissolved inorganic carbon (DIC), and hydrogen sulfide (H_2S).

Sediment samples (five for each core) were freeze-dried, homogenized, and ground to fine powder for analyses of total and organic C (C_{tot}, C_{org}), total N (N_{tot}), total P (P_{tot}), and biopolymeric carbon (BPC, as sum of carbohydrate (CHO), protein (PRT), and lipid (LIP) carbon). Part of the intact samples was used to determine granulometry and sediment water content (Emili et al. 2015).

Diffusive fluxes

Diffusive fluxes (F) represent an instantaneous measure of the flux of solutes diffusing from sediment porewaters to the overlying water column, along a concentration gradient. Positive values are indicative of an efflux, while negative values represent an influx or scavenging from the water column. In the present study, the diffusive benthic fluxes of DIC, DOC, and

Table 1 Environmental characteristics at the bottom of the two sampled stations

Station	Depth (m)	Temperature	Oxygen (% saturation)	Salinity	PAR (↑μE m^{-2} s^{-1})	% PAR
St. 1E	11.2	20.61	100.80	38.371	188.17	6.74
St. 1I	11.0	20.64	98.49	38.335	183.69	7.45

Data kindly provided by T. Cibic

PAR photosynthetic available radiation, *%PAR* benthic PAR expressed as the percentage of surface irradiance

N, P, Si nutrients and H_2S were calculated by application of Fick's first law as reported by De Vittor et al. (2012). In the absence of bioirrigation, Fick's first law can be expressed as follows:

$$F = -\left(\frac{\Phi D_w}{\theta^2}\right)\frac{\partial C}{\partial x}$$

where F is the flux of a solute with concentration C at depth x and $\partial C/\partial x$ is the concentration gradient of chemical species between porewater at the depth of 1 cm and the overlying water, Φ the sediment porosity (0.75), θ the tortuosity (dimensionless), and D_w is the diffusion coefficient of the solute in water (Ullman and Aller 1982; Alperin et al. 1994) in the absence of the sediment matrix.

Benthic flux chamber experiments

In situ benthic flux measurements were conducted using benthic chambers already tested in the Gulf of Trieste (Bertuzzi et al. 1997; Covelli et al. 1999) and in the Marano and Grado Lagoon (Covelli et al. 2008; De Vittor et al. 2012). The chamber, consisting of a transparent Plexiglas box, covers a sediment area of 0.25 m^2 containing ~53 L of seawater. The chamber waters were homogenized using a magnetic stirring mechanism, coupled to a rotating propeller on the chamber topside. Samples were periodically (t=0 and every ≅2 h for a total of five samplings) collected at sites 1E and 1I using 50-mL polypropylene syringes during day deployments of about 8 h. The volume removed from the chamber was replaced by in situ water flowing into the chamber from a valve. Flux rates calculated from concentration data were not corrected for dilution because of the low ratio of the sample to total chamber volume (0.2 %). The hourly metabolism rates were scaled to the number of light hours for each experiment to calculate diurnal net metabolism (McGlathery et al. 2001). In situ flux rates of solutes across the SWI were calculated on square meter basis adapting Rizzo (1990) and Nixon et al. (1976) protocols.

$$\text{Diurnal nutrients/DOC flux} = (\text{mean hourly chamber nutrients change} \times \text{photoperiod})$$

$$\text{Daily net production (as } O_2\text{production)} = (\text{mean hourly chamber oxygen change} \times \text{photoperiod})$$

$$\text{Daily net production (as } CO_2\text{uptake)} = (\text{mean hourly chamber DIC change} \times \text{photoperiod})$$

Unfortunately, as a consequence of the sampling schedule and the lack of overnight samples, daily respiration could not be estimated; furthermore, also nutrients and DOC fluxes reflect only daylight processes.

Analyses

Analyses of C_{tot} and N_{tot} in freeze-dried and homogenized sediment samples were performed using a Perkin Elmer 2400 CHNS/O Elemental Analyser. C_{org} was determined after acidification of samples with 1 M HCl (Hedges and Stern 1984) at a combustion temperature of 975 °C. P_{tot} was analyzed by extraction from freeze-dried and homogenized sediment with 1 M HCl after ignition at 550 °C (Aspila et al. 1976). Dissolved phosphate in extracts was determined using the same method described for inorganic nutrients in overlying and porewaters (see at the end of the paragraph). The precision of C_{tot}, C_{org}, N_{tot}, and P_{tot} was about 3 %.

Two different CHO fractions (water soluble, CHO_{H2O} and EDTA-extractable, CHO_{EDTA}) were determined following Blasutto et al. (2005). The carbohydrate fractions were measured spectrophotometrically using the phenol-sulfuric acid assay (Dubois et al. 1956), modified by Gerchacov and Hatcher (1972) for sediment samples. CHO concentrations were calculated from calibration curves of D-glucose. CHO concentrations, obtained as equivalent-glucose, were transformed into carbon using a conversion factor of 0.49 g C g^{-1} (Fabiano et al. 1995).

PRT analyses were carried out on lyophilized sediment samples after extractions with NaOH (0.5 M, 4 h). PRT were determined according to Hartree (1972) modified by Rice (1982) to compensate for phenol interference. PRT concentrations were calculated from calibration curves of serum albumin. Even if determination could be affected by the interference of humics (Rice 1982), this method was chosen due to its ease and high sensitivity. Moreover, the wide application of this protocol makes our results comparable with other studies (Fabiano et al. 1995; Fabiano et al. 2001; Pusceddu et al. 2009). Concentrations obtained as albumin equivalents were transformed into carbon using a conversion factor of 0.50 g C g^{-1} (Fichez 1991). Total LIP were extracted by direct elution with chloroform and methanol following the procedure of Bligh and Dyer (1959) and analyzed according to Marsh and Wenstein (1966). LIP concentrations were calculated from calibration curves of tripalmitine. Concentrations obtained as tripalmitine equivalents were transformed into carbon using a

conversion factor of 0.75 g C g^{-1} (Fichez 1991). All biochemical analyses were carried out in three to five replicates, with standard deviation lower than 5 %.

The sum of the carbon equivalents of CHO, PRT and LIP was referred as BPC (sensu Fichez 1991).

Dissolved O_2 (DO) was analyzed by the Winkler method (Grasshoff et al. 1983) using an automated titration system (Mettler Toledo, DL 21). The reproducibility of the methods was 5 %. DIC and DOC were determined using the Shimadzu TOC-V CSH analyzer. For DIC, samples were injected into the instrument port and directly acidified with H_3PO_4 (25 %). For DOC analysis, water samples were previously acidified (automatically into instrument syringe, 2 %—6 M HCl) and after CO_2 elimination, the concentration was determined using a high temperature catalytic method (Sugimura and Suzuki 1988). Phosphoric acidification for DIC and combustion conducted at 680 °C on a catalyst bed for DOC, generated CO_2 that was carried to a nondispersive infrared detector (NDIR). Analysis showed a variation coefficient <2 %. The reproducibility of the method was between 1.5 and 3 %. Nutrient analyses, including nitrate ($N\text{-}NO_3^-$) and nitrite ($N\text{-}NO_2^-$), ammonium ($N\text{-}NH_4^+$), phosphate ($P\text{-}PO_4^{3-}$), and silicate ($Si\text{-}Si(OH)_4$), were performed with a segmented flow Bran+ Luebbe AutoAnalyzer 3 following standard colorimetric methods (Hansen and Koroleff 1999). The precision was 3 %. Aliquots of 2.5 ml of overlying or porewater and stored in a dark place until analysis. Samples for hydrogen sulfide determination were preserved by adding zinc acetate and measured spectrophotometrically using a VARIAN CARY 100 Scan spectrophotometer at 670 nm according to Fonselius (1983).

To test if the concentrations of the biochemical compounds differed significantly between the two stations (1E and 1I), an analysis of variance (ANOVA) test was performed using the Oneway Analysis Platform analysis. To highlight relationships between analyzed biochemical variables, the nonparametric Spearman's rank correlation analysis was applied.

In order to verify the differences between impacted and control sites, principal component analysis (PCA) was applied on solid phase and porewater data.

All analyses were performed using the JMP 11 Pro statistics software package (SAS Institute Inc.).

Results and discussion

Sediment biogeochemistry

Surface sediment grain size at both stations was rather uniform over the 0–7-cm depth layers sampled, and it largely consisted of fine particles (<63 μm). Grain size distribution at station 1E (average 13.9 % sand, 72.6 % silt, and 13.5 % clay) lightly differed from station 1I characterized, on average, by 13.5 % sand, 76.7 % silt, and 9.8 % clay proportion (Emili et al. 2015).

The porewater oxygen penetration depth was between 0.16 and 0.29 cm (Rubino et al. 2015), indicating that the upper sample for porewater extraction and solid analyses included the whole oxic zone and the top of the anoxic sediment (Anschutz et al. 2007).

The redox potential (Eh) along sediment cores varied from −150 to −418 mV at station 1E and from −272 to −400 mV at 1I and are similar to those reported by Spada et al. (2012) who found values ranging from −348 to −457 mV in the surface sediments of the Mar Piccolo basin. Matijević et al. (2007) reported that the transition from suboxic to anoxic conditions (presence of HS^- or S^{2-}) takes place at potentials from 0 to to 150 mV. Thus, Eh values measured along the sediment cores indicate the presence of anoxic conditions, sulfate reduction and anaerobic organic matter degradation (Matijević et al. 2013). Vertical profiles displayed a clear decrease in Eh downcore at 1E while 1I, more subjected to anthropogenic inputs and characterized by more negative potential, showed an irregular trend (Fig. 2).

Similar C_{tot} contents (average 8.0±0.2 vs 7.7±0.3 %) and uniform trends with depth were encountered at sites 1E and 1I, while higher C_{org} contents (average 3.8±0.1 vs 4.2±0.3 %), with the exception of the surface layer, and N_{tot} contents (average 0.27±0.01 vs 0.39±0.03 %) were found at 1I (Fig. 2).

The ratio of total organic carbon to total nitrogen (C_{org}/N_{tot}) is widely applied for inferring the origin of organic matter (OM) in marine sediments. According to Goñi et al. (2003), C_{org}/N_{tot} (molar) ratios >14 are characteristic of vascular plant-derived OM dominated by carbon-rich (and nitrogen-poor) biochemical classes (i.e., lignin and cellulose), while C_{org}/N_{tot} (molar) values <10 may be defined as of autochthonous marine origin (from phytoplankton and bacterioplankton characterized by higher N content) (Ogrinc et al. 2003). The C_{org}/N_{tot} ratios (molar) were rather constant along sediment depth at site 1E, varying from 15.2 to 16.9 (average 16.3±0.7) while at 1I a wide range of variation was observed, from 8.9 to 14.4 (average 12.6±2.2), with a net increase with depth, mainly as a consequence of the decreasing N_{tot} trend downcore. The ratio in surface sediments (0–1 cm) found at 1E was twice higher (16.9) than at 1I (8.9), suggesting that OM is predominantly of marine origin at this station while 1E could be influenced by some terrestrial input. Concentrations of P_{tot} decreased slightly with depth from 809±4 μg g^{-1} (average 0–2 cm) to 761 μg g^{-1} at 1E and from 724 to 679 μg g^{-1} at 1I (Fig. 2), suggesting a recent enrichment in the surface sediment most likely due to urban and/or aquaculture inputs (Anschutz et al. 2007). C_{org}/P_{tot} ratio (Fig. 2) was quite constant along sediments of 1E with values, on average, of 123±1.4, typical of suboxic and intermittently anoxic environments (Algeo and Ingall 2007). At 1I, similar conditions (C_{org}/P_{tot}= 115) were found only in surface sediments (0–1 cm) while in

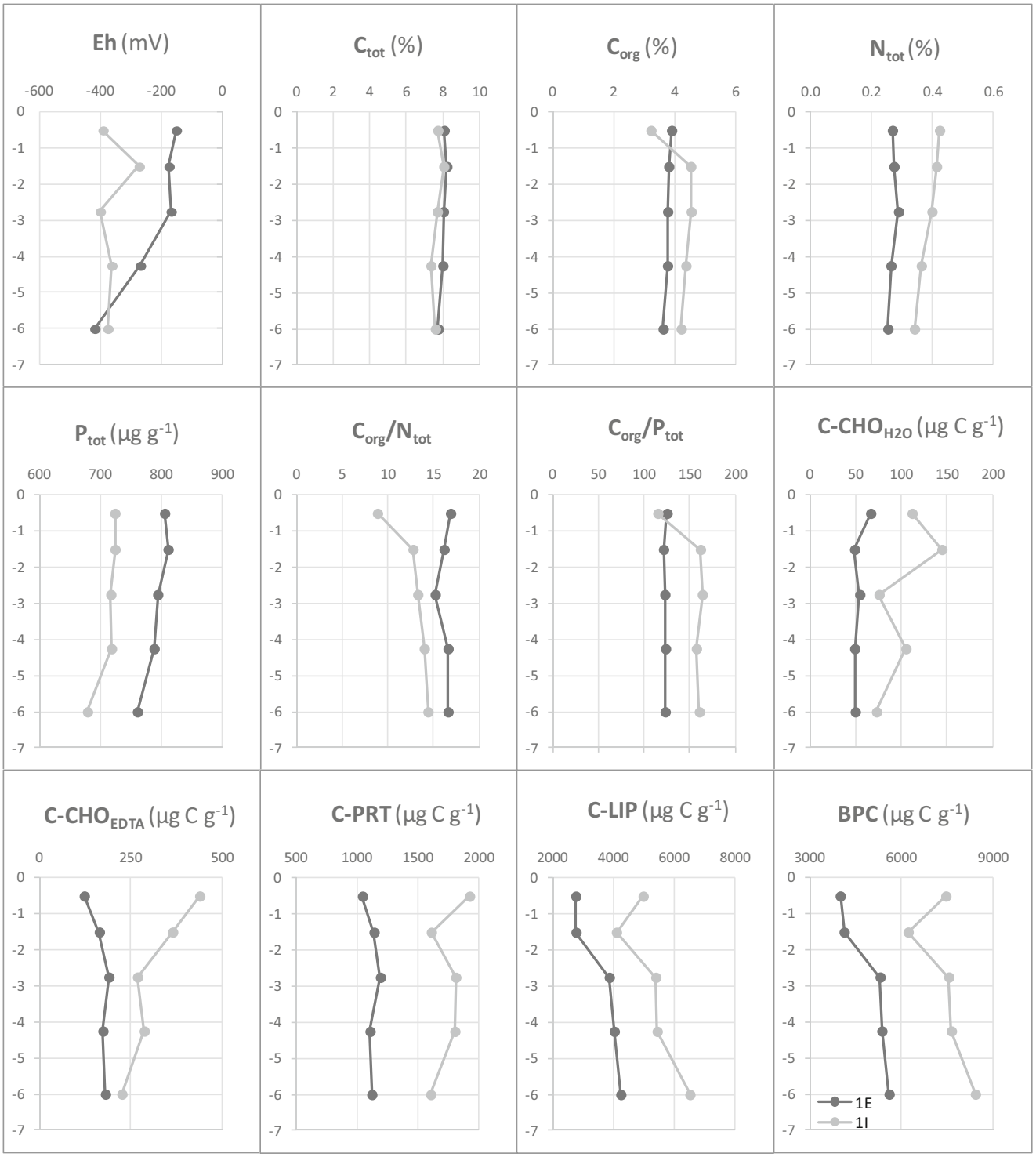

Fig. 2 Depth profiles of Eh, C_{tot}, C_{org}, N_{tot}, P_{tot}, C_{org}/N_{tot} (molar ratio), C_{org}/P_{tot} (molar ratio), C-CHO_{H2O} (water-soluble carbohydrates), C-CHO_{EDTA} (EDTA extractable carbohydrates), C-PRT (proteins), C-LIP (lipids), and BPC (biopolymeric carbon) in the experimental sites 1E and 1I

the deeper ones (1–7 cm), the ratio reached a mean value of 161±2.7, characteristic of permanently anoxic environments (Algeo and Ingall 2007).

The sediment concentrations of biochemical compounds, CHO_{H2O} and CHO_{EDTA}, PRT, LIP, and BPC (as sum of the carbon of the four components) differ significantly between stations 1E and 1I (CHO_{H2O}: $p<0.01$; CHO_{EDTA}: $p<0.01$; PRT: $p<0.01$; LIP: $p<0.005$; BPC: $p<0.005$) (Fig. 2). On average, 1I was characterized by 1.5–2-fold higher concentrations of all components, even if the relative percentage

composition is similar between the two stations. At both stations, the BPC was dominated by LIP (67–77 % of total BPC), followed by PRT (20–28 %) and CHO_{EDTA} (3–6 %). CHO_{H2O} contributed only for 1–2 % to total BPC. At 1E, LIP ranged from 2758 to 4244 μg C g^{-1} showing an increasing gradient with depth, PRT ranged from 1045 to 1193 μg C g^{-1} with a uniform trend along depth, CHO_{EDTA} varied between 123 and 190 μg C g^{-1} increasing slightly with depth, while CHO_{H2O} profile was quite uniform with concentrations ranging from 49 to 66 μg C g^{-1}. At 1I, LIP ranged from 4099 to 6523 μg C g^{-1} (maximum was reached at the deepest sediment layer of 5–7 cm), PRT varied between 1607 and 1927 μg C g^{-1} displaying an irregular vertical profile, CHO_{EDTA} decreased with depth from 439 to 226 μg C g^{-1}, while CHO_{H2O} showed a highly variable profile with a concentrations range of 73–144 μg C g^{-1}.

LIP concentrations found in our study, especially those of site 1I, are definitely higher than those reported worldwide for marine sediments (for a review, see Pusceddu et al. 2009). However, they are comparable to those measured by Cibic et al. (2012) at 2–6-cm sediment depth of an Adriatic lagoon, contaminated by hydrocarbon and heavy metal and by Pusceddu et al. (1999) in the top sediments (0–1 cm) at a station of the Marsala lagoon (Mediterranean Sea) characterized by *Posidonia oceanica* (and detritus of *Posidonia*) coverage. Similar concentrations with a maximum of more than 20,000 μg g^{-1} (lipid carbon=15,400 μg C g^{-1}) were also reported by Neira et al. (2001) in an upwelling region off Central Chile. The high lipid contribution to BPC (lipids are always the dominant component, up to 77 %) found in our study is the highest ever reported in the literature (for a review, see Pusceddu et al. 2009, 2010). Generally, the composition of the sedimentary organic detritus shows a dominance of carbohydrates or proteins (Pusceddu et al. 2009, 2010; Cibic et al. 2012) depending on its origin (primary organic carbon from microalgae vs aged and/or nonliving organic matter). The cause of the high concentration of lipids found especially at site 1I remains unknown. Although one possibility could be the natural production from diatoms like *Coscinodiscus*, one of the most important phytoplanktonic taxa in Mar Piccolo of Taranto (Caroppo and Cardellicchio 1995; Caroppo et al. 2006), deposited shortly before sampling (Neira et al. 2001), we believe that they derive from anthropogenic sources (e.g., untreated sewage discharges and petroleum-related compounds).

BPC vertical profiles reflected patterns observed for lipids concentrations. The BPC represented, on average, the 13.0± 2.4 % of C_{org} at station 1E and its contribution to C_{org} increased regularly with depth. At station 1I, the biopolymeric available fraction of total organic carbon constituted, on average, the 18.2±3.6 % of C_{org} showing the highest value of 23.2 % at the uppermost layer of sediment (0–1 cm), a clear decrease at 1–2 cm and then a regular increase up to the bottom layers (Fig. 2). Increasing accumulation of BPC in marine sediments is associated even in highly productive systems (such as estuaries, ponds, and fish farm sediments) with low algal carbon contributions to BPC. This suggests that, in eutrophic sediments characterized by high BPC concentrations and benthic algal biomass, algal carbon is progressively diluted in a complex and heterogeneous organic matrix (Pusceddu et al. 2009).

A PCA was performed on the correlation matrix of variables describing the solid phase of the two sediment cores to highlight differences between the two stations (Fig. 3). The first two eigenvalues explain 81.3 % of the original data variance. By plotting the original datapoints (each point representing a single sediment layer) onto a biplot with the first two principal components as the axes, two groups can clearly be distinguished, corresponding to the two stations. Principal component 1 is responsible for this separation, and it is well correlated with all original variables, except for C_{org} (factor loading<0.5). The highest loadings (>|0.94|) were associated with variables P_{tot}, BPC, and PRT. Differences among the different sediment layers in the same core are

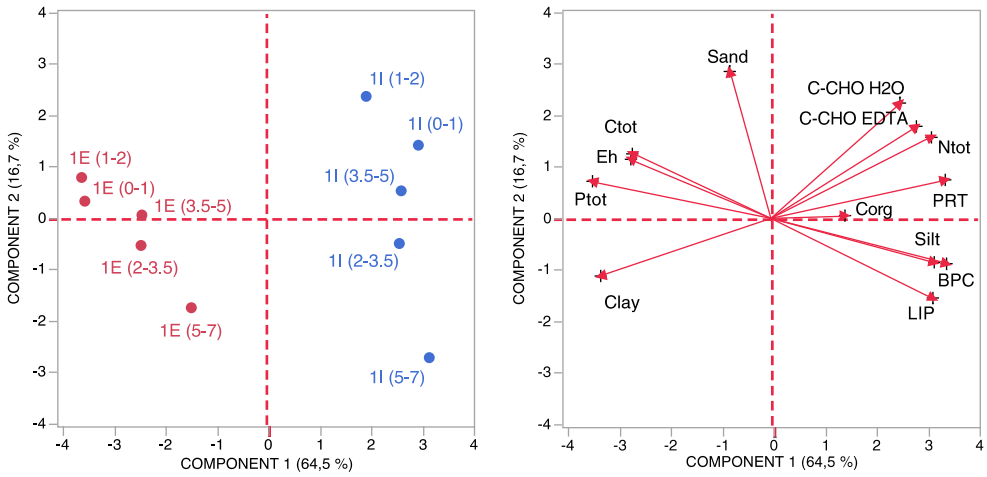

Fig. 3 Principal component analysis (PCA) score plot (*left*) and biplot (*right*) of solid phase samples (*red*: station 1E; *blue*: station 1I). *Numbers in parentheses* refer to the percentage of total variance explained by the principal components

explained by the second principal component, which is mostly represented by the percentage of sand in the sediment.

Porewater chemistry

The concentration and lability (freshness) of organic matter determine the efficiency of its mineralization and the concentrations of its by-products. Metabolite accumulation in porewaters results from the balance between reaction rates and transport processes (Metzger et al. 2007). Thus, porewater concentrations provide an image of ongoing diagenetic reactions and physical processes (Metzger et al. 2007).

The DIC profiles exhibited two different patterns: a regular but minor increase of concentration with depth along the sediment core (from 2879 μM, in the supernatant, to 3347 μM, at 5–7-cm depth) at 1E, and a marked increasing concentration downcore with a clear positive gradient at the SWI going to a maximum of 5714 μM at the deepest layer (5–7 cm), at 1I (Fig. 4). In the porewater concentration versus depth profiles, the increasing DIC concentrations are attributed to processes accompanying the decomposition of sedimentary organic matter (Lojen et al. 2004) as confirmed by the positive correlation found between DIC and P-PO_4^{3-} ($p<0.05$ and $p<0.01$ at 1E and 1I, respectively) and between DIC and N-NH_4^+ ($p<0.01$ at both stations). As DIC represents the ultimate product of organic carbon oxidation, the increasing DIC concentrations downcore evidenced at station 1I indicate that significant decomposition occurs within the sediment column (Alperin et al. 1999).

Porewater DOC concentrations reflect a balance between production and consumption reactions; dissolved compounds produced by hydrolysis of solid-phase organic matter are consumed by biotic and abiotic processes (Alperin et al. 1999). DOC concentrations in porewaters varied from 119 to 809 μM and from 345 to 714 μM, at 1E and 1I, respectively. Values increased irregularly downcore especially at 1E indicating DOC diagenetic formation within sediments (Alperin et al. 1999) with prevalently macromolecular (humic) nature and, hence, lower mobility (Burdige et al. 1992) (Fig. 4).

At both stations, the porewater N-NH_4^+ profiles showed a large increase in concentration with depth with a strong positive gradient at the SWI, but concentrations at each sediment depth of station 1I were always approximately 3-fold higher compared to 1E, reaching a maximum of 291 μM at the deepest sediment layer (Fig. 4). This behavior suggests the presence of more intense denitrification processes and organic matter mineralization rate at site 1I, characterized by higher biopolymeric carbon concentrations (i.e., proteins).

At station 1E, a considerable N-NO_2^- concentration gradient existed between the surficial interstitial water and the overlying seawater; immediately below, the concentrations decreased substantially to reach a quasi-constant value below 3-cm depth. N-NO_3^- concentrations increased sharply in the first centimeter of the sediment and then decreased to reach a constant concentration of about 2.5 μM at layers between 1 and 3 cm to increase again below 4-cm depth. At 1I, N-NO_2^- concentrations increased in the 1–2-cm layer of the sediment and then gradually declined to reach a steady state below 2-cm depth. The concentration of N-NO_3^- increased from 2.9 μM in the supernatant to 6.3 μM at 5–7-cm depth, except for a decrease at 2–4-cm depth (Fig. 4). This increasing N-NO_3^- concentration with depth suggests that bioturbation is actively reworking sediment as confirmed by the high presence of mobile species, which normally move in the first 10 cm of the sediment like the polychaetes *Lumbrineris latreilli*, *Glycera rouxii*, and *Eunice vittata* and the amphipod *Microdeutopus anomalus*. These bioturbators were not abundant at station 1E characterized by higher macrozoobenthic biomass but dominated by surface deposit feeders (Auriemma, personal communication; Franzo et al. 2015). The presence of N-NO_2^- and N-NO_3^- along the sediment depth, albeit in low concentrations, suggests an accumulation of the products of OM oxidation in the interstitial water. However, the presence of very high levels of N-NH_4^+ also in the upper sediment layers indicates that the ammonia produced during heterotrophic breakdown of OM was not immediately oxidized and accumulated in porewaters prior to its transport predominantly to the sediment below (Ram and Zingde 2000). As found by Lojen et al. (2004), the concentration vs. depth profiles of nitrate and ammonia (Fig. 4) can be explained in relation to the observed influx of nitrate and ammonia into the sediment in benthic chamber experiments (see "In situ benthic fluxes"). The increase of ammonia and nitrate with depth is typical of environments where rapid decomposition of sedimentary organic matter takes place (Lojen et al. 2004). Ram and Zingde (2000) suggested also that N-NO_3^- increase in the sediment depth could be due to a nonsteady-state condition derived from either the two following factors: the sediment could have been buried at a time when the bottom water N-NO_3^- concentrations were high or, else, the nitrate was consumed less rapidly than in surface sediments, due to the differences in OM and/or microbial populations.

The concentration profiles of P-PO_4^{3-} reflect the behavior of N-NH_4^+ with positive correlation coefficients of 0.94 ($p<0.01$), and 0.96 ($p<0.01$) at stations 1E and 1I, respectively, showing a large increase in concentration with sediment depth and higher concentrations (up to 6-fold) at each sediment depth at 1I (Fig. 4). The linear relationship indicates that porewater P-PO_4^{3-} is released in relation to ammonia by organic matter decomposition (Ogrinc and Faganeli 2006). The release of phosphate to porewaters is mostly due to the loss of capacity by the sediment to adsorb phosphate as it undergoes burial and to the aerobic and anaerobic mineralization of organic matter during early diagenesis, which produces dissolved phosphate (Anschutz et al. 2007). The observed

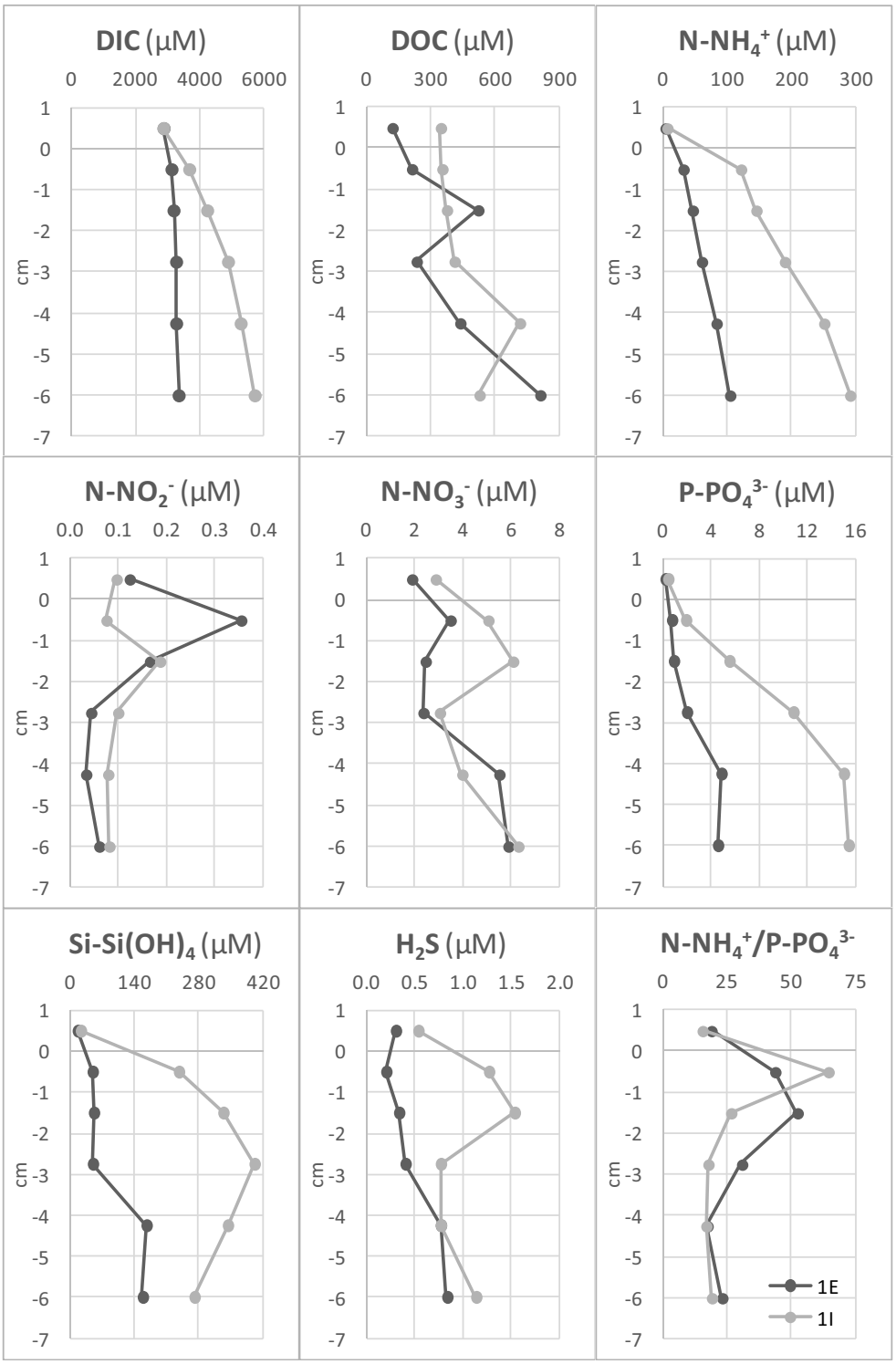

Fig. 4 Depth profiles of DIC, DOC, N, P, and Si nutrients, H_2S and $N\text{-}NH_4^+/P\text{-}PO_4^{3-}$ ratio in porewaters from the study sites 1E and 1I

differences between the two stations can be attributed to the different content of biopolymeric carbon and as a consequence of the different grade of OM mineralization in the cores.

The ratio between dissolved ammonium and phosphate can provide information about the processes of phosphate release and uptake in the sedimentary cores. A constant ratio indicates a stoichiometric nutrient regeneration due to organic matter mineralization. Variable ratios suggest that reactions of P removal or addition take place (Anschutz et al. 2007 and references therein). The ratio varied between 17 and 52 at 1E and

from 17 to 64 at 1I (Fig. 4). This variability indicates that the mineralization of marine organic matter alone cannot explain the profiles and that, in the surface sediments (0–2 cm), reactions of P removal, such as adsorption on iron oxides (De Vittor et al. 2012), precipitation as authigenic phosphate mineral, and biological uptake within the sedimentary column occurred (Anschutz et al. 2007). Remarkably, Mar Piccolo sediments are rich in iron (Petronio et al. 2012). The decrease of the NH_4^+/PO_4^{3-} ratio with depth instead confirms the release of phosphate from iron oxides as these are reduced, and the anaerobic mineralization of organic P (Sundby et al. 1992).

Silicate concentration, at station 1E, was 15.5 μM in the overlaying water, resulted homogenous in the first 3 cm of sediments with values of 48–51 μM, and then increased to 165 and 157 μM in the deeper layers. At 1I, a considerable concentration gradient of Si-$Si(OH)_4$ existed between the surficial interstitial water (236 μM) and the overlying seawater (22 μM); silicate increased up to 400 μM in the middle layer of the sediment core and then declined in the deeper layers (Fig. 4). The observed increasing Si-$Si(OH)_4$ concentrations with sediment depth at station 1I may be the result of biogenic silica dissolution in the sediment (Zhang et al. 2013 and references therein) which depends on temperature, pH, the nature and concentration of aqueous salt solutions, and Al content of the surrounding solution (Pastuszak et al. 2008). On the other hand, biogenic silica settled on the seafloor can be transformed into aluminosilicate materials (Ren et al. 2013) and precipitation of authigenic aluminosilicate minerals gives a low apparent solubility and contributes to low silicic acid concentrations, which could be the case of station 1E.

H_2S concentrations were very low at both stations, ranging from 0.2 to 0.8 μM and from 0.5 to 1.5 μM at 1E and 1I, respectively (Fig. 4). This could be due to bioturbation, as suggested by the presence of N-NO_3^- throughout the core lengths, which rules out the possibility of sulfate reduction (Ram and Zindge 2000), but also to very quickly reactions of reactive iron with sulfide, which leads to FeS precipitation (Middelburg and Levin 2009) reducing sulfide diffusion from the deeper anoxic sediment layers.

Similar to solid phase data, a PCA performed on porewaters (Fig. 5) showed that sediment layers can also be distinguished in two groups, corresponding to the two experimental stations. However, the distinction is not so sharp due to the deepest layer of 1E (5–7-cm depth) falling in the 1I group. This could be due to its high concentration of silicates and ammonia and the large negative value of Eh (−418 mV). Principal component 1 mostly summarizes the variables N-NH_4^+ (0.94), P-PO_4^{3-}, Si-$Si(OH)_4$, DIC, and Eh (factor loading >|0.87|) while N-NO_3^- has the strongest loading to the second component. Together, PC1 and PC2 explain 73.3 % of the original dataset variance.

Diffusive fluxes

The diffusive fluxes of all analyzed parameters at the two study sites are reported in Table 2.

Following the concentration gradient, the flux of all analytes occurred in one direction from the sediment porewater to the overlying bottom waters with the only exceptions of H_2S and N-NO_2^- at stations 1E and 1I, respectively. Excluding DOC and nitrite, the flux of all other inorganic nutrients, DIC and H_2S were considerably higher at station 1I than at 1E. The reason of this is related to the higher concentrations of this analytes in the porewater of 1I enhanced by the higher biopolymeric carbon content and biological activity. The lower DOC flux associated with the higher DIC flux registered at station 1I suggests that DOC was utilized as fast as it was produced (De Vittor et al. 2012). Looking at the diffusion of the inorganic nitrogen species, nitrite fluxes are negligible and nitrate ones appear marginal (up to one order of magnitude lower) compared to the fluxes of ammonium. Low

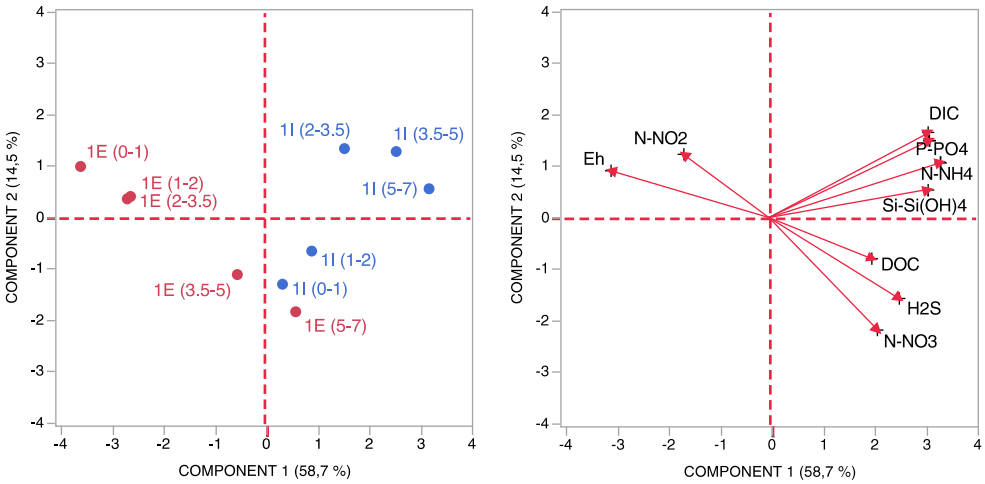

Fig. 5 Principal component analysis (PCA) score plot (*left*) and biplot (*right*) of porewater samples (*red*: station 1E; *blue*: station 1I). *Numbers in parentheses* refer to the percentage of total variance explained by the principal components

Table 2 Diffusive and in situ benthic fluxes at sites 1E and 1I

Parameter	Diffusive fluxes (μmol m^2 day^{-1})		Benthic fluxes (μmol m^2 day^{-1})	
	1E	1I	1E	1I
O_2			−1.6	−5.6
DIC	455	1969	−27.8	−30.4
DOC	36.2	3.6	−51.8	−5.8
$N\text{-}NH_4^+$	86.7	472.2	−73.1	−143.1
$N\text{-}NO_2^-$	0.7	−0.1	−6.2	1.5
$N\text{-}NO_3^-$	4.8	8.8	−87.8	−95.7
$P\text{-}PO_4^{3-}$	0.5	1.9	0.0	1.6
$Si\text{-}Si(OH)_4$	54.3	472.9	−282.3	−47.0
H_2S	−0.2	2.1	204.3	100.2

$N\text{-}NO_3^-$ fluxes toward the water column or $N\text{-}NO_3^-$ influxes have already been reported by several authors (Al-Rousan et al. 2004; Engelsen et al. 2008; De Vittor et al. 2012) and are related to the fact that $N\text{-}NH_4^+$ is the first inorganic product in the regeneration of nitrogenous organic material by microorganisms. $N\text{-}NO_2^-$ and $N\text{-}NO_3^-$ are formed in sediment only under well-oxygenated conditions by nitrifying bacteria throughout the nitrification processes (Al-Rousan et al. 2004 and references therein). The higher fluxes of $N\text{-}NH_4^+$ and $P\text{-}PO_4^{3-}$ found at station 1I could be related both to the more anoxic conditions, which increased the release rate of these species from sediments to the overlaying water (Al-Rousan et al. 2004 and references therein), and to the dependence of phosphate and ammonium regeneration on the quality of organic matter in the sediment (Clavero et al. 2000). Also, the higher $Si\text{-}Si(OH)_4$ flux is related to the increased porewater concentration of silicate, probably due to enhanced dissolution of biogenic Si under more reducing conditions, as suggested by the H_2S efflux at 1I compared to the influx at 1E. Hydrogen sulfide release from anoxic sediments, in fact, has been widely reported (Middelburg and Levin 2009).

Concentration variations in benthic chambers

A very good linear correlation ($p<0.01$) was observed between analyte concentration and incubation time only for DIC at station 1I, suggesting the absence of a constant flux during the duration of the deployment (Berelson et al. 2013). The concentration of oxygen did not fall below 249 μM during the time the benthic chambers were on the seafloor, showing slightly higher concentrations at station 1I (ranging from 295 to 335 μM) compared to 1E (249–279 μM). During the 8-h sediment incubation at both sites (Fig. 6), O_2 concentration showed temporal little decrease/increase or nearly constant levels, suggesting that the production was balanced by respiration. The trends in DIC versus time (Fig. 6) showed some scatter but in both stations were fit with a linear decreasing trend-line showing a decoupling with O_2, probably due to nonphotosynthetic utilization of CO_2, chemosynthetic removal of O_2 (Johnson et al. 1981), and carbonate precipitation, as previously postulated for the sediments of the Gulf of Trieste and the Marano and Grado lagoons (De Vittor et al. 2012 and references therein).

DOC values, whose release should be compatible with DIC and O_2 based rates for net system production (Johnson et al. 1981), showed substantial differences between the two stations (Fig. 6) and resulted not related to O_2 and DIC changes. The lack of DOC/O_2 and DOC/DIC correlations during the incubation time suggests that DOC may originate more from OM aerobic degradation and from dissolved OM (perhaps humic substances) benthic release rather than from extracellular photosynthetates (Ogawa et al. 2003), even if the inverse correlation ($p<0.05$) with silicates found at 1I supported the hypothesis of a diatoms role in DOC release. Looking at the inorganic nitrogen pool (Fig. 6), the $N\text{-}NO_3^-$ levels were low, often close to 0.5 μM, which is considered limiting to phytoplankton growth (Fasham et al. 1990) but always higher (1–2 orders of magnitude) than $N\text{-}NO_2^-$ (whose concentration was negligible) at both the sites, ranging from 0.3 to 0.9 μM and from 0.7 to 2.0 μM, at 1E and 1I, respectively. The changes of $N\text{-}NO_3^-$ concentrations, which could be also attributed to benthic infauna causing either increases or decreases in nitrate release from the sediment, depending on the depth of their burrowing and their amount of irrigation activity (Fields et al. 2014), showed that at both sites, nitrate, although low in concentration, did not become completely consumed during incubations.

Ammonium concentrations ranged from 1.1 to 2.8 μM and from 1.0 to 1.7 μM at 1E and 1I, respectively (Fig. 6). Even if a significant correlation was not

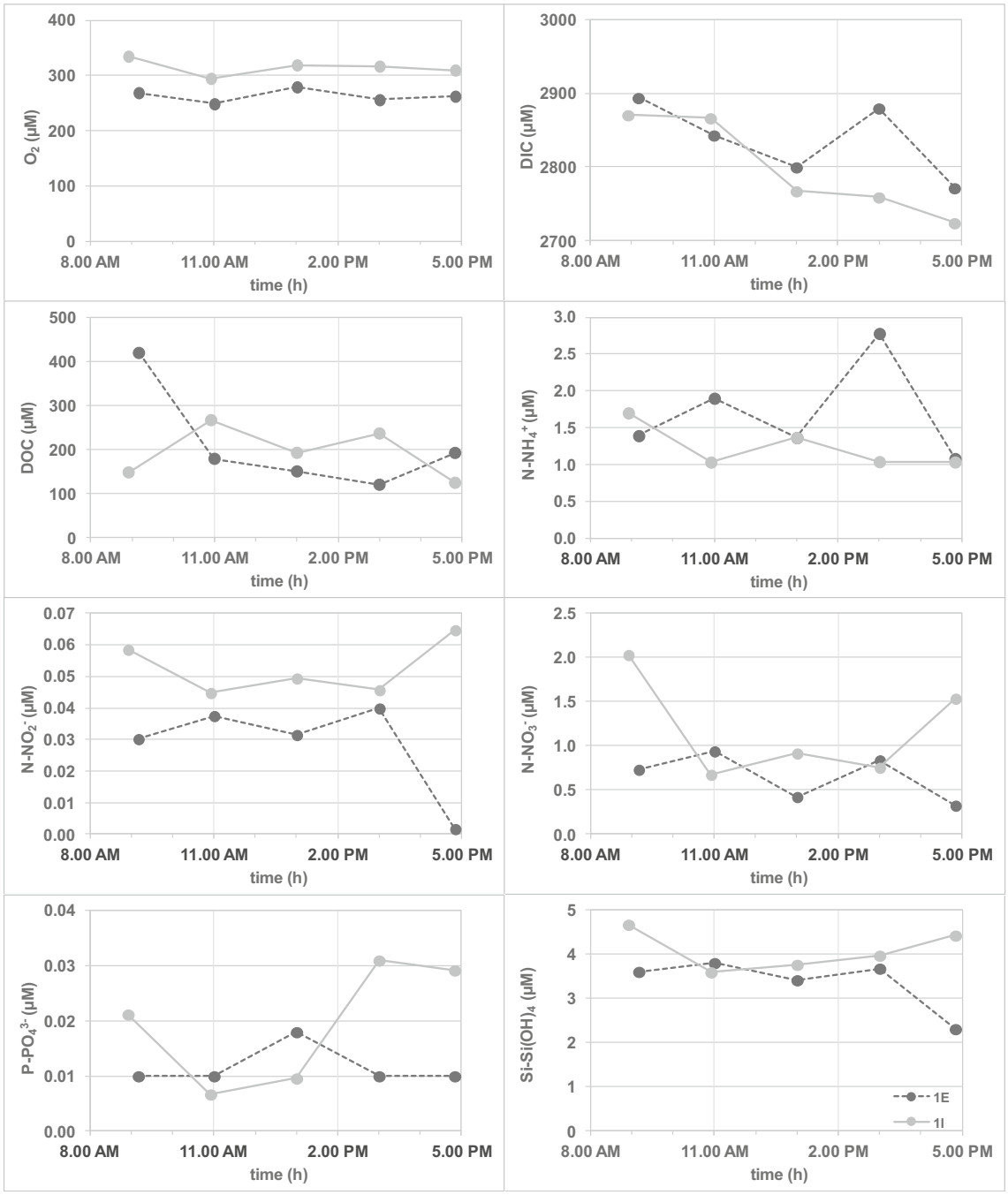

Fig. 6 Diurnal variations of O_2, DIC, DOC, and N, P, and Si nutrients in the benthic chambers at the study sites 1E and 1I

found at both sites, the variation of $N\text{-}NH_4^+$ inside the chambers followed that of nitrate, suggesting a simultaneous influence of denitrification (sediment)/nitrification (oxygenated water) processes and algal uptake.

$P\text{-}PO_4^{3-}$ concentrations (Fig. 6) were low at both stations (0.01–0.03 μM), suggesting that phosphate is the limiting nutrient for microalgal production. This hypothesis is supported by the high $DIN/P\text{-}PO_4^{3-}$ ratios, always higher than the Redfield ratio (De Vittor et al. 2012).

Silicate levels (Fig. 6) varied from 2.3 to 3.8 μM at 1E and from 3.6 to 3.8 μM at 1I. At both stations, silicate trends were highly correlated with nitrate ($p<0.05$ and $p<0.01$, at 1E and 1I, respectively), suggesting that benthic diatoms preferentially assimilate ammonium rather than nitrate. On the other hand, the fact that ammonium trends follow nitrate (even if not significantly related) suggests that nutrient fluxes are also controlled by external factors, such as the bioirrigation rate (Berelson et al. 2013).

In situ benthic fluxes

Fluxes calculated from chamber incubations, which represent the total fluxes (Rasheed et al. 2006) differed substantially from diffusive ones (Table 2). Unexpectedly, the flux of almost all analytes were negative, i.e., directed to the sediment porewater, with the only exceptions of P-PO_4^{3-} at both stations and N-NO_2^- at station 1I. This great difference suggests the enhancement of fluxes by bioturbation and that biogeochemically important processes occur at the SWI (De Vittor et al. 2012). Furthermore, total fluxes, in addition to diffusive fluxes, may include fluxes from advective porewater exchange (out of the chamber) although in mud sediments, like those of our study, this contribution can be minor (Rasheed et al. 2006). In our study, the discrepancy between benthic and diffusive fluxes is also due to the lack of data from overnight samples; thus, our calculations only reflect daylight processes without taking into account night respiration and fluxes, which generally differ substantially from the daylight ones. Several authors, in fact, have reported differences in night and day fluxes or during light and dark incubations (Rizzo 1990; Billerbeck et al. 2007; De Vittor et al. 2012; Dunn et al. 2013; Sospedra et al. 2015).

During the 8 h of diurnal incubation experiments, the oxygen uptake rate of −1.6 and −5.6 mmol $m^{-2}day^{-1}$ at sites 1E and 1I, respectively, showing daily net negative production, suggested that sediments were more heterotrophic at 1I, due to the increased respiratory demands for decomposition of the higher quantity of organic matter. On the other hand, the apparent community production measured from DIC reached highly negative values of −27.8 and −30.4 mmol $m^{-2}day^{-1}$, at 1E and 1I, respectively, thus suggesting that respiration processes exceeded the primary production but also that carbonate precipitation could have occurred.

The diurnal DOC influx was one order of magnitude higher at 1E (−51.8 mmol $m^{-2}day^{-1}$) than at 1I (−5.8 mmol $m^{-2}day^{-1}$), suggesting that larger amounts of DOC are removed at 1E, during daylight by biotic and abiotic pathways. For example, the photolysis of complex organic compounds may produce labile DOC from biologically less reactive riverine and marine DOC (Moran and Zepp 1997). On the other hand, the lack of new production of reactive DOC and different sources of organic matter, not equivalent in terms of biodegradability for heterotrophic bacteria, could have differently affected the functional performance of bacterial communities between the two stations. In addition, irrigation may be an important mass transfer process. Nevertheless, it seems that at both stations DOC utilization, within incubation time, exceeds DOC production. Differences between benthic and diffusive fluxes, which were directed out of the sediments, also suggest that the majority of porewater DOC was resistant towards microbial oxidative degradation and/or that porewater DOC differs in terms of molecular composition (i.e., different molecular weight with different diffusion coefficient) from bottom-water DOC; thus, the diffusive fluxes could have been overestimated.

Diurnal influxes of nitrate (nitrite fluxes were negligible) reached similar values at the two stations while the ammonium flux was double at station 1I. This behavior could be the consequence of intense autotrophic and heterotrophic assimilation but also of nitrification processes. Our data also support the idea that benthic microalgal community can function as a "filter" that controls the flux of dissolved nutrients at the sediment/water interface through assimilation and photosynthetic oxygenation of the sediment surface Sundbäck et al. (2000). Phosphate release, whose regeneration from sediments is a slow process (Liu et al. 2004) and whose exchanges are largely controlled by the oxygen status of the sediment (Rizzo 1990), was observed only at 1I probably due to degradation of higher content of sedimentary organic P. The measured influx of silicate was 6-fold greater at 1E suggesting a higher uptake by microphytobenthos as confirmed by the definitely higher abundance of benthic diatoms evidenced at this station (43,186±8861 cells cm^{-3} at 1E vs 9576±1732 cells cm^{-3} at 1I; Rubino et al. 2015). The differences in diffusive and benthic flux of silicate likely depend also on the remineralization of moribund, i.e., not actively photosynthesizing diatoms at the SWI (Warnken et al. 2007).

Summary and conclusion

1. In the Mar Piccolo of Taranto, the station 1I, placed just in front of the Navy Arsenal and more contaminated by anthropogenic activities, is characterized by more negative redox potential, higher biopolymeric carbon content (most of all lipids), and lower C/N ratios.
2. Steep near-surface gradients of porewater concentrations were observed for almost all analytes with stronger gradient again localized at 1I where diffusive fluxes were, with the exception of DOC and N-NO_2^-, always higher. These results highlight the role of the higher contaminated site in enhancing benthic fluxes.

PCA clearly emphasized the differences between impacted and control sites in relation of their different solid phase and porewater contents characteristics.

The higher content of DIC, nutrients, and H2S in the porewater of station 1I suggest the presence of higher diagenetic activities enhancing the release of this analytes which could result in a higher release of contaminants as already reported by several authors (Emili et al. 2012; Dang et al. 2014).

3. At both stations, diurnal benthic fluxes of O_2, DIC, DOC, N-NH_4^+, N-NO_3^-, and Si-$Si(OH)_4$ were negative while P-PO_4^{3-} efflux was negligible at 1E and low at 1I. Based on

oxygen diurnal influx, station 1I seems more heterotrophic with respect to 1E.

4. The low release of P-PO_4^{3-}, evidenced both by diffusive and benthic fluxes, suggests P to be a limiting nutrient for primary production in the Mar Piccolo of Taranto.

The great difference observed between diffusive and in situ benthic fluxes could be due to the lack of data from overnight samples during benthic incubation, but also suggests an important role of biological activity at or near the SWI.

5. The severe anthropogenic pressures suffered by the Mar Piccolo of Taranto (declared SIN in 1998), which caused a multi-contamination of both inorganic and organic pollutants in the sediments potentially transferable to the water column and to the aquatic trophic chain is of serious concern for its ecological relevance, also considering the widespread fishing and mussel farming activities in the area.

More research effort toward detailed analysis of the mobility and biogeochemical fate of dissolved porewater compounds in relation to contaminants (focusing in a larger study area and on seasonal variability) are needed to obtain a better understanding on the role of the sediment of the Mar Piccolo of Taranto as source of pollutants/nutrients toward the seawater column.

Acknowledgments The activities described in this publication were funded by the Project Bandiera RITMARE - La Ricerca Italiana per il Mare coordinated by the National Research Council and funded by the Ministry for Education, University and Research within the National Research Programme 2011–2013. The authors are warmly grateful to Nicola Cardellicchio and the team of the IAMC institute, section of Taranto, for their logistical support and hospitality. Thanks are due to M. Bussi and C. Landucci from DMG Trieste for their help in grain-size and CHN analyses and to T. Cibic for environmental data reported in Table 1. We are also grateful to three anonymous reviewers for their valuable suggestions.

References

Algeo TJ, Ingall E (2007) Sedimentary C_{org}:P ratios, paleocean ventilation and phanerozic atmospheric pO_2. Palaeogeogr Palaeocl 256: 130–155

Alperin MJ, Albert DB, Martens CS (1994) Seasonal variations in production and consumption rates of dissolved organic carbon in an organic-rich coastal sediment. Geochim Cosmochim Ac 58:4909–4930

Alperin MJ, Martens CS, Albert DB, Suayah IB, Benninger LK, Blair NE, Jahnke RA (1999) Benthic fluxes and porewater concentration profiles of dissolved organic carbon in sediments from the North Carolina continental slope. Geochim Cosmochim Ac 63:427–448

Al-Rousan S, Rasheed M, Badran M (2004) Nutrient diffusive fluxes from sediments in the northern Gulf of Aqaba, Red Sea. Sci Mar 68(4):483–490

Anschutz P, Chaillou G, Lecroart P (2007) Phosphorus diagenesis in sediment of the Thau Lagoon. Estuar Coast Shelf Sci 72:447–456

Aspila KI, Agemian H, Chau AS (1976) A semi-automated method for the determination of inorganic, organic and total phosphate in sediments. Analyst 101:187–197

Berelson WM, McManus J, Severmann S, Reimers CE (2013) Benthic flux of oxygen and nutrients across Oregon/California shelf sediments. Cont Shelf Res 55:66–75

Bertuzzi A, Faganeli J, Welker C, Brambati A (1997) Benthic fluxes of dissolved inorganic carbon, nutrients and oxygen in the Gulf of Trieste (Northern Adriatic). Water Air Soil Poll 99:305–314

Billerbeck M, Røy H, Bosselmann K, Huettel M (2007) Benthic photosynthesis in submerged Wadden Sea intertidal flats. Estuar Coast Shelf Sci 71:704–716

Blasutto O, Cibic T, De Vittor C, Fonda Umani S (2005) Microphytobenthic primary production and sedimentary carbohydrates along salinity gradients in the lagoons of Grado and Marano (Northern Adriatic sea). Hydrobiologia 550:47–55

Bligh EG, Dyer W (1959) A rapid method for total lipid extraction and purification. Can J Biochem Phys 37:911–917

Burdige DJ, Alperin MJ, Homstead J, Martens CS (1992) The role of benthic fluxes of dissolved organic carbon in oceanic and sedimentary carbon cycling. Geophys Res Lett 19:1851–1854

Cardellicchio N, Buccolieri A, Di Leo A, Spada L (2006) Heavy metals in marine sediments from the Mar Piccolo of Taranto (Ionian Sea, Southern Italy). Ann Chim-Rome 96:727–741

Cardellicchio N, Annicchiarico C, Di Leo A, Giandomenico S, Spada L (2015) The Mar Piccolo of Taranto: an interesting marine ecosystem for the environmental problems studies. Environ Sci Pollu R, in this issue

Caroppo C, Cardellicchio N (1995) Preliminary study on phytoplankton communities of Mar Piccolo in Taranto (Jonian sea). Oebalia 21:61–76

Caroppo C, Turicchia S, Margheri MC (2006) Phytoplankton assemblages in coastal waters of the northern Ionian Sea (eastern Mediterranean), with special reference to cyanobacteria. J Mar Biol Assoc UK 86:927–937

Cibic T, Franzo A, Celussi M, Fabbro C, Del Negro P (2012) Benthic ecosystem functioning in hydrocarbon and heavy-metal contaminated sediments of an Adriatic lagoon. Mar Ecol Prog Ser 458:69–87. doi:10.3354/meps09741

Cibic T, Bongiorni L, Borfecchia F, Di Leo A, Franzo A, Giandomenico S, Karuza A, Micheli C, Rogelja M, Del Negro P (2015) Ecosystem functioning nearby the largest steelworks in Europe and the main Italian naval base: the study case of the Mar Piccolo of Taranto. Environ Sci Pollu R, in this issue

Clavero V, Izquierdo JJ, Fernández NFX (2000) Seasonal fluxes of phosphate and ammonium across the sediment-water interface in a shallow small estuary (Palmones River, southern Spain). Mar Ecol Prog Ser 198:51–60

Covelli S, Faganeli J, Horvat M, Brambati A (1999) Porewater distribution and benthic flux of mercury and methylmercury in the Gulf of Trieste (northern Adriatic Sea). Estuar Coast Shelf Sci 48:415–428

Covelli S, Faganeli J, De Vittor C, Predonzani S, Acquavita A, Horvat M (2008) Benthic fluxes of mercury species in a lagoon environment (Grado Lagoon, northern Adriatic Sea, Italy). Appl Geochem 23: 529–546

Covelli S, Emili A, Acquavita A, Koron N, Faganeli J (2011) Benthic biogeochemical cycling of mercury in two contaminated northern Adriatic coastal lagoons. Cont Shelf Res 31:1777–1789

Dang DH, Lenoble V, Durrieu G, Mullot JU, Mounier S, Garnier C (2014) Sedimentary dynamics of coastal organic matter: an assessment of the porewater size/reactivity model by spectroscopic techniques. Estuar Coast Shelf Sci 151:100–111

De Vittor C, Faganeli J, Emili A, Covelli S, Predonzani S, Acquavita A (2012) Benthic fluxes of oxygen, carbon and nutrients in the Marano

and Grado lagoon (Northern Adriatic sea, Italy). Estuar Coast Shelf Sci 113:57–70

Dubois M, Gilles KA, Hamilton JK, Rebers P, Smith F (1956) Colorimetric method for determination of sugars and related substances. Anal Chem 28(3):350–356

Dunn RJK, Robertson D, Teasdale PR, Walthman NJ (2013) Benthic metabolism and nitrogen dynamics in an urbanized tidal creek: domination of DNRA over denitrification as a nitrate reduction pathway. Estuar Coast Shelf Sci 131:271–281

Emili A, Koron N, Covelli S, Faganeli J, Acquavita A, Predonzani S, De Vittor C (2011) Does anoxia affect mercury cycling at the sediment–water interface in the Gulf of Trieste (northern Adriatic Sea)? Incubation experiments using benthic flux chambers. Appl Geochem 26:194–204

Emili A, Acquavita A, Koron N, Covelli S, Faganeli J, Horvat M, Žižek S, Fajon V (2012) Benthic flux measurements of Hg species in a northern Adriatic lagoon environment (Marano & Grado Lagoon, Italy). Estuar Coast Shelf Sci 113:71–84

Emili A, Acquavita A, Covelli S, Spada L, Di Leo A, Giandomenico S, Cardellicchio N (2015) Water-sediment interactions controlling heavy metals mobility in a contaminated coastal environment (Taranto, Italy). Environ Sci Pollut R in this issue

Engelsen A, Hulth S, Pihl L, Sundbäck K (2008) Benthic trophic status and nutrient fluxes in shallow-water sediments. Estuar Coast Shelf Sci 78:783–795

Fabiano M, Danovaro R, Fraschetti S (1995) A three-year time series of elemental and biochemical composition of organic matter in subtidal sandy sediments of the Ligurian Sea (North-western Mediterranean). Cont Shelf Res 15:1453–1469

Fasham MJR, Ducklow HW, McKelvie SM (1990) A nitrogen based model of plankton dynamics in the oceanic mixed layer. J Mar Res 48:591–639

Fichez R (1991) Composition and fate of organic matter in submarine cave sediments; implications for the biogeochemical cycle of organic carbon. Oceanol Acta 14:369–377

Fields L, Nixon SW, Oviatt C, Fulweiler RW (2014) Benthic metabolism and nutrient regeneration in hydrographically different regions on the inner continental shelf of Southern New England. Estuar Coast Shelf Sci 148:14–26

Fonselius SH (1983) Determination of hydrogen sulphide. In: Grasshof K, Ehrhardt M, Kremling K (eds) Methods of seawater analysis, 2nd edn. Weinheim, Verlag Chemie, pp 73–80

Franzo A, Auriemma R, Nasi F, Vojvoda J, Pallavicini A, Cibic T, Del Negro P (2015) Benthic ecosystem functioning in the severely contaminated Mar Piccolo of Taranto (Ionian Sea, Italy): focus on heterotrophic pathways. Environ Sci Pollu R, in this issue

Gerchacov SM, Hatcher PG (1972) Improved technique for analysis of carbohydrates in sediments. Limnol Oceanogr 17:938–943

Goñi MA, Teixeira MJ, Perkey DW (2003) Sources and distribution of organic matter in a river-dominated estuary (Winyah Bay, SC, USA). Estuar Coast Shelf Sci 57:1023–1048

Grasshoff K, Ehrhardt M, Kremling K (1983) Methods of seawater analysis, 2nd edn. Weinheim, Verlag Chemie

Grenz C, Cloern JE, Hager SW, Cole BE (2000) Dynamics of nutrient cycling and related benthic nutrient and oxygen fluxes during a spring phytoplankton bloom in South San Francisco Bay (USA). Mar Ecol Prog Ser 197:67–80

Hansen HP, Koroleff F (1999) Determination of nutrients. In: Grasshoff K, Kremling K, Ehrhardt M (eds) Methods of seawater analysis, 3rd edn. Wiley-VCH, Weinheim, pp 159–228

Hartree EF (1972) Determination of proteins: a modification of the Lowry method that give a linear photometric response. Anal Biochem 48: 422–427

Hedges JI, Stern JH (1984) Carbon and nitrogen determinations of carbonate-containing solids. Limnol Oceanogr 29:657–663

Hyun JH, Kim SH, Mok JS, Lee JS, An SU, Lee WC, Jung RH (2013) Impacts of long-line aquaculture of Pacific oysters (*Crassostrea gigas*) on sulfate reduction and diffusive nutrient flux in the coastal sediments of Jinhae–Tongyeong, Korea. Mar Pollut Bull 74:187–198

Johnson KM, Burney CMMN, Sieburth J (1981) Enigmatic marine ecosystem metabolism by direct diel CO_2 and O_2 flux in conjunction with DOC release and uptake. Mar Biol 65:49–60

Kelly JR, Nixon SW (1984) Experimental studies of the effect of organic deposition on the metabolism of a coastal marine bottom community. Mar Ecol Prog Ser 17:157–169

Kralj M, De Vittor C, Comici C, Relitti F, Alabiso G, Del Negro P (2015) Recent evolution of the physical-chemical characteristics of a Site of National Interest - the Mar Piccolo of Taranto (Ionian Sea) - and changes over the last 20 years. Environ Sci Pollu R, in this issue

Liu SM, Zhang J, Li DJ (2004) Phosphorus cycling in sediments of the Bohai and Yellow Seas. Estuar Coast Shelf Sci 59: 209–218

Lojen S, Ogrinc N, Dolenec T, Vokal B, Szaran J, Mihelčić G, Branica M (2004) Nutrient fluxes and sulfur cycling in the organic-rich sediment of Makirina Bay (Central Dalmatia, Croatia). Sci Total Environ 327:265–284

Marsh JB, Weinstein WJ (1966) A simple charring method for determination of lipids. J Lipid Res 7:574–576

Matijević S, Kušpilić G, Kljaković-Gašpić Z (2007) The redox potential of sediment from the Middle Adriatic region. Acta Adriat 48(2): 191–204

Matijević S, Bogner D, Bojanić N, Žuljević A, Despalatović M, Antolić B, Nikolić V, Bilić J (2013) Biogeochemical characteristics of sediments under the canopy of invasive alga *Caulerpa racemosa* var. *cylindracea* (Pelješac peninsula, Adriatic Sea). Fresen Environ Bull 22(10a):3030–3040

McGlathery KJ, Anderson IC, Tyler AC (2001) Magnitude and variability of benthic and pelagic metabolism in a temperate coastal lagoon. Mar Ecol Prog Ser 216:1–15

McGlathery KJ, Sundbäck K, Anderson IC (2007) Eutrophication in shallow coastal bays and lagoons: the role of plants in the coastal filter. Mar Ecol Prog Ser 348:1–18

Metzger E, Simonucci C, Viollier E, Sarazin G, Prévot F, Jézéquel D (2007) Benthic response to shellfish farming in Thau lagoon: pore water signature. Estuar Coast Mar S 72: 406–419

Middelburg JJ, Levin LA (2009) Coastal hypoxia and sediment biogeochemistry. Biogeosciences 6:1273–1293

Moran MA, Zepp RG (1997) Role of photoreactions in the formations of biologically labile compounds from dissolved organic matter. Limnol Oceanogr 42:1307–1316

Neira C, Sellanes J, Soto A, Gutiérrez D, Gallardo VA (2001) Meiofauna and sedimentary organic matter off Central Chile: response to changes caused by the 1997–1998 El Niño. Oceanol Acta 24:313–328

Nixon SW, Oviatt CA, Garber J, Lee V (1976) Diel metabolism and nutrient dynamics in a salt marsh embayment. Ecology 57:740–750

Ogawa H, Usui T, Koike I (2003) Distribution of dissolved organic carbon in the East China Sea. Deep-Sea Res Pt II 5:353–366

Ogrinc N, Faganeli J (2006) Phosphorus regeneration and burial in near-shore marine sediments (the Gulf of Trieste, northern Adriatic Sea). Estuar Coast Shelf Sci 67:579–588

Ogrinc N, Faganeli J, Pezdic J (2003) Determination of organic carbon remineralization in near-shore marine sediments (Gulf of Trieste, Northern Adriatic) using stable carbon isotopes. Org Geochem 34: 681–692

Ortega T, Ponce R, Forja J, Gómez-Parra A (2008) Benthic fluxes of dissolved inorganic carbon in the Tinto-Odiel system (SW of Spain). Cont Shelf Res 28:458–469

Pastore M (1993) Mar Piccolo. Nuova Eolitrice Apulia, Martina Franca (In Italian)

Pastuszak M, Conley DJ, Humborg C, Witek Z, Sitek S (2008) Silicon dynamics in the Oder estuary, Baltic Sea. J Mar Syst 73:250–262

Petronio BM, Cardellicchio N, Calace N, Pietroletti M, Pietrantonio M, Caliandro L (2012) Spatial and temporal heavy metal concentration (Cu, Pb, Zn, Hg, Fe, Mn, Hg) in sediments of the Mar Piccolo in Taranto (Ionian Sea, Italy). Water Air Soil Poll 223:863–875

Pusceddu A, Sarà G, Armeni M, Fabiano M, Mazzola A (1999) Seasonal and spatial changes in the sediment organic matter of a semi-enclosed marine system (W-Mediterranean Sea). Hydrobiologia 397:59–70

Pusceddu A, Dell'Anno A, Fabiano M, Danovaro R (2009) Quantity and bioavailability of sediment organic matter as signatures of benthic trophic status. Mar Ecol Prog Ser 375:41–52

Pusceddu A, Bianchelli S, Canals M, Sanchez-Vidal A, De-Madron XD, Eussner S, Lykousis V, de-Stigter H, Trincardi F, Danovaro R (2010) Organic matter in sediments of canyons and open slopes of the Portuguese, Catalan, Southern Adriatic and Cretan Sea margins. Deep-Sea Res I 57:441–457

Ram A, Zingde MD (2000) Interstitial water chemistry and nutrients fluxes from tropical intertidal sediment. Indian J Mar Sci 29:310–318

Rasheed M, Al-Rousan S, Manasrah R, Al-Horani F (2006) Nutrient fluxes from deep sediment support nutrient budget in the oligotrophic waters of the Gulf of Aqaba. J Oceanogr 62:83–89

Ren H, Brunelle BG, Sigman DM, Robinson RS (2013) Diagenetic aluminum uptake into diatom frustules and the preservation of diatom-bound organic nitrogen. Mar Chem 155:92–101

Rice DL (1982) The detritus nitrogen problem: new observations and perspectives from organic geochemistry. Mar Ecol Prog Ser 9: 153–162

Rizzo WM (1990) Nutrient exchange between the water column and the subtidal benthic microalgal community. Estuaries 13:219–226

Rubino F, Cibic T, Belmonte M, Rogelja M, Del Negro P (2015) The microbenthic community structure and the trophic status of sediments in Mar Piccolo of Taranto (Ionian Sea). Environ Sci Pollu R, in this issue

Santos-Escheandia J, Prego R, Cobelo-García A, Millward GE (2009) Porewater geochemistry in a Galician Ria (NW Iberian Peninsula): implications for benthic fluxes of dissolved trace elements (Co, Cu, Ni, Pb, V, Zn). Mar Chem 117:77–87

Sospedra J, Falco S, Morata T, Gadea I, Rodilla M (2015) Benthic fluxes of oxygen and nutrients in sublittoral fine sands in a north-western Mediterranean coastal area. Cont Shelf Res 97:32–42

Spada L, Annicchiarico C, Cardellicchio N, Giandomenico S, Di Leo A (2012) Mercury and methylmercury concentrations in Mediterranean seafood and surface sediments, intake evaluation and risk for consumers. Int J Hyg Envir Heal 215:418–426

Spagnoli F, Bergamini MC (1997) Water-sediment exchange of nutrients during early diagenesis and resuspension of anoxic sediments from the Northern Adriatic Sea shelf. Water Air Soil Poll 99:541–556

Sugimura Y, Suzuki Y (1988) A high temperature catalytic oxidation method for the determination of non-volatile dissolved organic carbon in seawater by direct injection of liquid sample. Mar Chem 24: 105–131

Sundbäck K, Miles A, Göransson E (2000) Nitrogen fluxes, denitrification and the role of microphytobenthos in microtidal shallow-water sediments: an annual study. Mar Ecol Prog Ser 200:59–76

Sundby B, Gobeil C, Silverberg N, Mucci A (1992) The phosphorus cycle in coastal marine sediments. Limnol Oceanogr 37(6):1129–1145

Ullman WJ, Aller RC (1982) Diffusion coefficients in nearshore marine sediments. Limnol Oceanogr 27:552–556

Warnken KW, Santschi PH, Roberts LA, Gill GA (2007) The cycling and oxidation pathways of organic carbon in a shallow estuary along the Texas Gulf Coast. Estuar Coast Shelf Sci 76(1):69–84

Zhang L, Wang L, Yin K, Lü Y, Zhang D, Yang Y, Huang X (2013) Pore water nutrient characteristics and the fluxes across the sediment in the Pearl River estuary and adjacent waters, China. Estuar Coast Shelf Sci 133:182–192

CHAPTER 3

Recent evolution of the physical–chemical characteristics of a Site of National Interest—the Mar Piccolo of Taranto (Ionian Sea)— and changes over the last 20 years

Martina Kralj[1*], Cinzia De Vittor[1], Cinzia Comici[1], Federica Relitti[1,2], Rocco Auriemma[1], Giorgio Alabiso[3], Paola Del Negro[1]

[1] Oceanography Division, OGS (Istituto Nazionale di Oceanografia e di Geofisica Sperimentale), Trieste, Italy

[2] Department of Life Science, University of Trieste, Trieste, Italy

[3] Consiglio Nazionale delle Ricerche, Istituto Ambiente Marino Costiero (IAMC)

[*]**Corresponding author: Martina Kralj**

OGS (Istituto Nazionale di Oceanografia e di Geofisica Sperimentale), Oceanography Division

Via A. Piccard 54, 34151 Trieste, Italy

Tel.: +39 040 2249746

email: mkralj@inogs.it

Published in Environmental Science and Pollution Research

DOI 10.1007/s11356-015-5198-8

Environ Sci Pollut Res (2016) 23:12675–12690
DOI 10.1007/s11356-015-5198-8

Recent evolution of the physical–chemical characteristics of a Site of National Interest—the Mar Piccolo of Taranto (Ionian Sea)—and changes over the last 20 years

Martina Kralj[1] · Cinzia De Vittor[1] · Cinzia Comici[1] · Federica Relitti[1,2] · Rocco Auriemma[1] · Giorgio Alabiso[3] · Paola Del Negro[1]

Received: 9 April 2015 / Accepted: 10 August 2015 / Published online: 26 August 2015

Abstract The Mar Piccolo of Taranto, classified as a 'Site of National Interest' (SIN), is a semi-enclosed basin divided into two inlets with lagoon features and sea influences, seriously affected by anthropic activities. In the framework of the RITMARE project, a study has been carried out to evaluate the functionality of this ecosystem. As part of this work, measurements of the water abiotic parameters were performed in order to assess the physical–chemical features of this area after the activation, in the last decade, of treatment plants for various urban and industrial dumping. Seawater intrusions and continental inputs, as well as several submarine freshwater springs, clearly affect physical–chemical characteristics of the water column in the two inlets. This finding suggests that small-scale patterns in water circulation have the potential to influence the chemical properties of the seawater. The comparison with a 20-year dataset reveals a drastic decrease in nutrient concentrations after the year 2000, validating the functionality of the treatment plants. The reduction of nutrient inputs into the basin (up to −90 % in the first inlet characterized by lower hydraulic residence time) has changed the biogeochemical characteristics of the Mar Piccolo from being relatively eutrophic to moderately oligotrophic.

Responsible editor: Philippe Garrigues

✉ Martina Kralj
mkralj@ogs.trieste.it

[1] Sezione Oceanografia, OGS (Istituto Nazionale di Oceanografia e Geofisica Sperimentale), Via A. Piccard 54, 34151 Trieste, Italy

[2] Department of Life Sciences, University of Trieste, Via L. Giorgieri 10, 34127 Trieste, Italy

[3] Consiglio Nazionale delle Ricerche, Istituto Ambiente Marino Costiero (IAMC), Via Roma 3, 74123 Taranto, Italy

Keywords Mar Piccolo of Taranto · Site of National Interest · Long-term monitoring · Nutrients · Chlorophyll *a* · Dissolved and particulate carbon

Introduction

Coastal areas, lagoons and transitional areas form unique transitional systems as they are closely linked to both marine and terrestrial factors. The increase of municipal and industrial waters discharge, as consequence of the growth of human population and the development of agriculture, aquaculture and industrial activities, has led to environmental degradation to both water column and benthic habitats in these fragile areas. One of the worldwide largest issues caused by the increase of anthropogenic inputs is eutrophication, especially in areas with limited water exchange and restricted flushing, as estuaries (Cerco and Noel 2007; Mallin et al. 2005; Lopes et al. 2007), salt marshes and lagoons (Magni et al. 2008; Souchu et al. 1998; Velasco et al. 2006). Several studies have provided evidence of the sensitivity of marine systems to changes in nutrient loading and it has been highlighted that the intensity and frequency of eutrophication-related water quality problems are often (but not always) correlated with the supply rates of N and P to the receiving waters (Smith et al. 2006 and references therein). As reported for various coastal systems within the past four decades (Pinckney et al. 2001; Kemp et al. 2005; Cloern and Dufford 2005), also many Italian estuarine and coastal waters have changed from balanced and productive ecosystems to ones experiencing sudden trophic changes, biochemical alterations and a deterioration in the quality of natural habitats.

The identification of this problem has prompted management of discharges, through the construction, implementation or relocation (e.g. in the New River Estuary, North Carolina,

Mallin et al. 2005; in Massachusetts Bay, Oviatt et al. 2007; in the Boston Harbor, Taylor et al. 2011) of treatment plants and has allowed the reduction of organic matter and nutrient inputs (Conley et al. 2002).

This is the case of the area of Taranto, which during the 1960s was inundated by an intense industrialization process, with the construction of a large industrial district that completely changed the inner natural marine and land environment. The Mar Piccolo basin, in addition to the inlets of waters from the inland high-cultivated region and the municipality sewage pipes, became affected by numerous industrial and military wastewater discharges. Also the extensive fishing and aquaculture (Cardellicchio et al. 2006), in particular mussel culture, have led to the reduction of the environmental quality. Indeed, Mar Piccolo houses the biggest mussel farm in Italy, with plants widely distributed in both the inlets covering the 61 % of the total surface producing about 30,000 tons year^{-1} (Cardellicchio et al. 2015). Even if the extensive mussel cultivation is considered to have low impacts compared to fish farming, as it does not require any inputs of feeds, and bivalves can act as a buffer against eutrophication processes by controlling the phytoplankton biomasses, the intense filtration, coupled with the production and the subsequent deposition of faeces and pseudofaeces, increases inputs of labile organic matter to the superficial sediment. This organic matter load, which can be two to three times higher underneath the mussel farm compared to ambient outside the farm, fuels mineralisation processes, stimulating both aerobic and anaerobic metabolism, and nutrient recycling back to the water column by enhancing benthic fluxes (Nizzoli et al. 2005; Souchu et al. 2001; Christensen et al. 2003). Furthermore, the use of the waters in the cooling system of the steel factory quickened the circulation and reduced the flushing times of the waters in the basin to 2–3 weeks and increased the salinity due to the input of waters from the Mar Grande (Caroppo et al. 2012; Umgiesser et al. 2007). These numerous anthropogenic activities influenced the biogeochemical characteristics of waters and sediments, making the area seriously polluted by heavy metals and organics (Cardellicchio et al. 2007; Petronio et al. 2012). Moreover, the increase in the rate of supply of organic matter, the nutrients loading and the scarce hydrodynamism (De Serio et al. 2007) determined strong eutrophication events in the area (Alabiso et al. 1997, 2005; Caroppo and Cardellicchio 1995).

In 1998, with the Italian Legislative decree 426, the area of Mar Piccolo was declared a Site of National Interest for its high pollution. Under this initiative, the Italian Government enacted laws, in September 2001, in order to plan the remediation and environmental cleaning up. Since then, 7 of the 14 municipal discharges were fitted out with treatment plants or relocated to the Gulf of Taranto, with the consequent lowering of nutrient discharges and the improvement of the water quality.

Numerous studies have been done on the Mar Piccolo basin to estimate the impact of the anthropic activities on its physical–chemical characteristics up to the year 2009 (Alabiso et al. 1997, 2005, 2006; Caroppo and Cardellicchio 1995; Cavallo et al. 1999; Giacomini and Alabiso 2006; Umgiesser et al. 2007; Zaccone et al. 2005).

In order to evaluate the effectiveness of the treatment plants and the relocation of the sewage discharges for the reduction of eutrophication and the improvement of water quality of the Mar Piccolo of Taranto, two surveys in 2013 and two in 2014 have been performed, and data obtained were compared with a 20-year dataset. The aim was to achieve an overall physical–chemical evaluation of the environmental conditions of this area, useful for the planning of integrate long-term remediation actions required by the Water Framework Directive (WFD 2000/60/EC), which addresses all surface waters and groundwaters, and the Marine Strategy Framework Directive (MSFD 2008/56/EC), which establishes a framework for marine environmental policy.

Materials and methods

Study site

The Mar Piccolo of Taranto is an inner and semi-enclosed shallow sea located in the northern area of the Taranto Town (Fig. 1). It has a surface area of 20.72 km^2 and is divided by a promontory in two smaller basins named First and Second Inlet (FI and SI). The area is characterized by shallow waters; maximum depths are reached in the centre of the FI (15 m) and in the central part of the SI (10 m) (Pastore 1993).

The FI is directly connected with Mar Grande through two connection channels: the Navigabile channel and the Porta Napoli channel. The fluxes of water through these inlets are generally weak and depend on the difference of density between the two basins. Most of the water inputs derive from numerous small surface watercourses and 34 submarine freshwater springs, called ‘Citri’, which influence the salinity and the temperature of both inlets (Vatova 1972). The two most important ‘Citri’ for the freshwater discharges are Citro Galeso in the FI (0.6 m^3 s^{-1}) and Citro Copre in the SI (0.1–1.2 m^3 s^{-1}) (Umgiesser et al. 2007). As more than 80 % of the province of Taranto is used for farming, in particular for the cultivation of wheat, cereal crops and fodder (Calabrese et al. 2014), freshwater inputs carry chemicals drained from the surrounding agricultural soils in the basin (Caroppo et al. 2008; Di Leo et al. 2010). Furthermore, until the year 2000, the discharges of 14 sewage pipes from the nearby towns amounted to 0.21 m^3 s^{-1}, whereof 85 % in the SI (Caroppo et al. 2008).

The basin is generally characterized by low velocity currents (about 5–10 cm s^{-1}) driven by the sea tides, with the

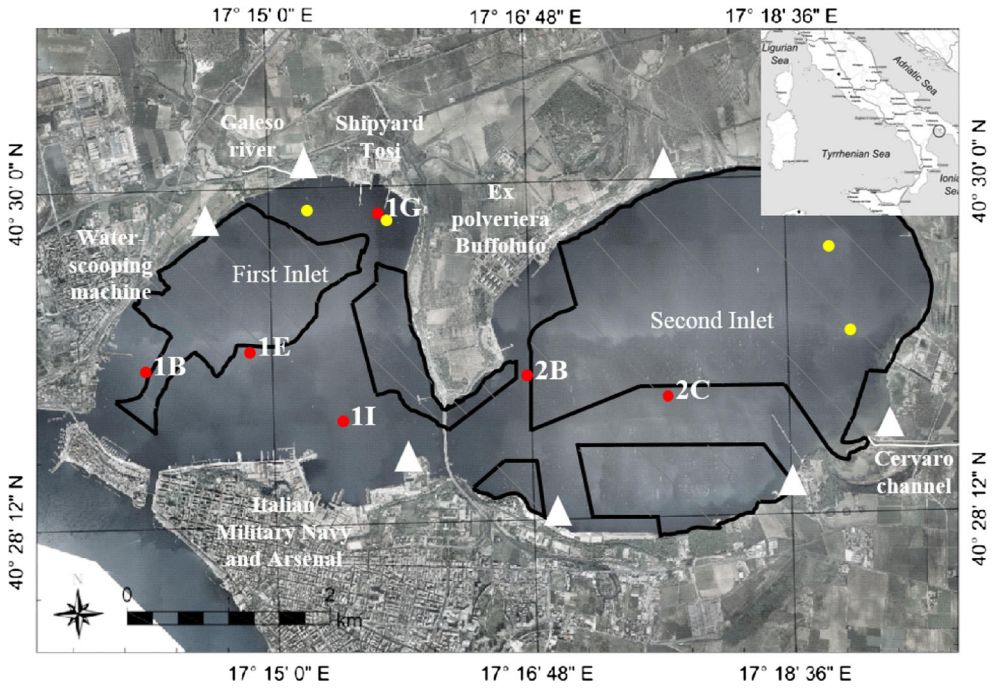

Fig. 1 Study area and location of stations sampled during 2013–2014 in the Mar Piccolo of Taranto. *White triangles* represent the active sewage outfalls, *yellow circles* are the principals freshwater springs 'Citri' and the *black lines* define the mussel farming areas. *Red circles* represent 2013-2014 sampling stations

maximum reached in the two connecting channels with the Mar Grande (up to 30–40 cm s^{-1}) (Umgiesser et al. 2007). From modelling studies (De Pascalis 2013), the dominant currents in the Mar Piccolo show two different components at surface and at 6 m depth. At surface (−1 m), the dominant current flux flows from the SI to the FI and discharges in the Mar Grande through the Navigabile and Porta Napoli channels. This flow generates clockwise currents inside both inlets. On the other hand, at 6 m depth, the current from the Mar Grande flows across the two channels into the FI and then enters in the SI.

The two inlets are characterized by different levels of confinement (Alabiso et al. 2006), i.e. by a different degree of connection to the sea and of sea water renewal time (Melaku Canu et al. 2012). In particular, the SI, due to the limited hydrodynamism and the low water exchange with the nearby Mar Grande, represents the most confined part of the system (Cardellicchio et al. 2007). The morphological characteristic of this inlet, together with the human activities, could be the reason of the reported increase of the fluctuation of nutrients, high water stratification in summer and hypoxia in the lower water layers (Alabiso et al. 2006; Caroppo et al. 2008).

Sampling strategy and analysis

Water samples were seasonally collected in June and October 2013 and in February and April 2014 at six different stations (Fig. 1). Sampling sites were chosen in order to better characterize the different areas of the subbasins. Four stations were located in the First Inlet: 1B, between the channels that connect the Mar Piccolo with the Mar Grande and the area of the cooling water intake (water-scooping machine); 1E, in the middle of the basin; 1G, near the freshwater submarine springs, Galeso River discharges and the former shipyard 'Tosi'; 1I, between the Navy Arsenal and Italian Military Navy and the connection with the Second Inlet. In the Second Inlet, two stations were sampled: the first near the Punta Penna Bridge at ex Polveriera Buffoluto (2B) and the second in the centre of the basin in correspondence of a long-term monitoring site (2C).

Depth profiles of temperature, salinity, oxygen concentration and saturation were recorded by a Sea Bird SBE 19 Plus Seacat multiparametric probe in June 2013 and April 2014, and with a Idromar IP050D multiparametric probe in October 2013. Unfortunately, during February 2014 survey, due to technical problems with multiparametric probes, depth profiles of the hydrological parameters were not recorded. Salinity (at surface and bottom of the six stations) and temperature (at the surface and bottom of stations 1B, 1I and 2C) were immediately measured on board on seawater samples with the conductivity method (CDM83 conductivity meter from Radiometer Copenhagen) while oxygen data are missing.

During each survey, discrete water samples were collected at surface (−1 m) and at bottom, using 5-L Niskin bottles. Subsamples were analysed for dissolved inorganic nutrients (nitrite N-NO_2, nitrate N-NO_3, ammonium N-NH_4, phosphate P-PO_4 and silicate Si-Si$(OH)_4$), dissolved organic and inorganic carbon (DOC, DIC), particulate organic carbon and particulate nitrogen (POC and PN), chlorophyll *a* and phaeopigments (chl-*a* and phaeo).

Samples for DIC analyses were collected minimizing gas exchange with atmosphere, treated with a mercuric chloride

solution in order to prevent biological activity and stored refrigerated until analyses. Samples for dissolved inorganic nutrients and DOC were filtered on board on pre-combusted Whatman GF/F filters and kept frozen (−20 °C) until laboratory analysis. Dissolved inorganic nutrients were determined with a segmented flow Bran+Luebbe AutoAnalyzer 3 following standard colorimetric methods (Hansen and Koroleff 1999). The detection limits of nutrient concentrations reported by the analytical methods are 0.02, 0.02, 0.04, 0.02 and 0.02 μM, respectively, for $N\text{-}NO_2$, $N\text{-}NO_3$, $N\text{-}NH_4$, $P\text{-}PO_4$ and $Si\text{-}Si(OH)_4$. The accuracy and precision of the analytical procedures at low concentrations are checked annually through the quality assurance programme QUASIMEME and the relative coefficient of variation for five replicates was less than 5 %. Internal quality control samples were used during each analysis.

DIC and DOC were determined using the Shimadzu TOC-V CSH analyser. For DIC, samples were injected into the instrument port and directly acidified with phosphoric acid (25 %). For DOC analysis, water samples were previously acidified (automatically into instrument syringe, 2 %–6 M HCl) and after CO_2 elimination, the concentration was determined using a high temperature catalytic method (Sugimura and Suzuki 1988). Phosphoric acidification for DIC and combustion conducted at 680 °C on a catalyst bed for DOC, generated CO_2 that was carried to a non-dispersive infrared detector (NDIR). Analysis from a minimum of three injections showed a variation coefficient <2 % and the reproducibility of the method tested with replicate field sampling was between 1.5 and 3 %. DOC results are periodically referenced against the international community of DOC analysts by using consensus reference material (CRM—University of Miami). The instrumental limit of detection (with high sensitivity measurement kit) is 0.33 μM, while it was 1–2 μM defined from measurement of certificated low carbon water (University of Miami) treated in the same way as samples. Analytical results from certified reference seawater of Quasimeme Laboratory Performance Study indicated a good agreement between determined concentrations and the certified values.

Subsamples for chlorophyll *a* analysis were stored in the dark and kept at 4 °C until filtration through 47 mm Whatman GF/F filters that were then stored frozen (−20 °C) until laboratory analysis. Pigments were extracted overnight (4 °C) with 90 % acetone from the homogenate filter and determined spectrofluorometrically according to Lorenzen and Jeffrey (1980). The measurements of chl-*a* and phaeo were performed, respectively, before and after acidification with two drops of HCl 1N using JASCO FP 6500 spectrofluorometer. The coefficient of variation for three replicate samples was lower than 5 %, and the detection limit, defined as twice the standard deviation of three blank filters treated in the same way as samples, was 0.002 and 0.068 μg L^{-1} for chl-*a* and phaeo, respectively. The procedures were quality controlled and monitored by participation in the QUASIMEME intercalibration programme.

POC and PN were measured using an elemental analyser CHNO-S Costech mod. ECS 4010 applying the methods performed by Pella and Colombo (1973) and Sharp (1974). Two subsamples of about 0.5 L each were filtered on 25-mm Whatman GF/F pre-combusted filters and were stored frozen at −20 °C. Before analysis, the filter was treated with the addition of 200 μl of HCl 1N to remove the carbonate and then dried in oven at 60 °C for about 1 h with the similar method of Lorrain et al. (2003). Before the analysis, the filter was inserted in a 10×10-mm tin capsule. Known amounts of standard acetanilide (C_8H_9NO—Carlo Erba; assay≥99.5 %) were used to calibrate the instrument. The detection limit for PN and POC, defined as twice the standard deviation of the blank (5–10 blank 25-mm filters), were 0.01 μmol-N L^{-1} and 0.001 μmol-C L^{-1}, respectively. The relative standard deviations for three replicates of internal quality control sample replicates were lower than 10 %. The accuracy of the method is verified periodically against the certified marine sediment reference material PACS-2 (National Research Council Canada).

Historical datasets (1991–2009)

The data obtained during the four-season surveys in the years 2013–2014 were compared with older data collected in the area in the periods between 1991 and 2009. This historical data are available from separate datasets deriving from different projects (with different sampling points) on hydrobiochemical and plankton distribution in the Mar Piccolo.

- March 1991–February 1992, surface and bottom monthly data from one station in each inlet of the basin (Caroppo and Cardellicchio 1995).
- June 1993–July 1994, monthly surface data from four stations in the FI and three stations in the SI (Alabiso et al. 1997).
- January 1996–December 2004, surface and bottom data at seven stations (four in the FI and three in the SI) (Alabiso et al. 2005, 2006; Giacomini and Alabiso 2006).
- January 2005–October 2009, surface samples of the same seven stations (Alabiso, unpublished data)

As, starting from 2000, the number of sewage pipes has been progressively reduced (Caroppo et al. 2010), the whole dataset was subdivided in two sampling periods: 1991–2000 and 2001–2009. Only the surface data were considered in the elaboration of the dataset because there was too little data from bottom depth.

The monthly evolution of the two groups of data for each inlet is represented by a graphical depiction, using box and whisker plots. This kind of plot represents the distribution of

data around the median, symbolized by the central line, the box gives the interval between 25 and 75 % percentiles, the segment indicates the range and the points the outliers. For the 2013–2014 dataset, the surface data were averaged for each inlet and graphically drawn as red diamonds in the second group of data.

Data elaboration and statistical analyses

Graphical representations and statistical analyses were performed using Golden Software Grapher 9, R statistical software (R Development Core Team 2011) and Primer-E Software package v7.0 (Plymouth Marine Laboratory, UK) according with Clarke and Warwick (2001). Different statistical analyses were performed on data in order to define trends and significant differences in the study area among the investigated periods and between inlets. The normality of the data was assessed with the Shapiro–Wilk test. Due to their non-normal distribution, a non-parametric approach was adopted. Spearman rank correlation analyses were performed on all the measured parameters, in order to examine significant relationships between the variables. Statistically significant differences among surveys and inlets for each parameter were tested with the ANOVA Kruskal–Wallis rank sum test. Principal component analysis (PCA), used to investigate patterns in the relative common variables over the stations and to compare the present situation with the former datasets, was performed on normalized variables after z-standardization. Tests for significant differences between the inlets and the surveys for the monitored variables were performed using the two-way crossed analysis of similarities (ANOSIM) test, which was performed considering all the studied variables, except for the parameters "Depth" and "Temperature" which could influence the statistics.

In order to assess the differences in water characteristics in response to the implementation of the treatment plants, a ANOSIM test was performed. The statistics was applied for the evaluation of the differences between the period 1991–2000 and 2001–2009 and between these two datasets and the data collected on 2013–2014.

R statistics for PCA and ANOSIM were interpreted according to Clarke and Warwick (2015): $R<0.25$=no differences in variables pattern; $0.25<R<0.50$=variables among the stations are overlapping but differ to a certain degree; $R>0.50$=parameters among the stations are different.

Results

Hydrology

Even if some data from February 2014 survey are lacking, general trends of hydrological parameters can be inferred. During 2013–2014, temperature, as expected, showed a marked dependency on seasonal conditions (Fig. 2). Surface maxima were registered in June in the SI (24.25±0.98 °C) while at the bottom the highest temperatures were measured, at both inlets, in October (23.91±0.33 °C). Minima were reached, at both inlets, in February, with values of 12.09± 0.14 and 13.06±0.22 °C, at surface and bottom, respectively. In June, the water column was generally characterized by thermal stratification favoured by the increasing air temperature, with surface values in the FI lower than in the SI, and similar temperature at the bottom waters of both inlets. In the same month, the maximum surface–bottom gradient (2.5 °C) was registered at the SI. During October, a seasonal reverse thermocline developed in both inlets at depths varying from 4 to 7 m. In April, a strong decrease of temperature was detected in both inlets, and the water column resulted quite homogeneous but SI showed weakly higher values than FI.

At each survey, vertical profile of salinity (only surface and bottom data for February survey) showed a positive surface–bottom gradient (Fig. 2). Both at surface and bottom, the maximum of salinity was reached in October (37.60 and 39.04, respectively) and the minimum in February (34.32 and 35.71, respectively).

In June, due to the different influence of freshwater springs in the area, the two inlets were characterized by a wide range of salinity values and by marked stratification. The halocline depth was quite variable: from 3 to 8 m, in the FI, and at 4 m, in the SI. In October, the first 4–5 m of the water column was homogenous (~37.5), while the variability persisted in the deeper waters, where the halocline was still present. In February, the surface mean salinity lowered to 35.12±0.68 with the minimum at St. 1E and the maximum at St. 1I. The bottom average salinity was 37.10±1.07, with the minimum in the St. 1G and the maximum in 1I. Water column stratification weakened in April when, with the exception of St. 1B (S=35.10), the surface salinity averaged 35.69±0.13, even if vertical profiles showed a slight increase.

In June, dissolved oxygen (DO) concentrations (Fig. 2) varied from ~5 to ~6 mL L^{-1} with the exceptions of the strong depletion evidenced at surface of St. 1B (3.99 mL L^{-1}) and of the strong increase up to 7.79 mL L^{-1} in the deeper layer of St. 2B. In October, the two inlets were definitely more oxygenated with DO mean concentrations of 7.43±1.29 mL L^{-1}. Vertical profiles resulted homogeneous in all stations with the only exception of the St. 1I, characterized by waters enriched in DO at surface and depleted at bottom. In April, the study area showed a general decrease in DO concentrations widely ranging from 4.80 mL L^{-1}, at surface of St. 1G, to 7.03 mL L^{-1} at bottom of St. 2B. No occurrence of anoxia was evidenced during the studied period. Unfortunately,

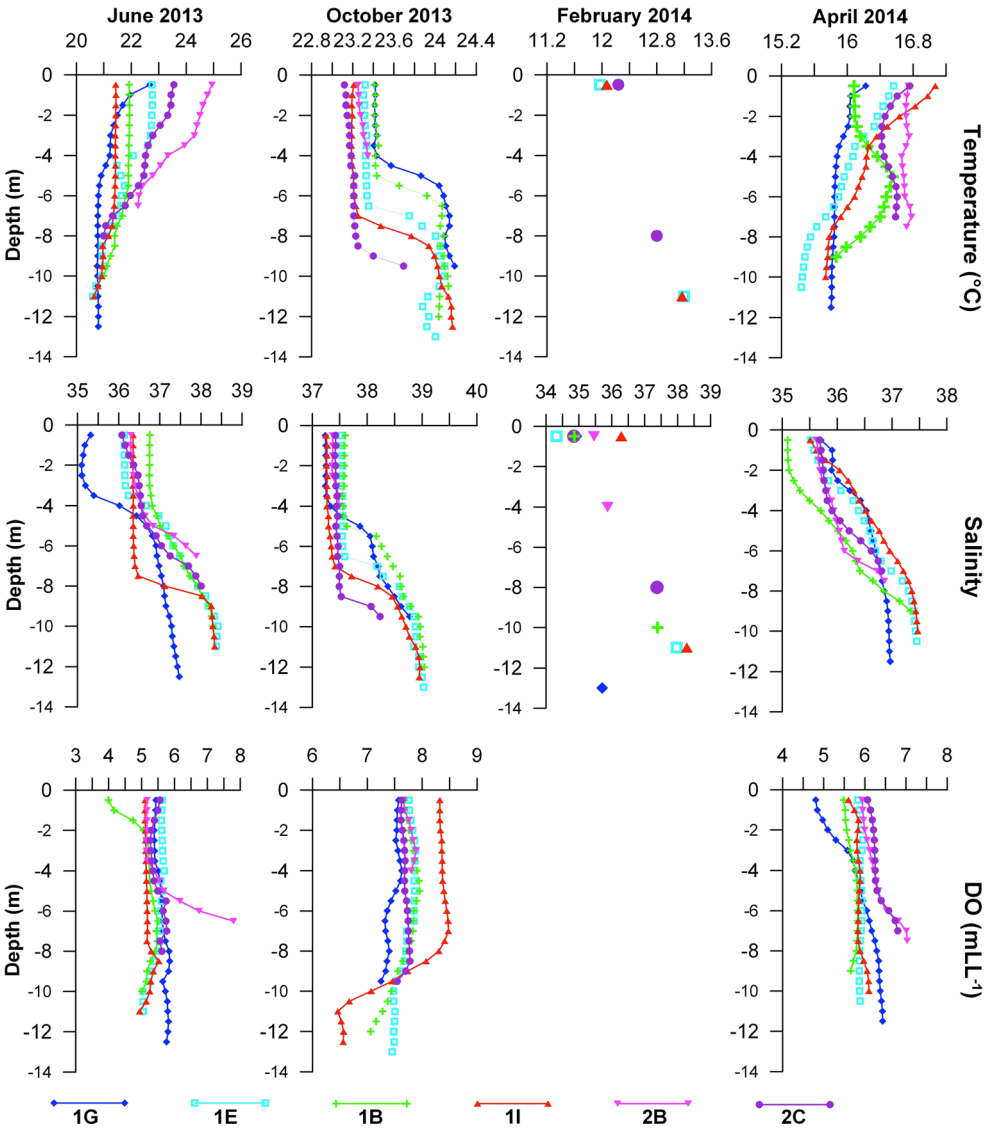

Fig. 2 Physical–chemical profiles of temperature, salinity and dissolved oxygen (DO) in the Mar piccolo of Taranto during June and October 2013 and February and April 2014

dissolved oxygen (DO) data are not available for the February 2014 survey.

Analysis of the former data sets showed a clear seasonal pattern with winter temperature, salinity and oxygen minima and summer maxima both during 1991–2000 and 2001–2009. This temporal evolution was observed at both inlets (Fig. 3). The dataset 2001–2009 was characterized by a large number of outliers in respect to the other group of data. No significant difference in temperature was observed at both inlets between the two considered periods, while the salinity showed significant differences ($p<0.05$) evidencing a general increase, in the second period, especially during summer. For oxygen, too little data were available before the 2001, therefore, the data are represented as a line. Observing the two graphical representations, no clear differences appeared, except for the month of December, characterized by a higher oxygen saturation, after 2000.

Biogeochemical properties of the water column

Seasonal variations of biogeochemical parameters measured during 2013–2014 are graphically shown in Figs. 4 and 5. DOC data are available only for June 2013 and April 2014. On average, concentrations were more heterogeneous and higher during June (119±19 μM) with a peak in St. 1G reaching 155 μM. The highest values, however, were observed in St. 2C in April (164 and 145 μM, at surface and at bottom, respectively) even if, excluding this station, the study area was characterized by a great homogeneity in DOC distribution and, on average, lower values (88±9 μM).

The distribution of DIC was similar in June, February and April with values ranging from 2648 to 2961 μM, while in October, higher values were detected in the whole study area (3289±90 μM). During all surveys, the highest concentrations were observed at surface in relation to the salinity minima. POC and PN spatial and temporal patterns were highly

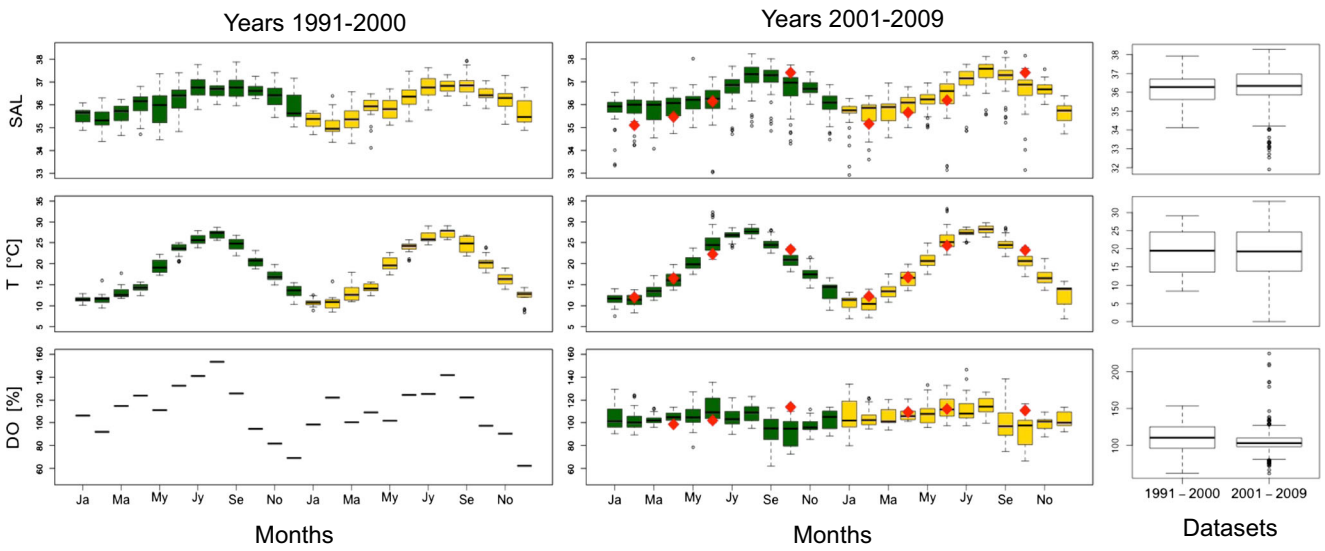

Fig. 3 Box and whiskers plots showing the variability of the monthly values of salinity, temperature and oxygen (SAL, T, DO) in the two different periods (1991–2000 and 2001–2009) at the surface water of the First (*green*) and Second Inlet (*yellow*). On the right, box and whiskers plots showing the variability of the two sets of historical analysed data. *Boxes* represent the interquartile range (25th to 75th percentile), the *horizontal line* is the median, the *ends of the whiskers* are the 5th and 95th percentiles and the *points* are the outliers. *Red diamonds* represent average values of 2013–2014 data

variable with concentrations ranging from 7.87 to 24.06 μM and from 1.02 to 3.52 μM, respectively (Fig. 4). In general, maxima of both parameters were observed in October, while minima were reached in February. The high correlation ($p<0.05$) found between POC and PN indicates a common source of C and N for the entire study area. The average molar ratio of Corg/Ntot (6.94±0.62) (Table 1) was very close to the Redfield ratio and inversely related with DOC ($p<0.05$) suggesting a more autochthonous marine origin of organic matter. The highest values of the ratio (>8) were measured at surface waters of stations more subject to continental input: 1G, in October and April, and 2C in February (Fig. 4). Chl-*a* showed a clear seasonality, with spring maxima (2.15±1.09 μg L^{-1}) and winter minima (0.68±0.69 μg L^{-1}); also spatial differences between the two inlets were found, with higher concentrations reached at the bottom waters of the SI. Phaeopigments, which represent the pigment degradation products, exhibited a different trend showing spring maxima, summer minima and similar values in October and February (Fig. 4). Chl-*a*/Phaeo ratio ranged between 0.27 and 4.68. The highest values and the wider variability were found in June.

Inorganic nutrient distribution showed a wide spatial and temporal variability (Fig. 5). Among nitrogenous species, nitrate concentrations ranged from 0.04 μM, minimum measured in June at the surface of St. 2B, to 36.92 μM, maximum detected at the surface of St. 1G, in April. In June, the water column was characterized by low bottom concentrations (<0.74 μM) at both inlets, while at surface, values ranged between 1.70 and 7.41 μM in the FI and were lower than 0.10 μM in the SI. A slight increase of concentrations, both at surface and at bottom, was detected at either inlets in October, followed by a sharp increase, especially at the surface, in February when a relative maximum of 19.92 μM was reached at St. 1B. In April, the two inlets differed substantially, with the FI clearly influenced by the continental input rising the N-NO_3 surface concentrations, and the SI characterized by quite homogeneous lower values along the water column.

Nitrite was detected in the range of 0.02–0.54 μM, and as for nitrate and ammonium, the highest concentrations characterized the surface waters, in February.

Ammonium concentrations varied from undetectable (at some sampling point, in April) to 3.14 μM (maximum reached at the surface of St. 2C, in February). During June, the two inlets were generally characterized by relatively low N-NH_4 concentrations (range 0.48–0.85 μM). Values increased in October, especially at bottom, where concentrations of two to three times higher (up to 2.27 μM) were reached. An opposite trend characterized February when the maximum concentrations of the study period (higher than 2.30 μM) were observed at surface. In April, at most of the stations, N-NH_4 values were close to or under the detection limit, never reaching values higher than 0.67 μM.

Dissolved inorganic nitrogen (DIN), as sum of ammonium, nitrite and nitrate, was characterized by a seasonal pattern, with lower concentrations in summer, due to the uptake of autotrophic organisms, and higher concentrations in winter, as result of the scarce biological activity and land runoff (Table 1).

At both inlets, N-NO_3 was the main component of DIN during October, February and April constituting from 49 to

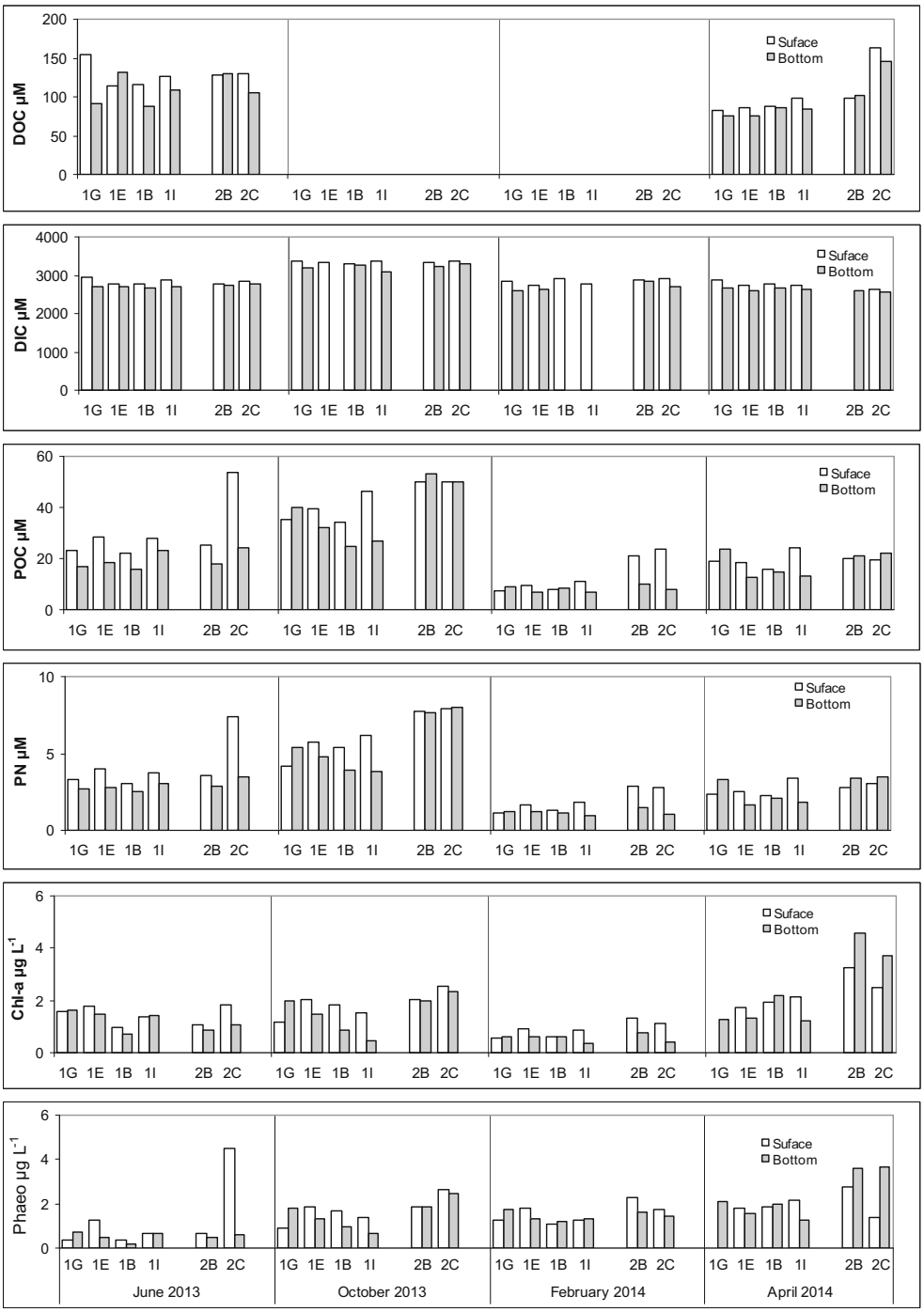

Fig. 4 Surface and bottom concentrations of DOC, DIC, POC, PN, chl-*a* and phaeo in the Mar Piccolo of Taranto during the four sampling surveys (June and October 2013, February and April 2014)

99 %, with the only exception encountered in October at the bottom of St. 2C, when N-NH_4 contributed up to the 67 %. In June, a great variability was observed between the two inlets. In the FI, N-NO_3 predominated at surface while at the bottom N-NH_4 was the main component (>51 %). The only exception was encountered at the bottom of St. 1I where N-NO_3 reached the 58 %. In the SI, the main component was N-NH_4 (>85 %) except for the bottom of St. 2C where predominate the N-NO_3. Nitrite represented less than 6 % of DIN ranging from 0.6 to 5.8 %.

Phosphate varied between under detection limit and 0.65 µM. The seasonal variability was higher than that of other nutrients, showing winter maxima and spring/summer minima. During June 2013 and April 2014, in fact, P-PO_4 concentrations were depleted to low values, often at or near the limits of detection. Temporal pattern at surface seemed to be more definite than in the bottom layer and among the sites, the SI experienced the highest amplitude of the annual phosphate cycle.

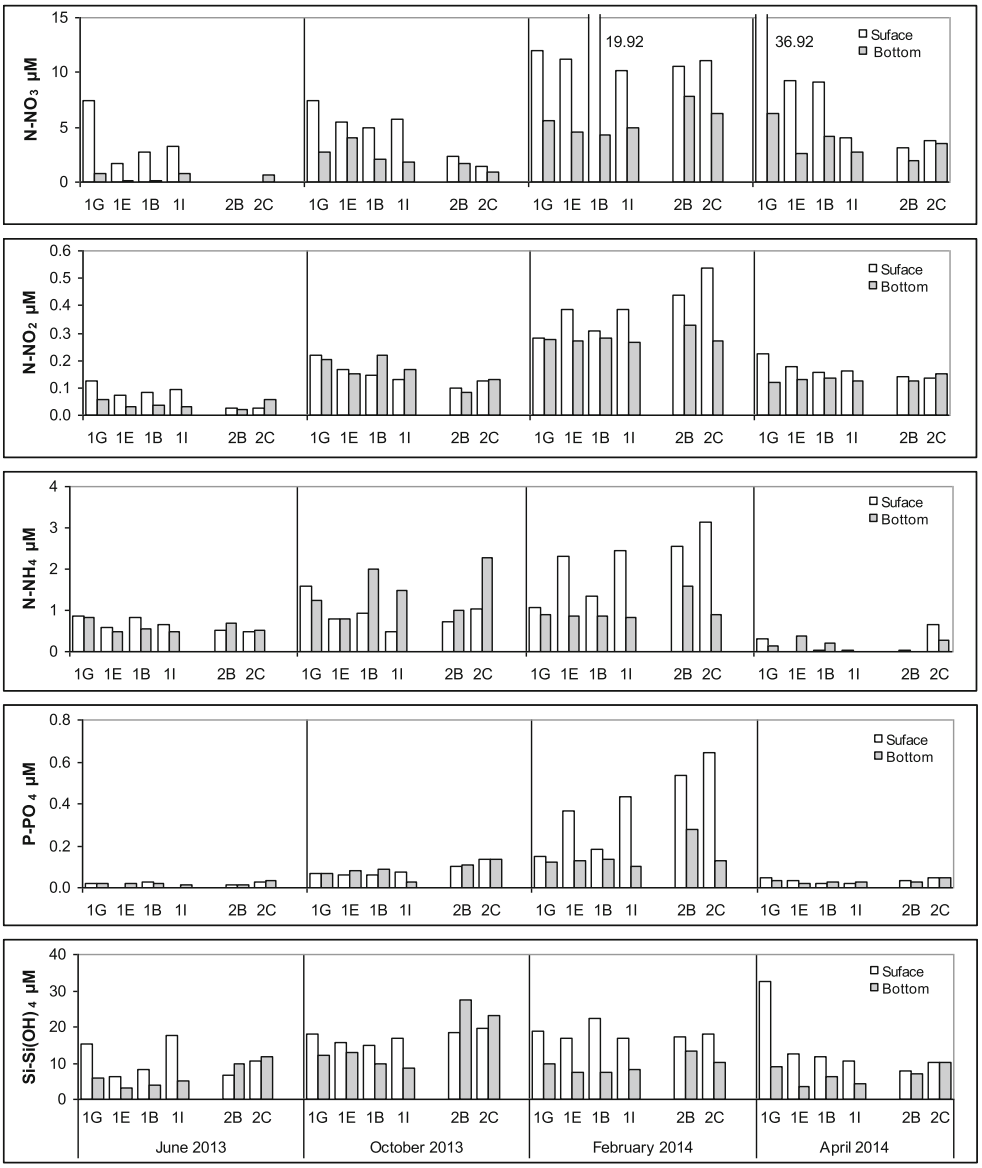

Fig. 5 Surface and bottom concentrations of N, P and Si nutrients in the Mar Piccolo of Taranto during the four sampling surveys (June and October 2013, February and April 2014)

Silicate concentration varied from 3.01 µM (minimum measured at the bottom of St. 1E, in June) and 32.53 µM (maximum reached in April at the surface of St. 1G). On average, seasonal higher concentrations were observed during October (16.50±5.41 µM) and February (13.84±5.08 µM) while lower values characterized June and April even if the absolute maximum was measured, as for $N\text{-}NO_3$, in April 2014 at the surface of St. 1G.

The PCA analyses on 2013–2014 biogeochemical data (Fig. 6) showed that the principal components 1 and 2 explained 71.5 % of the variance. All stations had a clear seasonal variation with DIN and phosphate concentrations characterizing February 2014 and POC, PN and DIC concentrations characterizing October. Between April and June, the distinction is not so sharp, probably due to the generally lower concentrations of ammonium and phosphate characterizing the spring/summer period. The only exceptions are the surface samples of two stations: 1G, in April, influenced by the river load supplying high nitrate and silicate concentrations, and 2C, in June, characterized by high levels of POC and PN.

The analysis of the data in the period extending from 1991 to 2000 (Fig. 7) indicates that N, P and Si show a similar behaviour with maximum values during autumn/winter and minimum values being reached during April–August. The high nutrient values, in January and February, could be ascribed to the high amount of discharges in the rainiest period as suggested by the high $N\text{-}NO_2+NO_3$ concentrations and low ammonia values, while in October, November and December, the remineralisation of organic matter prevailed as confirmed by the higher $N\text{-}NH_4$.

The depletion of silicates, which reaches values at or near the limits of detection, takes place between April and June, while nitrate minimum is observed 1–2 months later. Summer $P\text{-}PO_4$ minima were detected in the SI from April to June,

Table 1 Average and standard deviation values of Corg/Ntot ratios, DIN and chl-*a*/phaeo in the two inlets during the four sampling surveys (June and October 2013, February and April 2014)

		Surface				Bottom			
		FI		SI		FI		SI	
		Average	SD	Average	SD	Average	SD	Average	SD
Corg/Ntot	Jun 2013	7.19	0.20	7.20	0.11	6.77	0.58	6.68	0.47
	Oct 2013	7.28	0.87	6.38	0.07	6.86	0.47	6.61	0.50
	Feb 2014	6.13	0.29	7.89	0.86	6.92	0.70	7.22	0.69
	Apr2014	7.37	0.58	6.77	0.49	7.30	0.22	6.20	0.12
DIN (μM)	Jun 2013	4.62	2.62	0.59	0.01	1.06	0.46	0.98	0.32
	Oct 2013	7.01	1.47	2.85	0.42	4.21	0.59	3.05	0.46
	Feb 2014	15.47	4.09	14.13	0.89	5.89	0.58	8.53	1.65
	Apr2014	15.15	15.08	3.99	0.92	4.25	1.65	3.04	1.29
chl-*a*/phaeo	Jun 2013	2.70	1.42	1.01	0.84	2.91	0.76	1.85	0.07
	Oct 2013	1.15	0.10	1.04	0.10	1.04	0.13	1.00	0.07
	Feb 2014	0.55	0.10	0.61	0.03	0.40	0.11	0.39	0.14
	Apr2014	0.99	0.03	1.51	0.47	0.88	0.21	1.14	0.19

while in the FI no noticeable decrease from the high winter concentrations was evident.

The chlorophyll *a* concentrations appear to follow a classic pattern of annual succession with summer maxima and winter minima. Excluding some outliers and the months of August and September, when maxima up to 10 μg L^{-1} were registered, the concentrations generally did not exceed 5 μg L^{-1}.

Looking at the period 2001–2009, it appears that while before 2001, DIN exceeded 300 μM and phosphate and silicate peaked 15 and 1500 μM, respectively, after 2001 the DIN never reached 40 μM and P-PO_4 and Si-$Si(OH)_4$ were always lower than 0.8 and 40 μM, respectively (Fig. 7). The distribution of nutrient concentrations was in tune with the primary production cycle and the tributaries discharge. The temporal evolution of DIN concentration was characterized by a decrease throughout spring and summer and an evident increase in autumn. Less clear was the evolution of phosphate concentration during spring and summer; nevertheless, as for DIN, highest

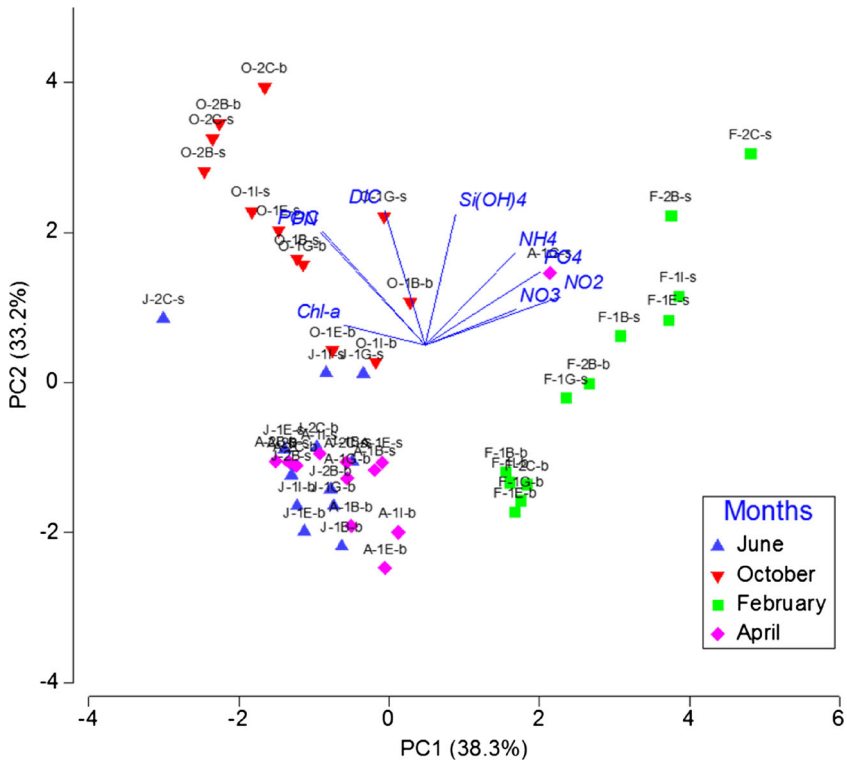

Fig. 6 Biplot of the PCA analyses on 2013–2014 biogeochemical data. Parameters and stations are plotted on the plane of the first two principal components (PC1 and PC2). The explained variance is shown on the axes

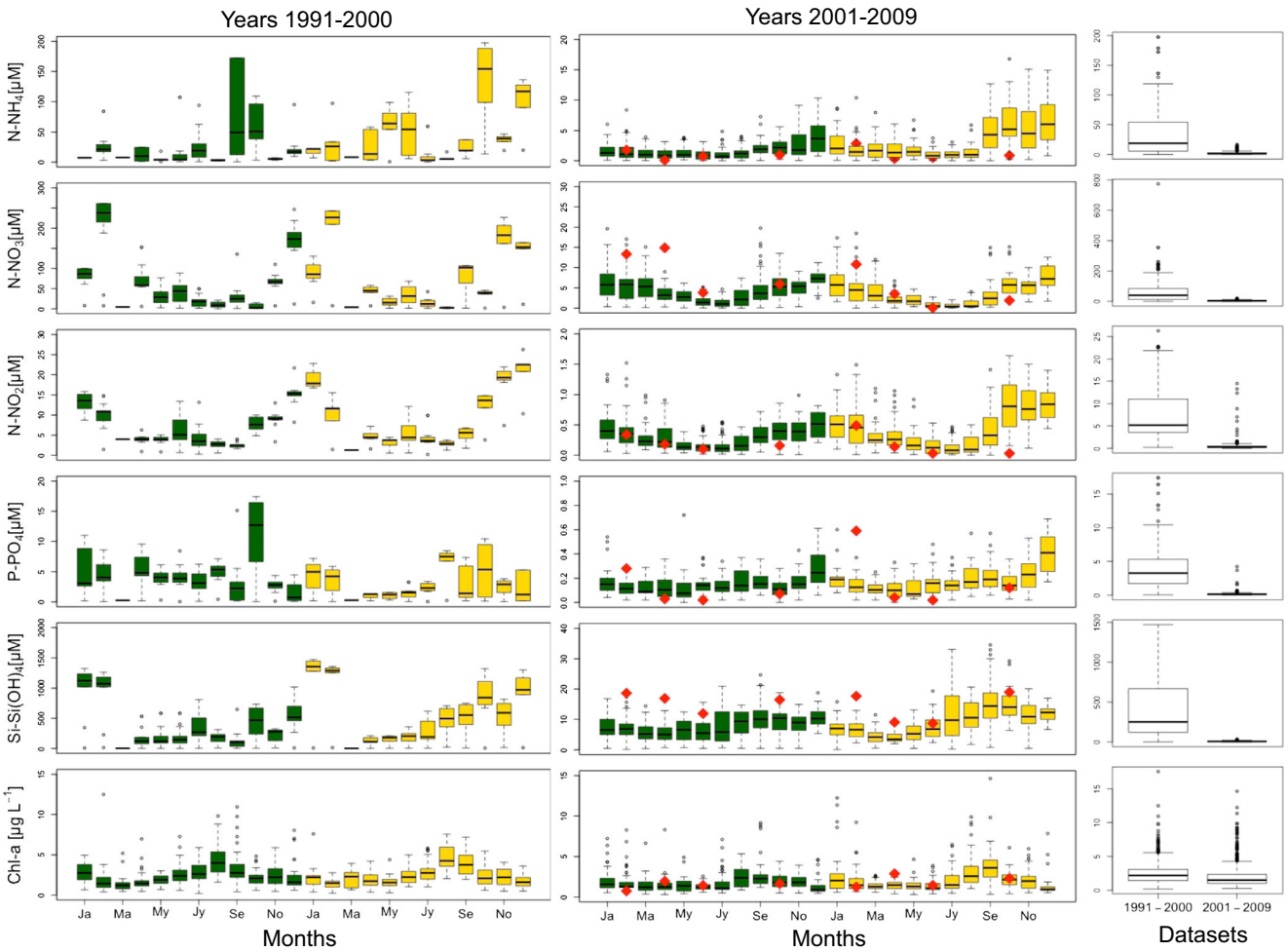

Fig. 7 Box and whiskers plots showing the variability of the monthly values of N-NH_4, N-NO_3, N-NO_2, P-PO_4, Si-Si$(OH)_4$ and chl-*a* in two different periods (1991–2000 and 2001–2009) at the surface water of the First (*green*) and Second Inlet (*yellow*). On the right, box and whiskers plots showing the variability of the two sets of historical analysed data. *Boxes* represent the interquartile range (25th to 75th percentile), the *horizontal line* is the median, the *ends of the whiskers* are the 5th and 95th percentiles and the *points* are the outliers. *Red diamonds* represent average values of 2013–2014 data. Note the different order of magnitude range

concentrations were registered in autumn. The monthly evolution of silicate showed a slight decrease in spring (March and April) and a progressive increase with maxima reached in late summer. Overall, the increase in concentrations registered from September to December was remarkably higher in the SI for N-NH_4, N-NO_2 and P-PO_4.

Chl-*a* did not show an evident seasonal trend even if a slight increase in concentrations from July to September, as before 2001, occurred.

PCA analyses (Fig. 8) performed to compare the present situation with the former datasets showed a remarkable separation between the dataset 1991–2000 and the dataset 2001–2009. Data collected during 2013–2014 were clearly included in the dataset 2001–2009. The first two principal components explained 71.5 % of the total variance. The principal component 1 explained approximately the 60 % of the variance and represents the distribution of all the nutrients, while the second principal component, which explained an additional 16.6 % of the variance, is represented by variations in the chl-*a* concentration.

Discussion

The transitional systems, like the Mar Piccolo of Taranto, are defined by a complex equilibrium of several factors, as the energy flows, the matter inputs and the biogeochemical processes inside the system. The geomorphologic characteristics of the basin act as a filter to modulate all these factors (Cloern 2001) determining space-time fluctuations in the biogeochemical heterogeneity of the system as yet encountered in other similar environments such as the Venice Lagoon (Bianchi et al. 2004; Sfriso et al. 1994; Solidoro et al. 2004), the Mar Menor (García-Pintado et al. 2007), the Arcachon Bay (Gle´ et al. 2008) and the Lesina Lagoon (Roselli et al. 2009).

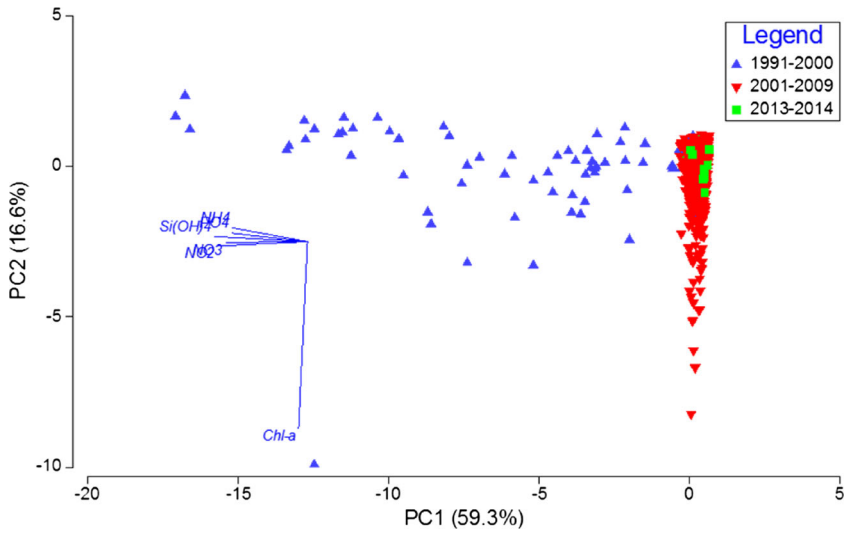

Fig. 8 PCA analyses performed to compare the present situation (2013–2014 surveys) with the former datasets (1991–2000 and 2001–2009). Parameters and data are plotted on the plane of the first two principal components (PC1 and PC2). The explained variance is shown on the axes

Spatial and temporal variability of hydrological and biogeochemical characteristics in the years 2013–2014

The data obtained during 2013–2014 show a considerable physical and biogeochemical inter-annual variability in the two inlets, as confirmed by the highly significant differences evidenced by ANOSIM analysis among the sampling periods ($p<0.001$) and by the PCA results (Fig. 6).

This can be ascribed to the concurrence of several meteorological, hydrological and biological forcing factors taking place in this basin. Irregular discharges of freshwater from its watershed intermittently provide nutrients to the water column. The differences between the two inlets were significant ($p<0.01$) even if ANOSIM demonstrated a certain degree of overlapping among variables ($R=0.27$) and can be attributed to the levels of confinement of the swallow waters, as previously reported by Alabiso et al. (2005). The shallowness of the basin, the strong influence of the freshwater and drainage discharges and the presence of extensive shellfish farming areas, acting as sinks of particulate matter and sources of nutrients for the water column (Souchu et al. 2001), make the elaboration of an annual cycle of nutrients difficult (Caroppo and Cardellicchio 1995).

Referring to the hydrological variables, the basin, despite its small extension, could be subdivided in different areas depending on sea water characteristics (Alabiso et al. 1997). The FI is clearly influenced by the freshwater discharges, derived from the inland tributaries and 'citri' in the northern part, and also from the seawater coming from the Mar Grande basin through the two connection channels, while the SI is characterized by lower water mass exchange and lower freshwater inputs (Caroppo and Cardellicchio 1995). That means that the biogeochemical characteristics of the basin are strongly dependent to the amount of discharges of tributaries. This was observed in the northern part of the FI basin during June 2013 when, both at bottom and surface waters, low salinity and an increase in nutrients, DIC and DOC concentrations were detected. Excluding this area of the FI, during this survey, the rest of the basin was characterized by the lowest DIN and marked depletion of P-PO_4, probably related to the phytoplankton uptake, as suggested by the high chlorophyll concentrations and high chl-*a*/phaeo ratio, which could be explained by a recent phytoplankton bloom mainly due to the phototrophs nanoflagellates fraction (Karuza et al. 2015).

The scarce hydrodynamism (De Serio et al. 2007) and the low water exchange with the nearby Mar Grande determine, mainly in summer, a high water stratification (Cardellicchio et al. 2007; Caroppo and Cardellicchio 1995). In 2013, this situation lasted until October, when the presence of thermocline and halocline regulated the vertical distribution of nutrients and their confinement and accumulation in the bottom waters as consequence of natural regeneration processes that occur at the water–sediment interface, determining an oxygen depletion in the deeper layer. The lower chl-*a*/phaeo ratio, compared with June, although could be related to senescent phytoplankton, suggests a higher herbivorous grazing pressure (Peña et al. 1991). This hypothesis is supported by the increase of particulate matter concentrations probably as consequence of a transfer of biomass from phytoplankton to zooplankton through grazing, as confirmed by the high concentrations of mesozooplancton observed in the same period by Karuza et al. (2015). Once a year, in fact, in late summer–early autumn, the study area is characterized by the maximum abundance of zooplankton (Belmonte et al. 2013).

The intense precipitation before the February 2014 survey (56.2 mm within 5 days, of which 33.8, 2 days before the sampling, data supplied by Servizio Protezione Civile of Puglia), produced a high discharge of freshwaters that carried riverine nutrients and lowered the surface salinity in the whole basin to the minimum registered during the study period. Freshwater transport supplied high concentrations of DIN and P-PO_4, which persisted in the water column also as

consequence of the scarce uptake from the phytoplanktonic community, reaching the lowest abundances during the winter months (Caroppo and Cardellicchio 1995), as evidenced by the low chl-*a* concentrations and chl-*a*/phaeo ratios. These results have been confirmed also by Karuza et al. (2015). The concentrations of reduced nitrogen forms and of P-PO_4 were higher in the SI, probably enhanced by the wide mussel rope community that covers the 61 % of the basin, which represents a large source of DIN (La Rosa et al. 2002) and phosphorus to the water column (Nizzoli et al. 2005).

Also in April 2014, the sampling was performed 4 days after an intense rainfall event (31.4 mm within four days), but the nutrient loads resulted quite different both quantitatively and qualitatively. Evidence of the freshwater input was present particularly in the northern area of the FI characterized by extremely high concentrations of nitrate and silicate but of really low phosphate. This could be due to the concurrence of other severe forcing factors such as the onset of intense biological processes, i.e. phytoplankton bloom (Caroppo et al. 2015) which, in shallow basins, may deeply modify the concentration and the coupling among the nutrients. The high chlorophyll *a* concentration detected especially in the SI supports the hypothesis of a crucial role of phytoplankton in P-PO_4 depletion. On the whole, these observations indicate that riverine loads of nutrients are, in early spring, an important factor for the rapid trigger of early phytoplankton blooms in the basin, even when other environmental conditions such as temperature and total irradiance are still close to the winter values.

In this study, even during intense discharge of freshwater, the dissolved pool was always deficient in phosphorous relative to nitrogen, and the highest DIN:P-PO_4 ratio were encountered in April straight after one of this events. These results suggest that the variability of nutrient loads is mainly linked to the runoff and to the concomitant presence of point and diffuse sources of nutrients ascribing to different levels of anthropogenic pressure.

Comparison of the present situation with the former dataset

The anthropogenic pressures that have taken place in the Mar Piccolo basin have caused significant alterations in its hydrological and chemical states and have probably influenced the biological communities (Caroppo and Cardellicchio 1995; Caroppo et al. 2008). Uninterrupted series of monitoring in multiple points of the basin and at different depths are lacking. Keeping in mind these difficulties, we tried to make preliminary considerations, with the aim to stress or to exclude the changes in the water quality of the Mar Piccolo after the closure of some sewage channels and the installation of depuration systems for the waters coming from the inland.

For what concerns the hydrological parameters, significant differences ($p<0.05$) were observed between the two climatological datasets (1991–2000 and 2001–2009) only for salinity.

The comparison between the climatological dataset (2001–2009) and the data collected during 2013–2014 and represented with red diamonds in the Fig. 3 shows that during February 2014, the observed salinity in the FI was slightly lower than the climatological values, but always in the range of variability, while there were no substantial differences in temperature. In June 2013 and April 2014, T, DO and SAL fell within the historical dataset, while in October 2013, these parameters were slightly higher with respect to the climatology even if always comprised between the 5th to 95th percentile. The only exception was the dissolved oxygen mean concentration in the FI, which exceeds the 95th percentile indicating the presence of more oxygenated waters. It was observed that October 2013 averaged data matched more with the September climatology (Fig. 3), suggesting that the basin still maintained summer environmental characteristics.

Differently, the analysis of the available biogeochemical data demonstrated the improvement of the water quality in the Mar Piccolo of Taranto after the treatment plant installation. As shown in the Fig. 7, nutrient concentrations were highly variable between the two inlets, and drastic changes in concentrations were found between the two analysed time series. The significant ($p<0.01$) lowering of the nutrient concentrations, evidenced by the ANOSIM test and confirmed by the PCA analysis (Fig. 8), suggests that an external cause determined the changes in the input regime, that is, the installation of the treatment plants (Taylor et al. 2011). The load of nutrients associated with inputs carrying inadequately treated waste waters from the inland, in the period before 2001, lead to concentrations of 1 order of magnitude higher than after 2001.

The 1991–2000 chl-*a* dataset significantly differed ($p<0.01$) from 2001–2009 ones due to a general reduction of chlorophyll concentration after the treatment plant installation. Nevertheless, high concentration values of chl-*a* were often reached also during 2001–2009, even if a drastic reduction of the total microphytoplankton and particularly of diatom abundance was observed (Caroppo et al. 2010, 2015). This could be due to a shift of the ecosystem towards a lower trophic level (Caroppo et al. 2010) as confirmed by the observations of Karuza et al. (2015) and in other systems tending to oligotrophication (Mozetič et al. 2010). The drastic reduction of diatom could explain the less marked spring chl-*a* peak, while the mean lower chl-*a* concentrations of July–September could be due to a reduction of dinoflagellates, which generally prevailed during summer (Caroppo et al. 2010).

Data collected during 2013–2014 and represented with red diamonds in the Fig. 7 were generally in the range of variability of the 2001–2009 climatology as evidenced also by the

PCA plot (Fig. 8). Values out of the 5th–95th percentiles were observed in February 2014, for P-PO_4 and Si-$Si(OH)_4$, in the SI; during April 2014, for nitrate and silicate, in the FI (as consequence of the extremely high concentrations detected at the St. 1G) and in October for nitrate, in the SI. This data confirms the lowering of the nutrient concentrations after the treatment plant installation yet observed in the 2001–2009 dataset.

Similar abrupt decrease in nutrient, up to −65 and −66 % of DIN and DIP, respectively, and −80 % of N-NH_4, were found also in other coastal systems, such as the Boston Harbor and the Kaneohe Bay, that have experienced decreases in nutrient loadings, while lower system responses were observed in areas with higher water residence time (Taylor et al. 2011 and references therein).

Conclusions

Coastal lagoon and basins with growing population densities and activities have undergone many environmental changes. In the Mar Piccolo of Taranto, several concurrent human actions have led to the alteration of the weak equilibrium characteristic of this transitional system and the increase of nutrients is among the main consequences because this coastal system acts as a trap for rivers and streams loadings during the high runoff periods. In the basin, the biological processes (production and mineralisation) affecting the nutrient budgets are largely influenced also by the intensive mussel culture (Cardellicchio et al. 2006), which by filtration and production and deposition of faeces and pseudofaeces, increases inputs of labile organic matter to the superficial sediment. Faeces and pseudofaeces are, in fact, characterized by a large bioavailability to microbial assemblages and by rapid degradation rates, which contribute to a rapid turnover of the organic biodeposits and to the massive release of nutrients at the water–sediment interface, which, in turn, can modify the nutrient budgets (La Rosa et al. 2002).

While relationships between anthropogenic nutrient loads and eutrophication processes in Mar Piccolo of Taranto have been previously demonstrated (Caroppo and Cardellicchio 1995), this is, in our knowledge, the first study that analyses and compares long-term seasonal variation of hydrological data and nutrient concentrations before and after the remediation and environmental cleaning up planned by the Italian Government.

The 20-year dataset analysis evidenced that the reduction of nutrient inputs into the basin from 1991 to 2009 has changed the biogeochemical characteristics of the Mar Piccolo from being relatively eutrophic before 2001, to moderately oligotrophic after 2001 when treatment plants began to be operational and phosphorous appeared to be the potential limiting nutrient for phytoplankton production in spring. The comparison between the two datasets shows that since 2001, an abrupt decrease in nutrient concentrations has occurred and that the response was higher, up to −90 % in the first inlet characterized by lower hydraulic residence time.

Our results, which represent a contribution to the characterization of the waters of the Mar Piccolo and an update of its climatology, demonstrate that, even if this costal ecosystem is still severely impacted by anthropogenic activities, the control of the point sources through depuration systems has been successful for the decrease in nutrient concentrations. Conclusions obtained from this study could be useful in the perspective of the water quality management for an overall understanding of the mechanistic linkages between man-made alterations of hydrologic and nutrients regimes, in order to plan integrate short and long-term remediation actions.

Acknowledgments The activities described in this publication were funded by the Project Bandiera RITMARE - La Ricerca Italiana per il Mare coordinated by the National Research Council and funded by the Ministry for Education, University and Research within the National Research Programme 2011–2013. The authors are warmly grateful to Nicola Cardellicchio and the team of the IAMC institute, section of Taranto, for their logistical support and hospitality. We would like to thank Gianmarco Ingrosso for helping in statistical elaborations and the Servizio Protezione Civile of Puglia (http://www.protezionecivile.puglia.it/centro-funzionale) for rainfall data supply. Four anonymous reviewers are warmly acknowledged for their helpful suggestions, which improved the manuscript.

References

Alabiso G, Cannalire M, Ghionda D, Milillo M, Leone G, Caciorgna O (1997) Particulate matter and chemical-physical conditions of an inner sea: the Mar Piccolo in Taranto. A new statistical approach. Mar Chem 58:373–388

Alabiso G, Giacomini M, Milillo M, Ricci P (2005) The Taranto sea system: 8 years of chemical–physical measurements. Biol Mar Medit 12:369–373

Alabiso G, Giacomini M, Milillo M, Ricci P (2006) Chemical-physical conditions in the Taranto sea system from 2002 to 2004. Biol Mar Medit 13:1055–1058

Belmonte G, Vaglio I, Rubino F, Alabiso G (2013) Zooplankton composition along the confinement gradient of the Taranto Sea System (Ionian Sea, South-eastern Italy). J Marine Syst 128:222–238

Bianchi F, Ravagnan E, Acri F, Bernardi-Aubry F, Boldrin A, Camatti E, Cassin D, Turchetto M (2004) Variability and fluxes of hydrology, nutrients and particulate matter between the Venice Lagoon and the Adriatic Sea. Preliminary results (years 2001–2002). J Marine Syst 51:49–64

Calabrese A, Massarelli C, Uricchio VF, Campanale C (2014) Safeguarding drinking water: use and quality of water, case study of Taranto Province. Procedia Engineering 89:232–238

Cardellicchio N, Buccolieri A, Di Leo A, Spada L (2006) Heavy metals in marine sediments from the Mar Piccolo of Taranto (Ionian Sea, southern Italy). Annali di Chimica 96:727–741

Cardellicchio N, Buccolieri A, Giandomenico S, Lopez L, Pizzulli F, Spada L (2007) Organic pollutants (PAHs, PCBs) in sediments from the Mar Piccolo in Taranto (Ionian Sea, Southern Italy). Mar Pollut Bull 55:451–458

Cardellicchio N, Annicchiarico C, Di Leo A, Giandomenico S, Spada L (2015) The Mar Piccolo of Taranto: an interesting marine ecosystem for the environmental problems studies. Environ Sci Pollu R. This issue

Caroppo C, Cardellicchio N (1995) Preliminary study on phytoplankton communities of Mar Piccolo in Taranto (Jonian Sea). Oebalia XXI: 61–76

Caroppo C, Rubino F, Giordano L, Trono A, Forleo M, Petrocelli A, Bellio G, Colella R, Palmieri N, Sclafani P, Siano R (2008) System design for SSA14 Mar Piccolo of Taranto (Southern Italy) Spicosa annual report. Available at http://www.academia.edu/1550097/System_Design_for_SSA14_Mar_Piccolo_of_Taranto_Southern_Italy_

Caroppo C, Giordano L, Rubino F, Bisci AP, Hopkins TS (2010) Phytoplankton communities as indicators of ecological change in the anthropogenically impacted Mar Piccolo of Taranto (Ionian Sea). Biol Mar Medit 17(1):102–105

Caroppo C, Giordano L, Bellio G, Bisci AP, Palmieri N, Portacci G, Sclafani P, Hopkins TS (2012) Progress toward sustainable mussel aquaculture in Mar Piccolo, Italy. Ecol Soc 17(3):10

Caroppo C, Cerino F, Auriemma R, Cibic T (2015) Phytoplankton dynamics with a special emphasis on harmful algal blooms in the Mar Piccolo of Taranto (Ionian Sea, Italy). This issue

Cavallo RA, Rizzi C, Vozza T, Stabili L (1999) Viable heterotrophic bacteria in water and sediment in 'Mar Piccolo' of Taranto (Ionian Sea, Italy). J Appl Microbiol 86:906–916

Cerco CF, Noel MR (2007) Can oyster restoration reverse cultural eutrophication in Chesapeake Bay? Estuaries Coasts 30(2):331–343

Christensen PB, Glud RN, Dalsgaard PG (2003) Impacts of longline mussel farming on oxygen and nitrogen dynamics and biological communities of coastal sediments. Aquaculture 218:567–588

Clarke KR, Warwick RM (2001) Change in marine communities: an approach to statistical analysis and interpretation. Primer-E- Ltd, Plymouth

Clarke KR, Warwick RM (2015) PRIMER v7: user manual/tutorial. PRIMER-E Ltd, Plymouth, p 296

Cloern JE (2001) Our evolving conceptual model of the coastal eutrophication problem. Mar Ecol-Prog Ser 210:223–253

Cloern JE, Dufford R (2005) Phytoplankton community ecology: principles applied in San Francisco Bay. Mar Ecol Prog Ser 285:11–28

Conley DJ, Markager S, Andersen J, Ellermann T, Svendsen LM (2002) Coastal eutrophication and the Danish National Aquatic Monitoring and Assessment Program. Estuaries 25:848–861

De Pascalis F (2013) Correnti e T/S nei mari di Taranto. CNR Report 09/2013 SP3_WP4_AZ5_UO01_D01 RITMARE La Ricerca Italiana per il MARE (in Italian)

De Serio F, Malcangio D, Mossa M (2007) Circulation in a Southern Italy coastal basin: modeling and field measurements. Cont Shelf Res 27(6):779–797

Di Leo A, Cardellicchio N, Giandomenico S, Spada L (2010) Mercury and methylmercury contamination in Mytilus galloprovincialis from Taranto Gulf (Ionian Sea, southern Italy): risk evaluation for consumers. Food Chem Toxicol 48:3131–3136

García-Pintado J, Martínez-Mena M, Barberá GG, Albaladejo J, Castillo VM (2007) Anthropogenic nutrient sources and loads from a Mediterranean catchment into a coastal lagoon: Mar Menor, Spain. Sci Total Environ 373:220–239

Giacomini M, Alabiso G (2006) Temperature study in the Mar Piccolo of Taranto (Italy, Mediterranean Sea). Biol Mar Medit 13:242–245

Gle´ C, Del Amo Y, Sautour B, Laborde P, Chardy P (2008) Variability of nutrients and phytoplankton primary production in a shallow macrotidal coastal ecosystem (Arcachon Bay, France). Estuar Coast Shelf S 76:642–656

Hansen HP, Koroleff F (1999) Determination of nutrients. In: Grasshoff K, Kremling K, Ehrhardt M (eds) Methods of seawater analysis, 3rd edn. Wiley-VCH, Weinheim, pp 159–228

Karuza A, Caroppo C, Camatti E, Di Poi E, Monti M, Stabili L, Pansera M, Cibic T, Del Negro P (2015) End to end planktonic trophic web and its implications for the mussel farms in the Mar Piccolo of Taranto (Ionian Sea, Italy). This issue

Kemp WM, Boynton WR, Adolf JE, Boesch DF, Boicourt WC, Brush G, Cornwell JC, Fisher TR, Glibert PM, Hagy JD, Harding LW, Houde ED, Kimmel DG, Miller WD, Newell RIE, Roman MR, Smith EM, Stevenson JC (2005) Eutrophication of Chesapeake Bay: historical trends and ecological interactions. Mar Ecol Prog Ser 303:1–29

La Rosa T, Mirto S, Favaloro E, Savona B, Sarà G, Danovaro R, Mazzola A (2002) Impact on the water column biogeochemistry of a Mediterranean mussel and fish farm. Water Res 36:713–721

Lopes CB, Lillebø AI, Dias JM, Pereira E, Vale C, Duarte AC (2007) Nutrient dynamics and seasonal succession of phytoplankton assemblages in a Southern European Estuary: Ria de Aveiro, Portugal. Estuar Coast Shelf S 71:480–490

Lorenzen CJ, Jeffrey SW (1980) Determination of chlorophyll in seawater. UNESCO Tech Pap Mar Sci 35:1–20

Lorrain A, Savoye N, Chauvaud L, Paulet YM, Naulet N (2003) Decarbonation and preservation method for the analysis of organic C and N contents and stable isotope ratio of low-carbonated suspended particulate material. Anal Chim Acta 491:125–133

Magni P, Como S, Cucco A, De Falco G, Domenici P, Ghezzo M, Lefrançois C, Simeone S, Perilli A (2008) A multidisciplinary and ecosystemic approach in the Oristano Lagoon-Gulf System (Sardinia, Italy) as a tool in management plans. Transit Waters Bull 2:41–62

Mallin MA, Mciver MR, Wells HA, Parsons DC, Johnson VL (2005) Reversal of eutrophication following sewage treatment upgrades in the New River Estuary, North Carolina. Estuaries 28:750–760

Melaku Canu D, Solidoro C, Umgiesser G, Cucco A, Ferrarin C (2012) Assessing confinement in coastal lagoons. Mar Poll Bull 64:2391–2398

Mozetič P, Solidoro C, Cossarini G, Socal G, Precali R, Francé J, Bianchi F, De Vittor C, Smodlaka N, Fonda Umani S (2010) Recent trends towards oligotrophication of the Northern Adriatic: evidence from chlorophyll *a* time series. Estuar Coasts 33:362–375

Nizzoli D, Welsh DT, Bartoli M, Viaroli P (2005) Impacts of mussel (Mytilus galloprovincialis) farming on oxygen consumption and nutrient recycling in a eutrophic coastal lagoon. Hydrobiologia 550:183–198

Oviatt CA, Hyde KJW, Keller AA, Turner JT (2007) Production patterns in Massachusetts with outfall relocation. Estuaries Coast 30:35–46

Pastore M (1993) Mar Piccolo. Nuova Editrice Apulia, Martina Franca, Taranto **(in Italian)**

Pella E, Colombo B (1973) Study of carbon, hydrogen and nitrogen determination by combustion-gas chromatography. Mikrochim Acta 5:697–719

Peña MA, Lewis MR, Harrison WG (1991) Particulate organic matter and chlorophyll in the surface layer of the Equatorial Pacific Ocean along 135 degree W. Mar Ecol-Prog Ser 72:179–188

Petronio BM, Cardellicchio N, Calace N, Pietroletti M, Pietrantonio M, Caliandro L (2012) Spatial and temporal heavy metal concentration (Cu, Pb, Zn, Hg, Fe, Mn, Hg) in sediments of the Mar Piccolo in Taranto (Ionian Sea, Italy). Water Air Soil Poll 223:863–875

Pinckney JL, Paerl HW, Tester P, Richardson TL (2001) The role of nutrient loading and eutrophication in estuarine ecology. Environ Health Persp 109:699–706

R Development Core Team (2011) R: a language and environment for statistical computing. R Foundation for Statistical Computing, Vienna, Austria

Roselli L, Fabbro A, Manzo C, D'Adamo R (2009) Hydrological heterogeneity, nutrient dynamics and water quality of a non-tidal lentic ecosystem (Lesina Lagoon, Italy). Estuar Coast Shelf S 84:539–552

Sfriso A, Marcomini A, Pavoni B (1994) Annual nutrient exchanges between the central lagoon of Venice and the northern Adriatic Sea. Sci Total Environ 156:77–92

Sharp JH (1974) Improved analysis for "particulate" organic carbon and nitrogen from seawater. Limnol Oceanogr 19(6):984–989

Smith VH, Joye SB, Hawarth RW (2006) Eutrophication of freshwater and marine ecosystems. Limnol Oceanogr 51:351–355

Solidoro C, Pastres R, Cossarini G, Ciavatta S (2004) Seasonal and spatial variability of water quality parameters in the lagoon of Venice. J Marine Syst 51:7–18

Souchu P, Gasc A, Collos Y, Vaquer A, Tournier H, Bibent B, Deslous-Paoli J-M (1998) Biogeochemical aspects of bottom anoxia in a Mediterranean lagoon (Thau, France). Mar Ecol-Prog Ser 164: 135–146

Souchu P, Vaquer A, Collos Y, Landrein S, Deslous-Paoli J-M, Bibent B (2001) Influence of shellfish farming activities on the biogeochemical composition of the water column in Thau Lagoon. Mar Ecol-Prog Ser 218:141–152

Sugimura Y, Suzuki Y (1988) A high temperature catalytic oxidation method for the determination of non-volatile dissolved organic carbon in seawater by direct injection of liquid sample. Mar Chem 24:105–131

Taylor DI, Oviatt CA, Borkman DG (2011) Non-linear responses of a coastal aquatic ecosystem to large decreases in nutrient and organic loadings. Estuar Coast 34:745–757

Umgiesser G, Scroccaro I, Alabiso G (2007) Mass exchange mechanisms in the Taranto Sea. Transit Water Bull 2:59–71

Vatova A (1972) Osservazioni fisico-chimiche periodiche nel Mar grande e nel Mar Piccolo di Taranto (1962–1969). Boll Pesca, Piscic Idrobiol 27:43–79 **(in Italian)**

Velasco J, Lloret J, Millan A, Marin A, Barahona J, Abellan P, Sanchez-Fernandez D (2006) Nutrient and particulate inputs into the Mar Menor lagoon (SE Spain) from an intensive agricultural watershed. Water Air Soil Poll 176:37–56

Zaccone R, Mancuso M, Modica A, Zampino D (2005) Microbiological indicators for aquaculture impact in Mar Piccolo (Taranto, Italy). Aquacult Int 13:167–173

CHAPTER 4

Stable carbon isotopes in phytoplankton as a tool to monitor CO_2 leakages at Carbon Capture and Storage sites

Federica Relitti[1,2*], Nives Ogrinc[3], Michele Giani[1], Federica Cerino[1], Cinzia De Vittor[1], Lidia Urbini[1], Bor Krajnc[3], Paola Del Negro[1]

[1] Oceanography Division, OGS (Istituto Nazionale di Oceanografia e di Geofisica Sperimentale), Trieste, Italy

[2] Department of Life Science, University of Trieste, Trieste, Italy

[3] Department of Environmental Sciences, Jožef Stefan Institute, Ljubljana, Slovenia

[*]**Corresponding author: Federica Relitti**

OGS (Istituto Nazionale di Oceanografia e di Geofisica Sperimentale), Oceanography Division

Via A. Piccard 54, 34151 Trieste, Italy

Tel.: +39 040 2249741

email: frelitti@inogs.it

Under review at Environmental Science and Pollution Research

Abstract

Carbon capture and storage technology (CCS) is expected to play a key role in climate change mitigation strategies by reducing CO_2 emissions into atmosphere from fossil fuel combustion. Although leakages from well-engineered storage sites are not expected, the environmental impacts related to potential CO_2 seepages are a major issue for the acceptance of this approach. This study aims to the evaluation of phytoplankton stable carbon isotopes as a tool for effective early warning of CO_2 migration from CCS, since different carbon sources have specific $\delta^{13}C$ values. Two culture experiments were conducted under controlled conditions for monitoring $\delta^{13}C$ changes in the diatom *Thalassiosira rotula* during growth in two different media; one prepared with natural seawater (NAT) and the other with artificial seawater (ASW). Carbonate system in ASW was derived from anthropogenic CO_2 and resulted in strongly ^{13}C-depleted dissolved inorganic carbon values (−44.7 ± 0.8‰). The uptake of inorganic carbon in ASW resulted in a rapid and significant change in microalgae $\delta^{13}C$ values (until −44.4‰), whereas in NAT phytoplankton $\delta^{13}C$ did not show important deviations from the starting value (−24.4 ± 0.3‰). The experiment results confirm the effectiveness of phytoplankton $\delta^{13}C$ as a tool for detecting different CO_2 sources.

Keywords

^{13}C; diatoms; CO_2 leakage; ^{13}C carbon fixation; Carbon Capture and Storage; Phytoplankton; CCS

1. Introduction

The global emissions of carbon dioxide (CO_2) from fossil fuels have been increasing by 2.7% annually since the past decade (Le Quéré et al. 2013). The increase of CO_2 concentration in atmosphere has been recognised as one of the main causes of climate change, resulting in strong impacts on natural and human systems on all continents and across the oceans (IPCC 2014). In order to prevent the adverse effects of climate change, several approaches have been studied for reducing CO_2 concentration in atmosphere. Among these, carbon capture and storage (CCS) technology has emerged as a promising option among the mitigation actions for the stabilization of atmospheric greenhouse gas concentrations (De Coninck & Benson 2014; IPCC 2005), by storing carbon dioxide either on-shore or off-shore. Although a well-engineered storage site is not expected to leak, the risk of failure of CO_2 containment and the subsequent environmental impact is a major issue for the acceptance of this approach. Monitoring strategies have been established in order to detect leakages from storage sites, including biological and chemical-physical approaches (Blackford et al. 2015;

Jones et al. 2015; Mayer et al. 2015; Noble et al. 2012). In off-shore sites, CO_2 released from CCS could impact marine environment in several different ways, mainly as a consequence of lower seawater pH because of CO_2 dissolution. Among the main adverse effects, shell formation in calcifying organisms could be inhibited, dissolution and desorption of metals could be enhanced and once mobilized they can accumulate in marine organisms inhibiting growth or even causing death. Moreover, microbial and faunal community could be altered in composition and metabolic activity (Lichtschlag et al. 2015 and references therein; Noble et al. 2012; Jones et al. 2015). With regards to primary producers, except from calcareous organisms which are detrimentally affected by the dissolution of CO_2, contradictory effects have been reported. CO_2 leakages seem not to affect phytoplankton and seaweed species. Indeed, these species seem to benefit from high CO_2 levels, by enhancing carbon and nitrogen fixation and stimulating photosynthesis (Jones et al. 2015; Tait et al. 2015 and references therein). However, as reviewed by Kim et al. (2016), lower pH could affect the physiological processes of some phytoplankton species, including photosynthesis, uptake rates of trace metals and toxin production of some harmful algal species. Moreover, natural phytoplankton assemblages and community composition could be modified by high dissolved CO_2 concentrations (Kim et al. 2016). Therefore, an effective management of storage sites is required in order to early detect leakages and prevent risks for the surrounding environment. Given the natural heterogeneity of sediment and water column chemistry and biology, a robust knowledge of the baseline of the site is required for characterising spatial and temporal dynamics, thus avoiding false positive and/or negative results (Blackford et al. 2015).

Stable isotopes have been largely applied to estimate the effects of anthropogenic pressures on natural ecosystems (Mancinelli & Vizzini 2015, and references therein) and carbon isotope analysis is considered a suitable tool for tracing the fate of CO_2 in the reservoir and for detecting leakages from storage sites, provided that the isotope composition of injected CO_2 is different from that of the surrounding environment (Mayer et al. 2015). The isotope composition ($\delta^{13}C$) of CO_2 stored in CCS ranges from −51 to −4.7‰ (Flude et al. 2016) depending on the feed-stock used and on the combustion process. Most of the CO_2 injected in CCS derives from fossil fuels and its $\delta^{13}C$ is usually ^{13}C-depleted, similar to the isotope composition of the bulk coal (from −28.5 to −23.9‰, Warwick & Ruppert 2016). Atmospheric $\delta^{13}C_{CO_2}$ has changed significantly since the 19th century, from a value of about −6.5‰ to a present-day value below −8.0‰ as a consequence of the addition of ^{13}C-depleted carbon from fossil fuel and land-use changes (the so-called Suess effect) (Hellevang & Aagaard 2015). $\delta^{13}C$ of total dissolved carbon in ocean ranges from 0 to −2‰ (Zeebe & Wolf-Gladrow 2001), because of biological activity and fractionation occurring during CO_2 dissolution in seawater. The difference between the isotope composition of combustion CO_2 and the natural baseline makes $\delta^{13}C$

the most widely analysed tracer, as it allows leakage monitoring with minimal economic and environmental impact compared to other tracers (Flude et al. 2016). Most of the applications of carbon stable isotope analysis is related to the monitoring of the movement of injected CO_2 inside the reservoir (Mayer et al. 2015; Mayer et al. 2013; Jeandel et al. 2010; Becker et al. 2011). To our knowledge, stable carbon isotope analysis has not yet been applied in the assessment of potential impact of CO_2 release on the environment surrounding a CCS site.

The present study aims to evaluate carbon stable isotope analysis as a tool for detecting CO_2 migration from CCS by the analysis of the variation of $\delta^{13}C$ of phytoplankton after the exposure to combustion CO_2. The performed experiments have been designed in a model case approach, considering the extreme case in which the isotope composition of the whole carbonate chemistry has been modified by a massive anthropogenic CO_2 sub-seabed leakage. A weak leakage does not alter the whole carbonate system and the anthropogenic CO_2 released from a storage site mixes and equilibrates in the environment, therefore the effects of a leakage may not be detectable unless sampling is simultaneous to CO_2 emissions. In the case of a strong CO_2 leakage, pH tends to decrease as CO_2 dissolves, and conditions that are not favourable for phytoplankton could be reached. The resulting stressful environment could hence alter carbon uptake and isotope fractionation. The purpose of the performed experiments is to verify how phytoplankton isotope composition changes when only the $\delta^{13}C$ of the carbon source is modified, but the whole carbonate system remains comparable to natural conditions in terms of concentrations of carbonate species. The only change of isotope composition of CO_2 in the medium should not alter algal metabolism and thus the interpretation of isotope results could not be affected by other factors than the $\delta^{13}C$ of the source of inorganic carbon.

2. Material and methods

2.1. Experimental setup

Two culture experiments (I and II) were conducted within 2L-photobioreactors (Kbiotech®) under controlled conditions of light (light/dark cycle: 14:10, intensity 100 µE m^{-2} s^{-1}) and temperature (20 ± 0.02 °C) (Figure 1). Clonal cultures of the diatom *Thalassiosira rotula* were established in September 2012 from a sample collected in the Gulf of Trieste (North Adriatic Sea) (45°42.06' N, 13°42.60' E). The strain was maintained in 100 mL glass Erlenmeyer flasks filled with modified L1 medium obtained from sterile-filtered Adriatic Sea water (0.2 µm pore size). The medium was supplemented with nutrients (nitrate, $NaNO_3$, 5.49 10^{-4} M, phosphate, $NaH_2PO_4 \cdot H_2O$, 2.24 10^{-5} M and silicate, $Na_2SiO_3 \cdot 9H_2O$, 1.06 10^{-4} M, final concentrations), metals and vitamins. The culture

was grown at 15 ± 2 °C and at a light intensity of about 53 µE m^{-2} sec^{-1}, under a light/dark regime (14:10). Before starting the experiments, cells were transferred within sterilized 2L glass Erlenmeyer flasks to allow growth until the exponential phase for the inoculation.

In each experiment, microalgae were grown simultaneously in two different media; one prepared with natural seawater (NAT) and the other with artificial seawater (ASW). Natural seawater was collected at 1174 m depth in the South Adriatic Sea (March 2015, 41°44.53' N, 17°41.35' E), whereas artificial seawater was prepared according to Andersen (2005) except for the sodium carbonate, that was artificially created by bubbling CO_2 into a solution of NaOH. CO_2 was supplied to the ASW medium by mixing carbon dioxide from cylinder with CO_2-free air, until typical marine pH value was reached (8.07–8.19). An industrial compressed CO_2 supply was used after verifying its different value from natural atmospheric CO_2, and after ensuring that no changes due to Rayleigh process occurred ($\delta^{13}C$ value was −48.3 ± 0.1‰ as average of the measurements performed during the two experiments). Both media were supplied with the same amount of nutrients and microelements proposed by Andersen (2005) and were added to the photobioreactors by filtration (hydrophilic PTFE filter, nominal pore size 0.2 µm, Merk), with the purpose of minimizing bacterial interference, and in an attempt to prevent gas exchange with the atmosphere. During experiments, variations of pH, temperature and dissolved oxygen were monitored and recorded by on-line probes (Figure 1). An intermittent CO_2-free air flow was maintained (on/off cycle: 10:50 min) in both conditions, and a continuous gentle stirring prevented stratification and favoured medium mixing. At the beginning of the experiments (0 h), diatoms were inoculated in the same concentration in both conditions (250 cell mL^{-1} in I and 1000 cell mL^{-1} in II). The first culture experiment lasted 96 h, while the second 140 h, and periodic samplings were performed by means of a peristaltic pump in order to minimize atmospheric gas exchange.

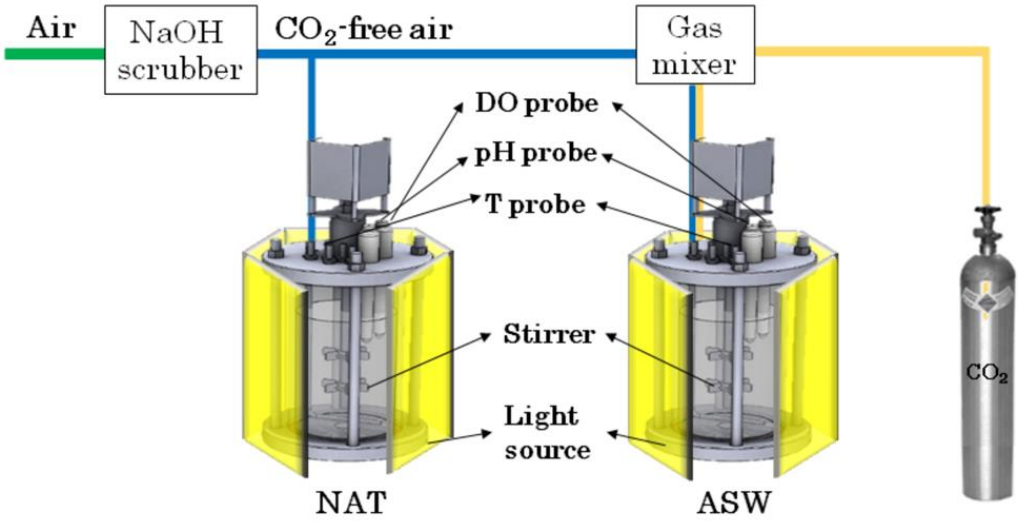

Fig. 1: Experimental setup description. During algal growth only CO2-free air was used (on/off cycle: 10:50 min) both for artificial seawater medium (ASW) and natural seawater medium (NAT). CO2 from cylinder was only supplied during ASW medium preparation. Dissolved oxygen (DO; % sat), temperature (T; °C) and pH (NBS scale) were recorded by on-line probes. Light/dark regime: 14/10 h; continuous gentle stirring. Photobioreactor outline modified from Kbiotech®.

2.2. Sampling and analyses of carbonate system

For cell density (cell mL^{-1}), 10 mL of culture were sampled every day and immediately fixed with pre-filtered and neutralized formaldehyde (1.6% final concentration) (Throndsen 1978). Cell counts were performed in triplicates in a Sedgewick Rafter counting chamber at a light microscope (Leica DM2500, Germany) at a magnification of 100-200x, counting a minimum of 200 cells in random fields or transects. Growth rate of the diatoms (μ, d^{-1}) was calculated in the exponential phase of the culture (Andersen 2005) as:

$$\ln cell_{t2} - \ln cell_{t1}/(t_2 - t_1) \quad (1)$$

where $cell_{t1}$ represents the abundance of phytoplankton (cell mL^{-1}) at the beginning of the time interval in which the culture exhibited an exponential growth (t_1; days) and $cell_{t2}$ the population size and the end of the time interval analysed (t_2; days). For molecular phytoplankton species identification, 25 mL (~40000 cells mL^{-1}) of the cell culture from the experiment was filtered on a 1.2 µm cellulose filter and frozen on –80 °C. Genomic DNA was isolated with the DNeasy Plant Mini Kit (Qiagen) according to manufacturer instructions. 5' end region of the ribulose bisophosphate carboxylase large subunit (*rbc*L) gene was amplified using primer pair rbcL66+ (5'-TTAAGGAGAAATAAATGTCTCAATCTG-3') and DtrbcL3R (5'-

ACACCWGACATACGCATCCA-3') according to Alverson (2008) and MacGillivary & Kaczmarska (2011) and sequenced at the Macrogen Inc. The resulting sequences (from both ends) were aligned using Geneious 7.1.7 software (Kearse et al. 2012). BLAST (Altschul et al. 1997) was used for searches and comparisons of the NCBI GenBank database (Clark et al. 2016).

The abundance of prokaryotes (cell mL^{-1}) was estimated by a FACSCanto II (Becton Dickinson) flow cytometer, equipped with an air-cooled laser at 488nm and standard filter setup. Samples were treated according to Marie et al. (1999) as described in Celussi et al. (2015).

To measure total alkalinity (A_T, µmol $kgSW^{-1}$), samples of 100 mL culture suspension were filtered over pre-combusted Whatman GF/F filters (450 °C for 4 h) to remove phytoplankton cells (Gattuso et al. 2010). Each bottle was poisoned with 50 µL of saturated mercuric chloride ($HgCl_2$) to halt biological activity and stored at 4 °C in the dark until analysis. Total alkalinity was determined by potentiometric titration in an open cell (SOP 3b, Dickson et al. 2007) as described in Ingrosso et al. (2016).

pH (NBS scale) was continuously recorded by on-line probes (Hamilton EasyFerm BIO Arc 225) previously calibrated on the National Bureau of Standards (NBS) scale with certified buffer solutions of pH 7 ± 0.02 and 9 ± 0.03 (at 25 °C, Certipur®).

Samples for dissolved inorganic nutrients (nitrite - NO_2, nitrate - NO_3, ammonium - NH_4, phosphate - PO_4, and silicate - SiO_4) were filtered over pre-combusted Whatman GF/F filters (450 °C for 4 h) in acid washed polyethylene vials and kept frozen (–20 °C) until laboratory analysis. Inorganic nutrient concentrations were determined colorimetrically with a QuAAtro Seal Analiytical autoanalyser according to Hansen & Koroleff (1999). Detection limits reported by the analytical methods were 0.02 µM, 0.02 µM, 0.04 µM, 0.02 µM, and 0.02 µM for NO_2, NO_3, NH_4, PO_4, and SiO_4, respectively. The accuracy and precision of the analytical procedures are annually checked through the quality assurance program QUASIMEME (AQ1) and the relative coefficient of variation for five replicates was less than 5%. Internal quality control samples were used during each analysis.

Dissolved oxygen (DO) was continuously recorded by on-line probes (Hamilton OxyFerm FDA Arc 225), previously calibrated with 0% DO and 100% DO solutions. In order to convert probe values in µmol L^{-1}, discrete samples were collected during the experiments (I: 0 h, 24 h, 96 h; II: 0 h, 140 h) and DO concentration was determined following the Winkler method (Hansen 1999) using the automated titration system Mettler Toledo G20 with potentiometric end-point detection (Oudot et al. 1988).

2.3. Sampling and analysis of stable isotope of carbon

Samples for the analysis of stable carbon isotopes of $CO_{2(gas)}$ and DIC were collected in 12 mL Exetainer® evacuated glass tubes, preventing gas exchange with atmosphere. Stable carbon isotope composition of $CO_{2(gas)}$ ($\delta^{13}C_{CO_{2(gas)}}$) was determined with an isotope ratio mass spectrometer (IRMS) Europa Scientific 20-20 with ANCA-TG preparation module for trace gas samples.

Samples for stable isotope composition of dissolved inorganic carbon ($\delta^{13}C_{DIC}$) were filtered over pre-combusted Whatman GF/F filters (450 °C for 4 h) to remove phytoplankton cells and analysis was performed by injecting aliquots of sample into evacuated septum tubes with phosphoric acid. Released $CO_{2(gas)}$ was then analysed with continuous-flow IRMS Europa 20-20 with ANCA TG trace gas separation module. In order to determine the optimal extraction procedure for water samples, a standard Na_2CO_3 solution was prepared with a known $\delta^{13}C$ value of −10.8 ± 0.2‰.

Bulk particulate organic matter isotope composition ($\delta^{13}C_{POC}$) was determined by filtering aliquots of culture suspension (~20 mL) over pre-combusted (450 °C for 4 h) Whatman GF/F filters (nominal porosity 0.7 µm, ø 25 mm). In order to estimate the potential influence of bacteria isotope composition on the bulk $\delta^{13}C_{POC}$ value ($\delta^{13}C_{POC<10\mu m}$), other aliquots of culture suspension (~20 mL) were filtered over pre-combusted Whatman GF/F filters after a pre-filtration on a 10 µm mesh in order to remove phytoplankton cells. The dimension of the mesh was chosen according to the average *Thalassiosira rotula* cell dimension of 20 µM (Hasle & Syvertson 1997). Samples for $\delta^{13}C_{POC}$ and $\delta^{13}C_{POC<10\mu m}$ analysis were collected in duplicate, rinsed with deionised water, oven-dried at 60 °C for 30 min and stored in desiccators until analysis. Before the analysis, filters for $\delta^{13}C_{POC}$ and $\delta^{13}C_{POC<10\mu m}$ were treated with 1 M HCl to remove carbonate minerals and inserted into tin capsules for further analysis. Measurements were performed on a Europa Scientific 20-20 IRMS with an ANCA-SL preparation module for solid and liquid samples.

All stable isotope values are given conventionally in δ-notation in per mil deviation (‰) from the Vienna Peed Dee Belemnite (VPDB) standard. IRMS was calibrated against reference materials: IAEA-CH-6 and IAEA-CH-7 for $\delta^{13}C_{POC}$ analysis and "CO_2 ISO-TOP, High" with $\delta^{13}C$ value of −4.3 ± 0.2‰ for $\delta^{13}C_{CO_2}$. The precision based on replicate analysis was ±0.2‰ for all stable isotope analysis ($\delta^{13}C_{CO_{2(gas)}}$, $\delta^{13}C_{DIC}$, $\delta^{13}C_{POC}$ and $\delta^{13}C_{POC<10\mu m}$).

2.4. Calculation of carbonate system parameters and isotopic fractionation

The other carbonate system parameters, including total dissolved inorganic carbon (DIC), dissolved CO_2 (CO_2) and bicarbonate (HCO_3^-) concentrations, were calculated using the CO2SYS program (Lewis & Wallace 1998) through in situ A_T, pH_{NBS} (20 °C), temperature, salinity, phosphate, and silicate data. Carbonic acid dissociation constants (i.e., pK1 and pK2) of Mehrbach et al. (1973) refitted by Dickson & Millero (1987) were used for the computation, as well as the Dickson constant for the ion HSO_4^- (Dickson, 1990) and borate dissociation constant of Uppström (1974).

A mass balance relation was used to calculate the isotope composition of dissolved CO_2 ($\delta^{13}C_{CO_2}$) and HCO_3^- ($\delta^{13}C_{HCO_3^-}$) from $\delta^{13}C_{DIC}$, by the temperature-fractionation relationships from Rau et al. (1996), based on Mook et al. (1974):

$$\delta^{13}C_{CO_2} = \delta^{13}C_{DIC} + 23.644 - \frac{9701.5}{T_K} \quad (2)$$

$$\delta^{13}C_{HCO_3^-} = \delta^{13}C_{CO_2} - 24.12 - \frac{9866}{T_K} \quad (3)$$

where T_K is the absolute temperature in Kelvin.

Diatom isotope fractionation associated with photosynthetic CO_2 fixation (ε_p) was calculated relative to the isotope composition of CO_2 in the bulk medium according to (Farquhar et al. 1989; Freeman & Hayes 1992):

$$\varepsilon_p = 1000 \frac{\left(\delta^{13}C_{CO_2} - \delta^{13}C_{POC}\right)}{\left(1000 + \delta^{13}C_{POC}\right)} \quad (4)$$

2.5. Statistical analysis

The Spearman rank correlation test was used to investigate time variation of the variables and relationships between phytoplankton/prokaryotes, abiotic parameters and isotope composition.

In order to verify the differences between natural and artificial seawater conditions, Kruskal-Wallis ANOVA test was applied to the variables. Kruskal-Wallis ANOVA and Spearman tests were conducted using STATISTICA 7 (StatSoft, Inc., USA) and only significant data ($p < 0.05$, $p < 0.01$)

are presented. Multivariate analysis was performed in order to verify the overall difference between the two conditions applying a non-metric multidimensional scaling analysis (nMDS) ordination model. nMDS was based on *z*-normalised data and phytoplankton abundance data were first square-root transformed because of the wide distribution of values that could have affected analysis. One-way ANOSIM was also performed for the analysis of similarity between the two conditions. nMDS and ANOSIM analysis were performed using PRIMER 7 (PRIMER-E Ltd., Plymouth, UK) software (Clarke et al. 2014).

3. Results

3.1. Biotic and abiotic parameters

Species identity was confirmed as *Thalassiosira rotula* by molecular analysis, using *rbc*L gene as a DNA barcode. New *Thalassiosira rbc*L nucleotide sequence was deposited in GenBank under accession number: **MG214782**.

T. rotula nearly followed a typical exponential growth in both experiments and conditions (Figure 2). Despite the same inoculation abundance in both medium (I: 250 cell L^{-1}; II: 1000 cell L^{-1}), in NAT microalgae started to decrease after reaching the highest abundances at 48 h and 72 h, respectively in the I experiment (4.24 10^3 cell L^{-1}) and II experiment (2.04 10^4 cell L^{-1}). At the end of the first experiment, in the natural seawater condition, an abundance lower than the inoculation was reached (196 cell L^{-1}). On the contrary, in the artificial seawater condition, the maximum abundances of microalgae were detected at the end of the experiments (1.50 10^4 cell L^{-1} and 4.17 10^4 cell L^{-1} respectively in I and II).

As diatom abundances started to increase earlier in NAT than in ASW, and as a consequence of the different inoculation abundance between I and II, the exponential phase of culture was not coincident in the two conditions and experiments. Therefore, growth rates (μ) were not calculated in the same time interval however, no significant differences were detected among all conditions. *T. rotula* exponential growth in NAT was detected in the first two days of culture in both experiments, and growth rate was 1.3 d^{-1}. In the artificial seawater condition, the exponential phase was detected in the last period of the culture (24 h – 96 h in I; 72 h – 140 h in II), and diatom growth rate was 1.2 d^{-1} in I and 1.0 d^{-1} in II.

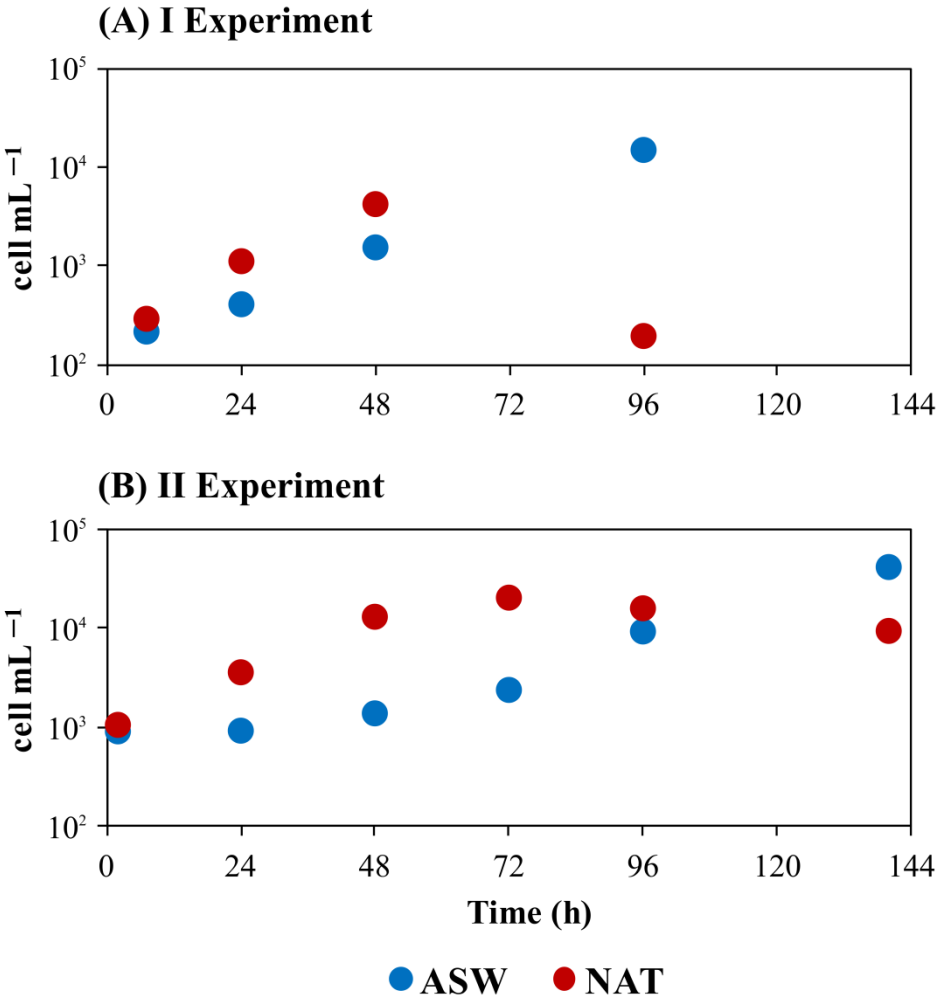

Fig. 2: Time variation of *T. rotula* abundance during the first (A) and second (B) culture experiment. Blue symbols represent the artificial seawater medium (ASW) and red symbols the natural seawater medium (NAT).

Prokaryotes abundance (Figure 3) significantly increased throughout the culture growth ($p < 0.05$) in both experiments and conditions. The abundance of prokaryotes after the inoculation was one order of magnitude higher in I than II, however similar values were detected at the end of the two culture experiments.

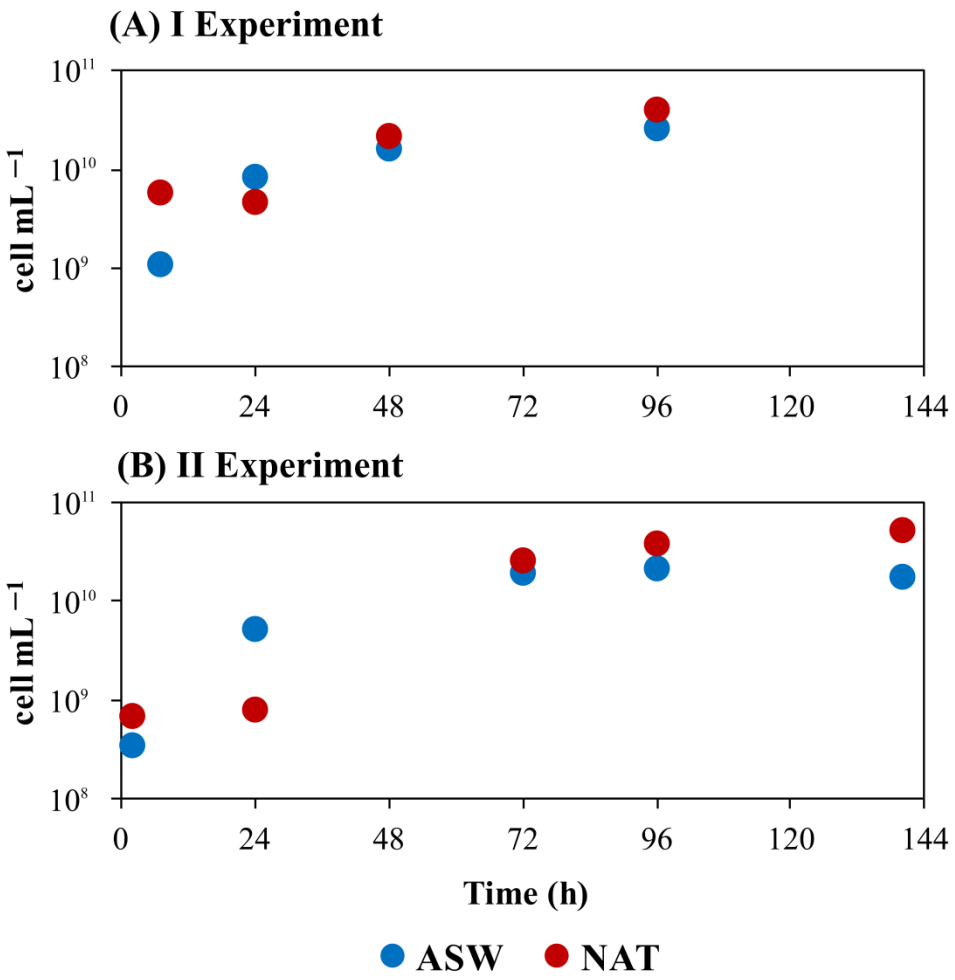

Fig. 3: Time variation of prokaryotes abundance during the first (A) and second (B) *T. rotula* culture experiment. Blue symbols represent the artificial seawater medium (ASW) and red symbols the natural seawater medium (NAT).

Dissolved oxygen (Figure 4 A) and pH (Figure 4 B) followed the typical day/night fluctuation due to photosynthetic activity, with decreasing values during the dark period and increasing values during the light one. The highest dissolved oxygen concentrations (Figure 4 A) coincided with the highest diatom abundance. Indeed in the artificial seawater condition maxima were detected at the end of the experiments (249 µmol L^{-1} at 95 h in I ASW, 346 µmol L^{-1} at 123 h in II ASW), whereas in NAT maximum values were recorded at 47 h and 52 h (respectively, 231 µmol L^{-1} in I NAT and 270 µmol L^{-1} in II NAT). Unfortunately, oxygen and pH data of I NAT are not available after 48 h because of technical problems. pH values (Figure 4 B) showed an increasing trend throughout the experiments in both medium, except for II ASW where values started to increase after 46 h, when also the diatoms showed higher abundance.

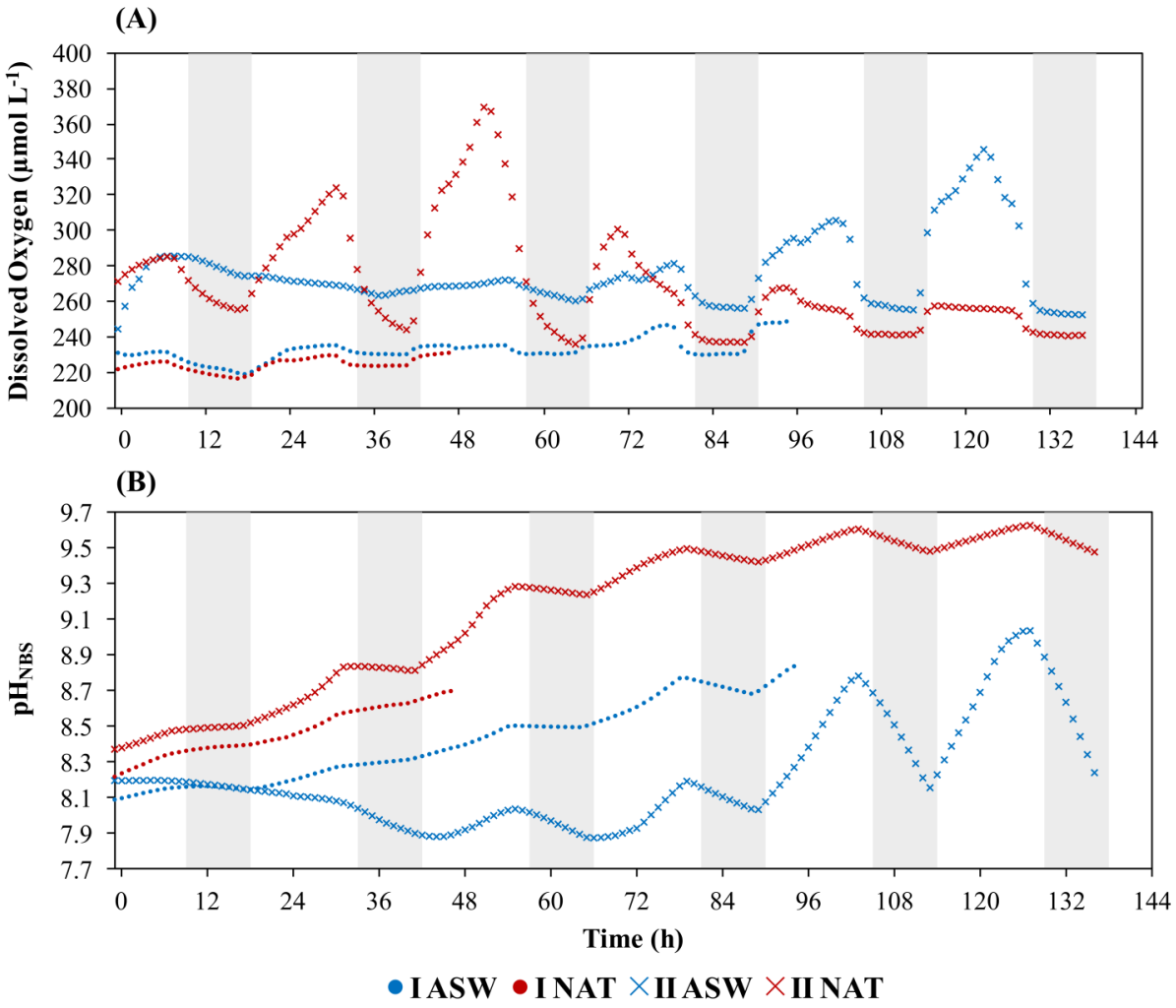

Fig. 4: Time variation of (A) dissolved oxygen (µmol L^{-1}) and (B) pH during the two *T. rotula* culture experiments (I and II). Grey bars represent the dark phase of the day/night cycle. Blue symbols represent the artificial seawater medium (ASW) and red symbols the natural seawater medium (NAT).

Total alkalinity (A_T, Figure 5 A) did not vary significantly during the experiments in both medium. Apart from I ASW, in which A_T values slightly decreased until the end of the culture experiment, A_T decreased in the first half of the experiments, and increased afterwards reaching the maximum values at the end of the experiments. Notwithstanding an error in the preparation of the medium in II ASW that caused lower A_T concentration, diatoms growth was not affected by lower carbon availability, as *T. rotula* abundances were similar to I ASW. DIC concentrations (Figure 5 B) exhibited a decreasing trend ($p < 0.01$) throughout the culture growth and reached approximately half of the initial amount at the end of the experiments. Bicarbonate (HCO_3^-) concentrations (Figure 5 C) approached similar values to DIC, and dissolved CO_2 (Figure 5 D) constituted less than 1% of DIC in both experiments and conditions, as expected at the experimental pH. Both HCO_3^- and dissolved CO_2 followed the same decreasing trend ($p < 0.01$) of DIC, and, due to the low initial concentration and the diatom uptake, dissolved CO_2 was almost depleted at the end of the culture experiment.

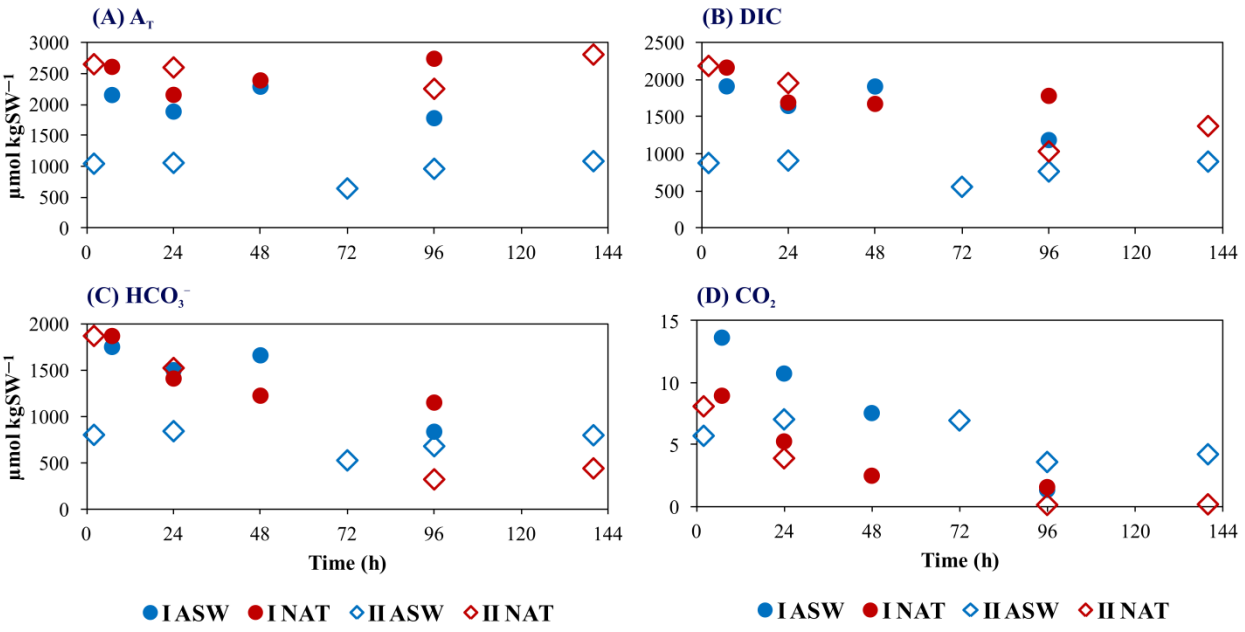

Fig. 5: Time variation of the concentrations of (A) total alkalinity (A_T), (B) dissolved inorganic carbon (DIC), (C) bicarbonate (HCO_3^-) and (D) dissolved CO_2 during *T. rotula* culture experiments. First (I) experiment is represented by circles and second (II) by diamonds. Blue symbols represent the artificial seawater medium (ASW) and red symbols the natural seawater medium (NAT).

Among the inorganic nitrogen species, nitrate (NO_3, Figure 6 A) was the most abundant in both conditions and experiments. NO_3 concentrations significantly decreased ($p < 0.05$) throughout the culture growth, with the highest values detected at the beginning and the lowest at the end of experiments. In the second experiment nitrate concentrations decreased to almost half of the initial value in both media, whereas a smaller variation (about 10%) was observed in the first experiment. Nitrite (NO_2, Figure 6 B) accounted for less than 1% of the total inorganic nitrogen species, and showed an opposite trend to nitrate ($p < 0.05$). Increase in nitrite concentrations could be related to ammonium oxidation and diatom release during nitrate uptake as a result of the accumulation of intermediate compounds during the reduction pathway leading to protein synthesis (Collos 1998). As well as nitrite, ammonium concentration (NH_4, Figure 6 C) was about 1% of the total inorganic nitrogen species, but exhibited different trend in the two experiments performed. In I, ammonium concentrations decreased throughout the culture growth, whereas in II ammonium decreased on the first day and then increased until the end of the experiment. The increase in NH_4 concentration could be related to prokaryotic remineralisation activity. Phosphate (PO_4, Figure 6 D) concentrations followed the same trend described for nitrate, with decreasing values throughout the culture growth. Only II ASW experiment showed a different pattern, indeed phosphate concentrations remained constant until 72 h, and then decreased to the minimum detected at 96 h (data of the last sampling are not available). As nitrate and phosphate, also silicate concentration (SiO_4, Figure 6 E) decreased after

the inoculation due to diatom uptake. At the end of the culture, in the second experiment silicate concentration was almost half of the initial amount, whereas a slighter decrease was observed in the first experiment.

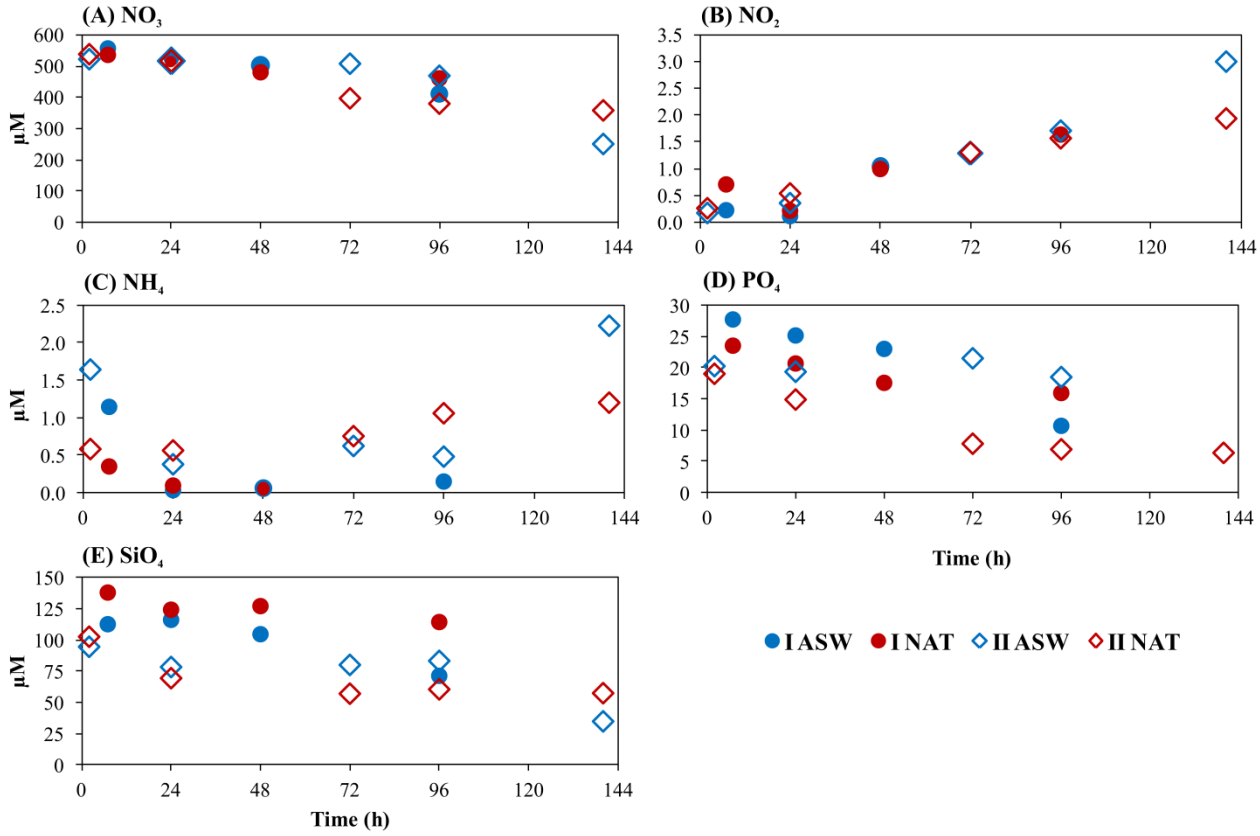

Fig. 6: Time variation of the concentrations of (A) nitrate (NO_3), (B) nitrite (NO_2), (C) ammonium (NH_4), (D) phosphate (PO_4), (E) silicate (SiO_4) during *T. rotula* culture experiments. First (I) experiment is represented by circles and second (II) by diamonds. Blue symbols represent the artificial seawater medium (ASW) and red symbols the natural seawater medium (NAT).

3.2. Isotope analysis

Dissolved inorganic carbon isotope values ($\delta^{13}C_{DIC}$) in the artificial seawater medium (Figure 7) increased with the proceeding of the algal growth in both experiments ($p < 0.05$). Indeed, in ASW minimum values were recorded at the beginning and the maxima on the last day of culture experiment, ranging from –43.2‰ to –30.1‰ in the I ASW, and from –44.5‰ to –33.1‰ in II ASW. Instead, $\delta^{13}C_{DIC}$ values in the natural seawater condition did not vary significantly, and ranged from –3.8‰ to –1.9‰ in I NAT, and from –2.5‰ to 1.6‰ in II NAT. $\delta^{13}C_{CO_2}$ and $\delta^{13}C_{HCO_3^-}$ (Figure 7) followed, as expected, the same trend as $\delta^{13}C_{DIC}$. $\delta^{13}C_{CO_2}$ values were lower of ~9‰ in both conditions because of carbonate system fractionation (Mook et al. 1974), whereas $\delta^{13}C_{HCO_3^-}$ values corresponded to $\delta^{13}C_{DIC}$ ones as bicarbonate was the most abundant carbonate species in the two media.

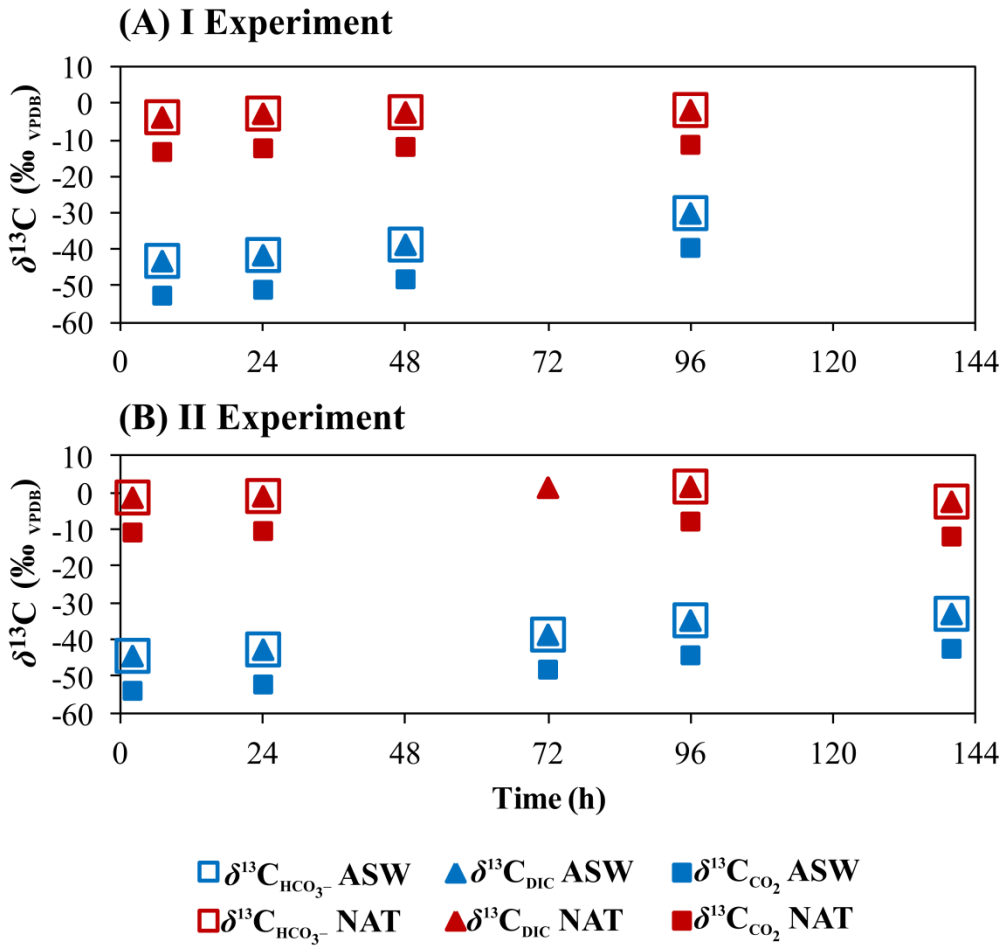

Fig. 7. Time variation of the isotopic composition of dissolved inorganic carbon ($\delta^{13}C_{DIC}$), dissolved CO_2 ($\delta^{13}C_{CO_2}$) and bicarbonate ($\delta^{13}C_{HCO_3^-}$) in the first (A) and second (B) experiment of *T. rotula* culture. Blue symbols represent the artificial seawater medium (ASW) and red symbols the natural seawater medium (NAT).

The initial POC isotope composition was similar in both conditions and experiments, with an overall average value of –24.4 ± 0.3‰ (Figure 8), as expected because of the same culture origin of the inoculated cells. However, algae $\delta^{13}C$ exhibited an opposite trend between the two conditions during diatom growth. In ASW, $\delta^{13}C_{POC}$ values significantly decreased ($p < 0.05$), reaching –39.0‰ in I ASW and –43.4‰ in II ASW at the end of the experiments. On the other hand, in the natural seawater condition, $\delta^{13}C_{POC}$ values slightly increased after the inoculation ($p < 0.05$), reaching the highest values at the end of the culture (–22.8‰ in I NAT; –18.5‰ in II NAT).

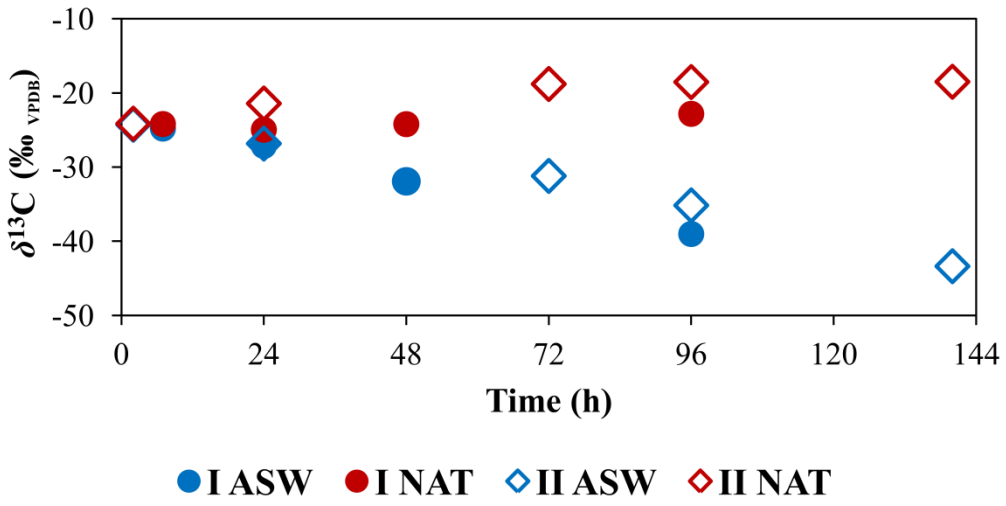

Fig. 8: Time variation of the isotopic composition of particulate organic carbon ($\delta^{13}C_{POC}$) during *T. rotula* culture experiments. First (I) experiment is represented by circles and second (II) by diamonds. Blue symbols represent the artificial seawater medium (ASW) and red symbols the natural seawater medium (NAT).

In order to take into account the effect of prokaryote biomass on $\delta^{13}C$ of the diatoms, the fraction of POC smaller than 10 µm ($\delta^{13}C_{POC<10µm}$) was analysed (Figure 9). Despite the common starting value (–25.2 ± 0.7‰), $\delta^{13}C_{POC<10µm}$ in ASW showed an opposite trend than in NAT, as already described for $\delta^{13}C_{POC}$. Indeed in ASW $\delta^{13}C_{POC<10µm}$ values decreased ($p < 0.05$), whereas in NAT values increased until the end of the experiments ($p < 0.05$).

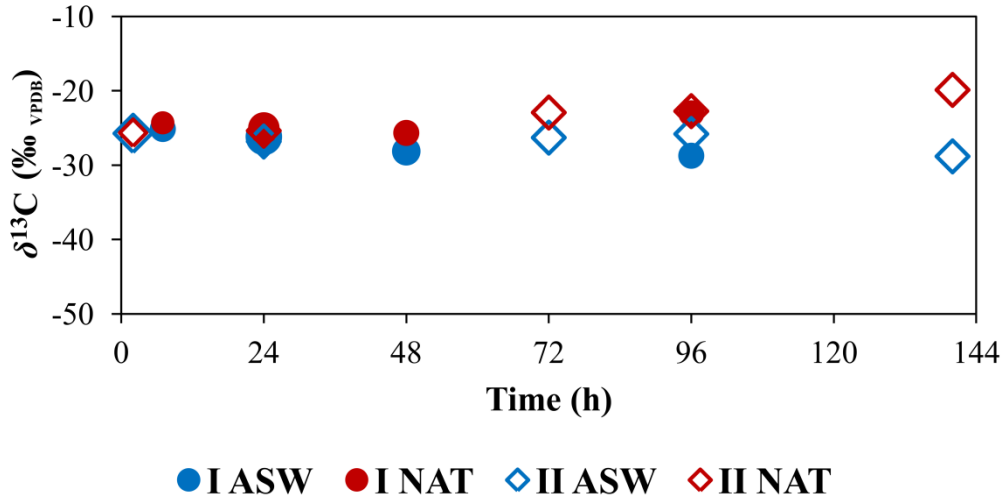

Fig. 9: Time variation of the isotopic composition of the fraction of POC smaller than 10µm ($\delta^{13}C_{POC<10µm}$) during *T. rotula* culture experiments. First (I) experiment is represented by circles and second (II) by diamonds. Blue symbols represent the artificial seawater medium (ASW) and red symbols the natural seawater medium (NAT).

4. Discussion

4.1. Phytoplankton growth and carbon stable isotopes

Thalassiosira rotula growth is well supported by the evolution of the chemical parameters analysed. The observed decrease of CO_2, HCO_3^- and NO_3 concentrations and the inverse correlation of phytoplankton abundance with PO_4 and SiO_4 concentrations ($p < 0.05$) in both media confirm microalgae growth. Moreover, the high fluctuations of pH and DO support diatom photosynthetic activity. Indeed, the highest values of pH and DO were always detected during the light period of the culture in relation with the highest diatom abundances as a result of inorganic carbon uptake and oxygen production. Microalgae did not show a simultaneous growth in the two conditions. Actually, in ASW the culture started to increase later than in NAT due to the acclimation time needed after the inoculation in the different medium. For this reason, in the natural condition, the maximum abundance was reached before the end of the experiments and consequently the culture started to decrease. Degradation of organic matter by the prokaryotes and remineralisation of nutrients are therefore expected to increase after the death of cells. The increase of NH_4 in the second half of the second experiment would support this assumption, but no correlation exists with prokaryotes abundances neither with nitrite concentrations. As Glibert et al. (2016 and references therein) reported, during nitrate uptake reduced nitrogen could be released as ammonium and nitrite in a dissimilatory pathway. The increase of nitrite concentrations also supports this hypothesis and could be the consequence of internal accumulation of intermediate compounds during nitrogen reduction for protein synthesis (Collos 1998).

The main purpose of the study is to test if stable isotope analysis could be a reliable tool in the identification of a leakage in an isotopically modified carbonate system. $\delta^{13}C_{DIC}$ values confirm that the experimental set-up was successful in the modification of the isotope composition of the carbonate species dissolved in water. CO_2 from cylinder used for the artificial medium preparation was strongly ^{13}C-depleted compared to atmospheric CO_2, therefore the isotope composition of DIC obtained in ASW was significantly lower than $\delta^{13}C_{DIC}$ in NAT ($p < 0.01$), and the same difference consequently applies to $\delta^{13}C_{CO_2}$ and $\delta^{13}C_{HCO_3^-}$ values. After the inoculation, diatoms immediately started to take up the inorganic carbon available, reflecting this information in their carbon isotope composition. Indeed, during photosynthesis, carbon fractionation occurs due to the preferential uptake of the lightest species (^{12}C) leading to ^{13}C-depleted values in phytoplankton in respect to the inorganic carbon source, and enriching the residual DIC in ^{13}C (Fry 1996). This typical behaviour of residual source enrichment is observed in both media, but a different pattern is detected in POC values

between ASW and NAT (Fig. 10). In the natural condition, $\delta^{13}C_{POC}$ values were always lower than $\delta^{13}C_{DIC}$, and this difference between source and phytoplankton isotope composition persisted throughout the whole duration of the experiments (Fig. 10 B). An apparent contradictory behaviour is observed in ASW condition, as $\delta^{13}C_{POC}$ values were higher than $\delta^{13}C_{DIC}$ until the third day of culture (72 h, Fig. 10 A). This apparent isotopic anomaly depends on the source of inorganic carbon used and on the experimental set-up. The aim of the experiments was to verify how the isotope composition of diatoms changed after the exposure to a modified medium, therefore no acclimation time followed inoculation. The diatom strain was grown in natural marine conditions until inoculation and consequently no significant change in $\delta^{13}C_{DIC}$ was experienced by the microalgae cultivated in NAT, resulting in slight modifications in POC isotope composition. On the other hand, once inoculated in the artificial seawater condition, microalgae still had their natural isotope composition, while $\delta^{13}C_{DIC}$ was strongly depleted, thus phytoplankton higher $\delta^{13}C$ values at the beginning of the experiments. In ASW a higher relative abundance of ^{12}C was available than in NAT due to the depleted source of CO_2 used for medium preparation, therefore $\delta^{13}C_{POC}$ values significantly decreased ($p < 0.05$) since the first day after the inoculation, even if diatom growth was slightly delayed than in NAT. A parallel significant enrichment ($p < 0.05$) in residual DIC was observed, until reaching similar values to $\delta^{13}C_{POC}$ at 96 h and higher values at the end of the II ASW experiment (Fig. 10 A). The rapid $\delta^{13}C_{POC}$ variation and the strong inverse correlations ($p < 0.01$) of $\delta^{13}C_{POC}$ with $\delta^{13}C_{DIC}$ and with phytoplankton abundance in ASW confirm that $\delta^{13}C_{POC}$ values depend mostly on the isotope ratio of the inorganic source of carbon used, and thus the isotope composition of phytoplankton could be used as an indicator of the $\delta^{13}C$ of anthropogenic CO_2 dissolved in seawater.

ASW and NAT exhibited a similar $\delta^{13}C_{POC}$ value at the beginning of the experiments, which is comparable to values observed in POC collected in the Gulf of Trieste (Faganeli et al. 2009; Tamše et al. 2014), typical for marine phytoplankton in estuarine area. The isotope composition of POC reached at the end of NAT experiments is closer to typical marine phytoplankton values in open Northern Adriatic Sea (–20.6‰, Giani et al. 2009), indicating that probably the starting values may be influenced by the culture medium in which the strain was grown before the inoculation.

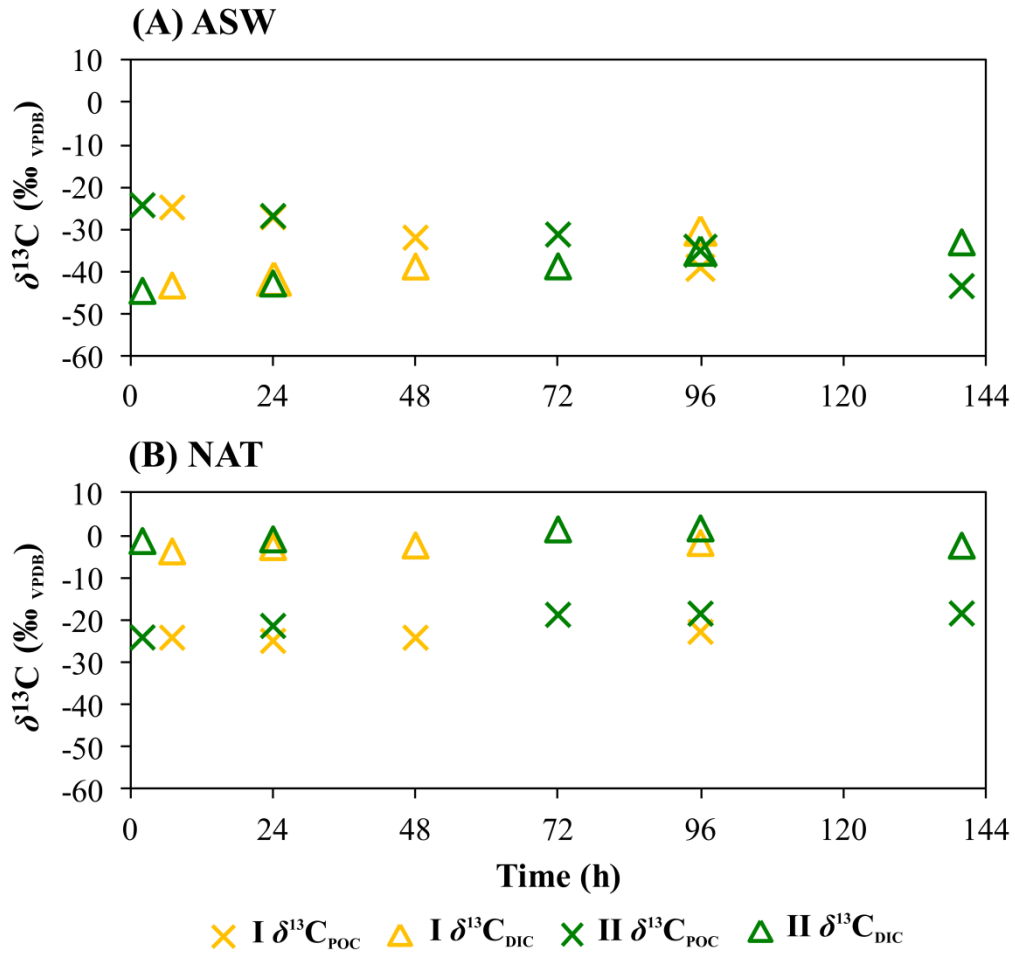

Fig. 10: Time variation of the isotopic composition of dissolved inorganic carbon ($\delta^{13}C_{DIC}$; triangles) and POC ($\delta^{13}C_{POC}$; crosses) in the artificial (ASW) (A) and natural (NAT) (B) medium during *T. rotula* culture experiments. Yellow symbols represent results from the first experiment (I) and green those of the second (II).

The isotope composition of diatoms grown in ASW is significantly different from that of the microalgae in NAT ($p < 0.01$), therefore carbon stable isotope analysis of phytoplankton could be a valid tool for the identification of different sources of carbon. This is confirmed by the non-metric multidimensional scaling analysis (nMDS), from which two groups can be clearly distinguished (Figure 11). The separation of the groups reflects the two conditions diatoms were exposed to (ASW and NAT), depending mostly on the vertical axis that includes the isotope composition of both POC and DIC. The strongest separation is evident at the final sampling times (96 h for I, 140 h for II), when the difference in $\delta^{13}C_{POC}$ values was the highest between ASW and NAT. The analysis of similarity (one-way ANOSIM) confirmed the significant difference between ASW and NAT ($p < 0.05$), even if with a certain degree of overlapping of the data ($R = 0.35$), probably related to the common starting condition of microalgae culture.

The presence of prokaryotes has been monitored in order to take into account its potential effect on the bulk POC isotope composition, since prokaryotes abundance increased in both media throughout the duration of the experiments. The results suggest that POC isotope composition was not altered by prokaryotes activity, indeed $\delta^{13}C_{POC<10\mu m}$ values followed the same trend as $\delta^{13}C_{POC}$ and no significant difference existed. Previous studies (Coffin et al., 1989; Hullar et al., 1996), actually, confirmed that heterotrophic prokaryotes isotope composition is generally close to or similar to that of the organic substrate provided, and this is consistent with the results of both experiments because, during algal growth in bioreactors, the only substrate for prokaryotes degradation was the phytoplankton-derived organic matter. Since no difference was detected between $\delta^{13}C_{POC<10\mu m}$ and the bulk $\delta^{13}C_{POC}$, it is possible to assume that the increase in prokaryotes biomass might have been non-significant in order to modify the bulk POC isotope composition. Moreover, $\delta^{13}C_{POC<10\mu m}$ values may not completely depend on prokaryotes biomass, but could be directly influenced by phytoplankton cells. *T. rotula* cell average dimension is about 20 µm (Hasle & Syvertson 1997), hence the choice of 10 µm mesh for removing phytoplankton from the bulk POC. Nevertheless, some isolated small or broken cells, not connected in chains, could have passed through 10 µm filter, and therefore could have affected the final $\delta^{13}C_{POC<10\mu m}$ results.

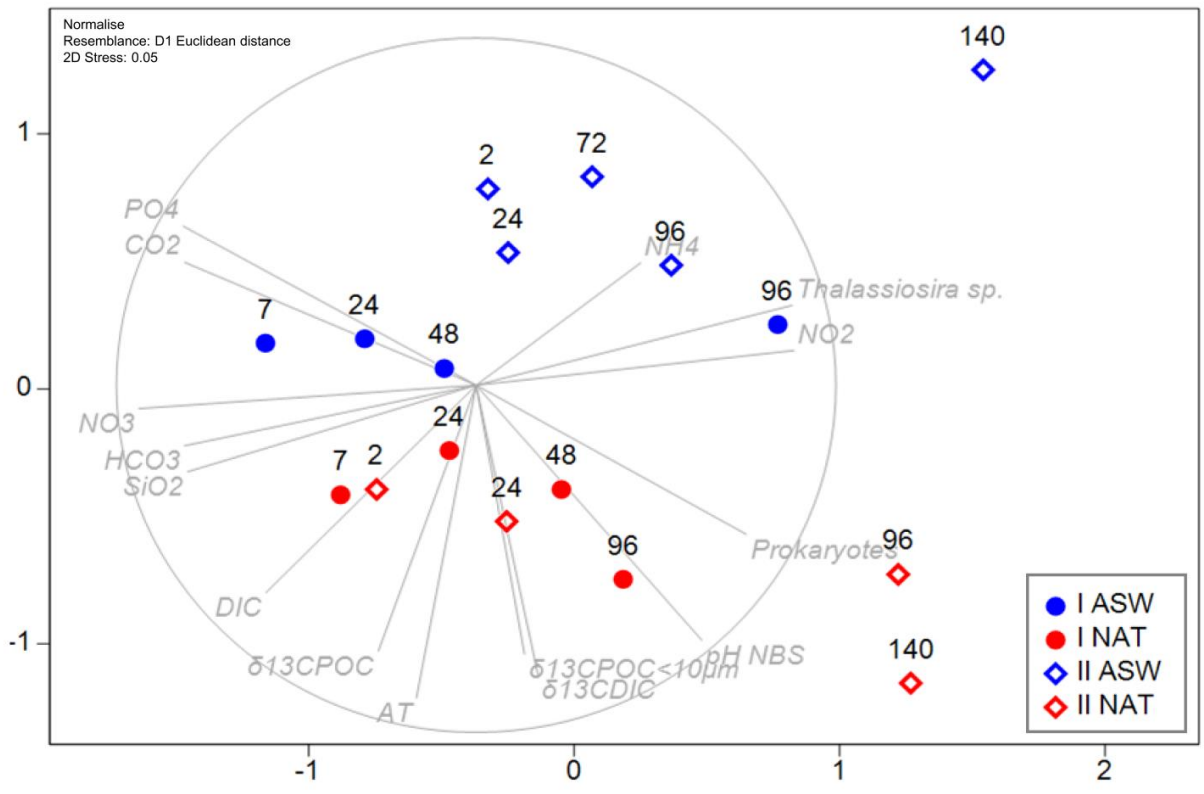

Fig. 11: Non-metric multidimensional scaling analysis of the *T. rotula* culture experiments. First (I) experiment is represented by circles and second (II) by diamonds. Blue symbols represent the artificial seawater medium (ASW) and red symbols the natural seawater medium (NAT). Numbers above symbols represent the sampling time (h).

According to the experiments results, carbon stable isotopes could be considered as valid tracers of the origin of inorganic carbon. Indeed, both $\delta^{13}C_{DIC}$ and $\delta^{13}C_{POC}$ were significantly influenced by the different source of carbon in the medium. In a real CCS site, the chemical composition of water column quickly changes after a leakage, and $\delta^{13}C_{DIC}$ is modified depending on CO_2 concentration released and on the environmental conditions. However, $\delta^{13}C_{DIC}$ values return to background levels due to mixing currents that rapidly disperse CO_2 both horizontally and vertically (Jones et al. 2015). In porewaters, where mixing processes could be slower than in the water column, $\delta^{13}C_{DIC}$ may return to baseline levels after a few weeks once the CO_2 release stopped (Lichtschlag et al. 2015). Therefore, a CO_2 leakage could be detected from $\delta^{13}C_{DIC}$ analysis only if sampling is close enough in time. On the other hand, the assessment of CO_2 leakages through microalgae $\delta^{13}C$ analysis gives the opportunity to gather a time integrated information, and thus even sporadic emissions, that otherwise would be hardly detectable from seawater analysis, could be identified.

4.2. Carbon isotope fractionation of *Thalassiosira rotula*

During the uptake of inorganic carbon for photosynthesis, fractionation (ε_p) occurs due to the inorganic carbon species used as substrate, to the different method of acquisition and to the enzyme involved in carboxylation (Ribulose-1,5-bisphosphate carboxylase/oxygenase – RuBisCO). The dominant physiological forcing factor of the CO_2-dependent ^{13}C fractionation in primary producers is the kinetic fractionation by RuBisCO, that fixes the lightest isotope ($^{12}CO_2$) at a rate 1.03 times faster than the heaviest ($^{13}CO_2$), leading to ^{13}C-depleted values in phytoplankton respect to the inorganic carbon source (Raven 1991).

Diatoms, as many other phytoplankton species, have developed CO_2-concentrating mechanisms (CCMs) for actively take up inorganic carbon and for increasing CO_2 concentration around RuBisCO. These mechanisms have evolved in order to prevent C-limitation as the high pH of the modern seas and the slow CO_2 diffusion rate in water are limiting factors for dissolved CO_2 availability and CO_2 concentrations in water are usually not sufficient to saturate RuBisCO fixation rates (Shen et al. 2017, and references therein). CCMs increase available inorganic carbon by active CO_2 and HCO_3^- transport and by the reversible dehydration of bicarbonate to CO_2 mediated by intra- and extra-cellular carbonic anhydrase (CA) enzymes. Experimental and genetic data confirmed that both HCO_3^- and CO_2 are possible substrates for diatom photosynthesis (Nimer et al. 1997; Colman et al. 2002, Giordano et al. 2005; Shen et al. 2017), and during the conversion of HCO_3^- to CO_2 a fractionation of ~10‰ occurs making bicarbonate uptake indistinguishable from direct CO_2 uptake (Riebesell & Wolf-Gladrow 1995). Because of the fractionation occurring in the conversion of HCO_3^- to CO_2,

$\delta^{13}C_{CO_2}$ values are used as external carbon source for the calculation of phytoplankton fractionation (Fig. 12), being CO_2 the carbon species ultimately used for photosynthesis.

Isotope fractionation (Fig. 12) of *Thalassiosira rotula* in the artificial seawater condition significantly increased during the experiments ($p < 0.01$) ranging from –28.6‰ to –0.6‰ in I, and from –30.4‰ to 0.9‰ in II. No significant variation was observed in I NAT fractionation, which ranged from 11.2‰ to 13.0‰, whereas a decrease was detected in II NAT (from 13.6‰ to 6.7‰). The approaching to 0‰ fractionation in ASW could be thought as an indication of C-limitation (Fry 2006). However, CO_2 and HCO_3^- concentrations in ASW were similar to those of NAT, but fractionation in the natural condition did not change significantly and did not indicate possible carbon limitation. In addition, in II ASW, despite the lower concentration of carbonate species and the highest abundance of diatoms, ε_p values were similar to I ASW, suggesting that the strong increase in fractionation in the artificial seawater medium depended mostly on the different $\delta^{13}C$ of the source of inorganic carbon, as also confirmed by the highly significant correlation of ε_p and $\delta^{13}C_{DIC}$ ($p < 0.01$). Moreover, despite the extremely low CO_2 concentrations at the end of the experiments in both conditions, *T. rotula* should not have suffered carbon limitation as HCO_3^- and DIC concentrations were still high enough for maintaining phytoplankton growth, even if no inorganic carbon was supplied after the inoculation.

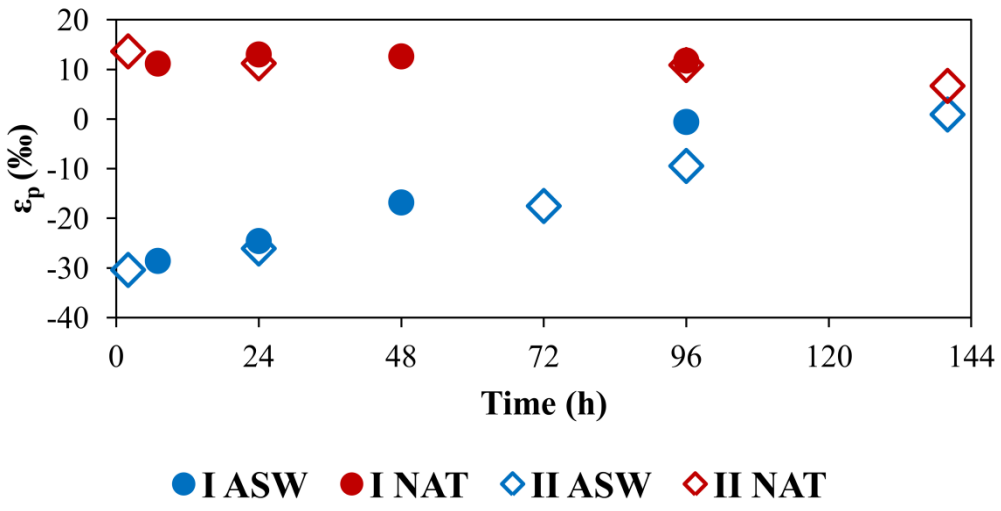

Fig. 12: Time variation of carbon fractionation (ε_p) of phytoplankton during *T. rotula* culture experiments. First (I) experiment is represented by circles and second (II) by diamonds. Blue symbols represent the artificial seawater medium (ASW) and red symbols the natural seawater medium (NAT).

The relationship between fractionation (ε_p) and growth rate/dissolved CO_2 concentration ratio ($\mu/[CO_2]$) was investigated (Fig. 13) to verify possible diffusive uptake of CO_2 in diatoms. As fractionation values in the artificial condition strongly depend on the highly ^{13}C-depleted carbon source, absolute ε_p values were used in the plot in order to bypass the influence of the very negative

values of fractionation in ASW. Moreover, as growth rates refer to the time interval of *T. rotula* exponential growth, the relationship between fractionation and $\mu/[CO_2]$ was only investigated in the same period of algal culture growth.

According to existing models of isotope fractionation in marine phytoplankton, a linear inverse relationship is predicted between ε_p and $\mu/[CO_2]$ if inorganic carbon uptake occurs only by CO_2 diffusive processes (Laws et al. 1995; Laws et al. 1997; Rau et al. 1996). The linear relationship ($p < 0.01$) was also observed in our study (Fig. 13) with ε_p of 22.6‰ at $\mu/[CO_2] = 0$. This value is lower than the expected range of fractionation due to Rubisco (25-28‰), but is consistent with the fractionation effect of carbon fixation in *Porosira glacialis* (Keller & Morel 1999). However, the observed correlation does not allow a certain differentiation between active uptake of CO_2 and of HCO_3^-. In the case of intracellularly conversion of HCO_3^- to CO_2, the carbon dioxide available for photosynthesis would be ^{13}C-enriched and ε_p would be smaller than predicted by purely diffusional transport. This effect would make data lie below the regression line, while $\delta^{13}C_{POC}$ data will be higher. In the case of the experiments presented, all data fit the regression line, except for one sample of II ASW (140 h) which plots completely away. This sample was obtained at the end of the culture experiment and is related to the lowest determined $\delta^{13}C_{POC}$ value (–43.4‰), and to the highest ASW fractionation of 0.9‰. The distance of this point from the others may be associated with C-limitation toward the end of the experiment, as a consequence of phytoplankton uptake and of the general lower carbonate species concentration due to an error in the preparation of the medium. For this reason, this point has been excluded from the regression line, as it would strongly condition the correlation. The possible CO_2 limitation could be confirmed by the other data of II ASW that lie below the regression line (96 h). *T. rotula*, as many other diatoms, has the potential to use bicarbonate as substrate, as also inferred by genetic analysis (Shen et al. 2017), and, as previous discussed, should not have suffered carbon limitation. Therefore, when CO_2 concentrations were too low, as in the case of II ASW, diatoms may have increased bicarbonate uptake through CCMs for sustaining culture growth, and the decrease in HCO_3^- concentrations (Fig. 5 C) supports this assumption.

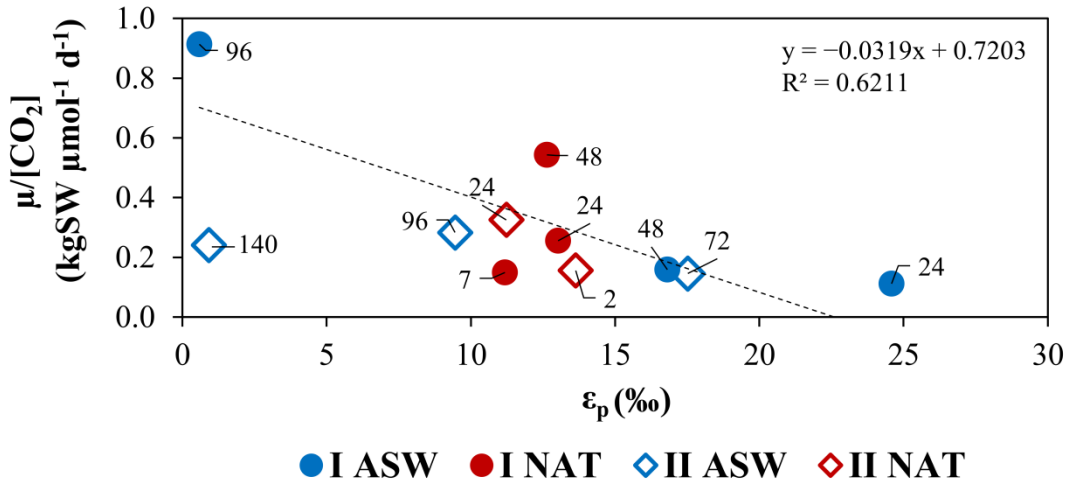

Fig. 13: Relationship between fractionation and the ratio of growth rate (μ) and dissolved CO_2 concentration ($[CO_2]$). Numbers associated to the symbols in the plot indicate sampling time (in hours). First (I) experiment is represented by circles and second (II) by diamonds. Blue symbols represent the artificial seawater medium (ASW) and red symbols the natural seawater medium (NAT).

5. Conclusions

The experiments demonstrate that the method tested is effective in the detection of changes in phytoplankton isotope composition depending on the different inorganic carbon source. Diatoms grown in the artificially modified condition were exposed to $\delta^{13}C_{DIC}$ values significantly different than the natural ones and, through photosynthetic fractionation, their carbon isotope composition quickly changed during algal growth. Therefore, this novel approach could give a valuable contribution for ocean management in the evaluation of anthropogenic impacts due to CO_2 release from carbon storage sites. The study was conducted in a model case approach, where the whole carbonate system isotope composition was modified. Further experiments will consider slighter anthropogenic CO_2 perturbations in a natural seawater carbonate system. Moreover, since the leakages are more likely to form plumes that impact the bottom and a few meters of water column, benthic microalgae will be tested as better indicators of a specific site (Jones et al. 2015; Tait et al. 2015).

Acknowledgments

This work has been done using the ECCSEL RI funded by the European Union's Horizon 2020 research and innovation program under grant agreement No 675206. It also represents a part of the project J1-8156: "Stable isotopes in the study of the impact of increasing CO_2 levels on C and Hg cycling in coastal waters" financially supported by Slovenian Research Agency and EU project

MASSTWIN - Spreading excellence and widening participation in support of mass spectrometry and related techniques in health, the environment and food analysis (H2020, grant agreement No 692241). We would like to thank Mirta Smodlaka Tankovic and Ana Baričević of the Ruđer Bošković Institute (Rovinj, Croatia) for performing genetic analysis, Sergio Predonzani and Matteo Bazzaro for the valuable help in the experiments set-up and sampling, Martina Kralj for nutrients analysis, Mauro Celussi for prokaryotes analysis and Alfred Beran for providing the culture and for the experiment preparation support.

References

Altschul SF, Madden TL, Schäffer AA, Zhang J, Zhang Z, Miller W, Lipman DJ (1997) Gapped BLAST and PSI-BLAST: a new generation of protein database search programs. Nucleic Acids Res 25:3389–402.

Alverson AJ (2008) Molecular systematics and the diatom species. Protist 159, 339–353. doi:10.1016/j.protis.2008.04.001.

Andersen RA (2005) Algal Culturing Techniques, 1st ed. Elsevier Academic Press, Burlington, Mass.

Becker V, Myrttinen A, Blum P, Van Geldern R, Barth JAC (2011) Predicting $\delta^{13}C_{DIC}$ dynamics in CCS: A scheme based on review on inorganic carbon chemistry under elevated pressures and temperatures. Int J Greenh Gas Control 5:1250–1258. doi:10.1016/j.ijggc.2011.05.001.

Blackford J, Bull JM, Cevatoglu M, Connelly D, Hauton C, James RH, Lichtschlag A, Stahl H, Widdicombe S, Wright IC (2015) Marine baseline and monitoring strategies for carbon dioxide capture and storage (CCS). Int J Greenh Gas Control 38:221–229. https://doi.org/10.1016/j.ijggc.2014.10.004.

Celussi M, Malfatti F, Franzo A, Gazeau F, Giannakourou A, Pitta P, Tsiola A, Del Negro P, (2015) Ocean acidification effect on prokaryotic metabolism tested in two diverse trophic regimes in the Mediterranean Sea. Estuar Coast Shelf Sci 186:125-138. https://doi.org/10.1016/j.ecss.2015.08.015.

Clark K, Karsch-Mizrachi I, Lipman DJ, Ostell J, Sayers EW (2016) GenBank. Nucleic Acids Res. 44:D67-72. doi: 10.1093/nar/gkv1276.

Clarke KR, Gorley RN, Somerfield PJ, Warwick RM (2014) Change in marine communities: An approach to statistical analysis and interpretation, 3rd ed. PRIMER-E, Plymouth, UK.

Coffin RB, Fry B, Wright RT (1989) Carbon isotopic compositions of estuarine bacteria. Limnol Oceanogr 34:1305–1310.

Collos Y (1998) Nitrate uptake, nitrite release and uptake, and new production estimates. Mar Ecol Prog Ser 171:293–301. doi: 10.3354/meps171293.

Colman B, Huertas E, Bhatti S, Dason JS (2002) The diversity of inorganic carbon acquisition mechanisms in eukaryotic microalgae. Funct Plant Biol 29:261–270. doi: 10.1071/PP01184.

De Coninck H, Benson SM (2014) Carbon dioxide capture and storage: issues and prospects. Annu Rev Environ Resour 39:243–270. 10.1146/annurev-environ-032112-095222.

Dickson AG (1990) Standard potential of the reaction: $AgCl_{(s)} + 1/2\ H_{2(g)} = Ag_{(s)} + HCl_{(aq)}$, and the standard acidity constant of the ion HSO_4^- in synthetic sea water from 273.15 to 318.15 K. J Chem Thermodyn 22:113-127. doi: 10.1016/0021-9614(90)90074-z.

Dickson AG, Millero FJ (1987) A comparison of the equilibrium constants for the dissociation of carbonic acid in seawater media. Deep-Sea Res A, Oceanogr Res Pap 34:1733–1743.

Dickson AG, Sabine CL, Christian JR (2007) Guide to best practices for ocean CO_2 measurements. PICES Special Publication 3, 191 pp. Standard operating procedure (SOP) 3b, Determination of total alkalinity in sea water using an open-cell titration.

Faganeli J, Ogrinc N, Kovac N, Kukovec K, Falnoga I, Mozetič P, Bajt O (2009) Carbon and nitrogen isotope composition of particulate organic matter in relation to mucilage formation in the northern Adriatic Sea. Mar Chem 114:102–109. doi:10.1016/j.marchem.2009.04.005.

Farquhar GD, Ehleringer JR, Hubick KT, City SL (1989) Carbon isotope discrimination and photosynthesis. Annu Rev Plant Physiol 40:503–537. doi:10.1146/annurev.pp.40.060189.002443.

Flude S, Johnson G, Gilfillan SMV, Haszeldine RS (2016) Inherent tracers for carbon capture and storage in sedimentary formations: composition and applications. Environ Sci Technol 50:7939-7955. doi: 10.1021/acs.est.6b01548.

Freeman KH, Hayes JM (1992) Fractionation of carbon isotopes by phytoplankton and estimates of ancient CO_2 levels. Global Biogeochem Cycles 6:185–198.

Fry B (1996) $^{13}C/^{12}C$ fractionation by marine diatoms. Mar Ecol Prog Ser 134:283-294.

Fry B (2006) Stable isotope ecology, 1st ed., Springer, New York.

Gattuso JP, Gao K, Lee K, Rost B, Schulz KG (2010) Approaches and tools to manipulate the carbonate chemistry, in: Riebesell U, Fabry VJ, Hansson L, Gattuso JP (Eds.), Guide for best practices in ocean acidification research and data reporting. Office for official publications of the European Union, Luxembourg.

Giani M, Berto D, Rampazzo F, Savelli F, Alvisi F, Giordano P, Ravaioli M, Frascari F (2009) Origin of sedimentary organic matter in the north-western Adriatic Sea. Estuar Coast Shelf Sci 84:573-583.8

Giordano M, Beardall J, Raven JA (2005) CO_2 concentrating mechanisms in algae: mechanisms, environmental modulation, and evolution. Annu Rev Plant Biol 56:99–131. doi: 10.1146/annurev.arplant.56.032604.144052.

Glibert PM, Wilkerson FP, Dugdale RC, Raven JA, Dupont CL, Leavitt PR, Parker AE, Burkholder JM, Kana TM (2016) Pluses and minuses of ammonium and nitrate uptake and assimilation by phytoplankton and implications for productivity and community composition, with emphasis on nitrogen-enriched conditions. Limnol Oceanogr 61:165–197. doi:10.1002/lno.10203.

Hansen HP (1999) Determination of oxygen. In: Grasshoff K, Kremling K, Ehrhardt M (Eds.), Methods of seawater analysis, 3rd ed. Wiley-VCH, Weinheim.

Hansen HP, Koroleff F (1999) Determination of nutrients. In: Grasshoff K, Kremling K, Ehrhardt M (Eds.), Methods of seawater analysis, 3rd ed. Wiley-VCH, Weinheim.

Hasle GR, Syvertson EE (1997) Marine Diatoms. In: Tomas CR (Ed.) Identifying marine phytoplankton, 1st ed. Academic Press, USA.

Hellevang H, Aagaar P (2015) Constraints on natural global atmospheric CO_2 fluxes from 1860 to 2010 using a simplified explicit forward model. Sci Rep 5:17352; doi: 10.1038/srep17352.

Hullar MAJ Fry B, Peterson BJ, Wright RT (1996) Microbial utilization of estuarine dissolved organic carbon: a stable isotope tracer approach tested by mass balance. Appl Environ Microbiol 62: 2489–2493.

Ingrosso G, Giani M, Cibic T, Karuza A, Kralj M, Del Negro P (2016) Carbonate chemistry dynamics and biological processes along a river–sea gradient (Gulf of Trieste, northern Adriatic Sea). J Mar Syst 155:35–49. https://doi.org/10.1016/j.jmarsys.2015.10.013.

IPCC (2005) IPCC special report on carbon dioxide capture and storage. Prepared by Working Group III of the Intergovernmental Panel on Climate Change [Metz B, Davidson O, de Coninck HC, Loos M, Meyer LA (eds.)]. Cambridge University Press, Cambridge, United Kingdom and New York, NY, USA.

IPCC (2014) Climate Change 2014: Impacts, Adaptation, and Vulnerability. Part A: Global and Sectoral Aspects. Contribution of Working Group II to the Fifth Assessment Report of the Intergovernmental Panel on Climate Change [Field CB, Barros VR, Dokken DJ, Mach KJ, Mastrandrea MD, Bilir TE, Chatterjee M, Ebi KL, Estrada YO, Genova RC, Girma B, Kissel ES, Levy AN, MacCracken S, Mastrandrea PR, White LL (eds.)]. Cambridge University Press, Cambridge, United Kingdom and New York, NY, USA.

Jeandel E, Battani A, Sarda P (2010) Lessons learned from natural and industrial analogues for storage of carbon dioxide. Int J Greenh Gas Control 4:890–909. doi:10.1016/j.ijggc.2010.06.005.

Jones DG, Beaubien SE, Blackford JC, Foekema EM, Lions J, De Vittor C, West JM, Widdicombe S, Hauton C, Queirós AM (2015) Developments since 2005 in understanding potential environmental impacts of CO_2 leakage from geological storage. Int J Greenh Gas Control 40:350–377. http://dx.doi.org/10.1016/j.ijggc.2015.05.032.

Kim H, Kim YH, Kang SG, Park YG (2016) Development of environmental impact monitoring protocol for offshore capture and storage (CCS): A biological perspective. Environ Impact Asses Rev 57:139–150. http://dx.doi.org/10.1016/j.eiar.2015.11.004.

Kearse M, Moir R, Wilson A, Stones-Havas S, Cheung M, Sturrock S, Buxton S, Cooper A, Markowitz S, Duran C, Thierer T, Ashton B, Meintjes P, Drummond A (2012) Geneious Basic: an integrated and extendable desktop software platform for the organization and analysis of sequence data. Bioinformatics 28:1647–9. doi:10.1093/bioinformatics/bts199.

Keller K, Morel FMM (1999) A model of carbon isotopic fractionation and active carbon uptake in phytoplankton. Mar Ecol Prog Ser 182:295–298.

Laws EA, Popp BN, Bidigare RR, Kennicutt MC, Macko SA (1995) Dependence of phytoplankton carbon isotopic composition on growth rate and $[CO_2]_{aq}$: theoretical considerations and experimental results. Geochim Cosmochim Acta 59:1131–1138.

Laws EA, Bidigare RR, Popp BN (1997) Effects of growth rate and CO_2 concentration on carbon isotopic fractionation by the marine diatom *Phaeodactylum tricornutum*. Limnol Oceanogr 42:1552–1560.

Le Quéré C, Peters GP, Andres RJ, Andrew RM, Boden T, Ciais P, Friedlingstein P, Houghton RA, Marland G, Moriarty R, Sitch S, Tans P, Arneth A, Arvanitis A, Bakker DCE, Bopp L, Canadell JG, Chini LP, Doney SC, Harper A, Harris I, House JI, Jain AK, Jones SD, Kato E, Keeling RF, Goldewijk K, Körtzinger A, Koven C, Lefèvre N, Omar A, Ono T, Park GH, Pfeil B, Poulter B, Raupach MR, Regnier P, Rödenbeck C, Saito S, Schwinger J, Segschneider

J, Stocker BD, Tilbrook B, van Heuven S, Viovy N, Wanninkhof R, Wiltshire A, Zaehle S, Yue C (2013) Global carbon budget 2013. Earth Syst Sci Data Disc 6:689–760.

Lewis E, Wallace DWR (1998) Program developed for CO_2 System calculations, ORNL/CDIAC-105, Carbon Dioxide Information Analysis Center, Oak Ridge National Laboratory, U.S. Department of Energy, Oak Ridge, Tennessee.

Lichtschlag A, James RH, Stahl H, Connelly D (2015) Effect of a controlled sub-seabed release of CO_2 on the biogeochemistry of shallow marine sediments, their pore waters, and the overlying water column. Int J Greenh Gas Control 38:80–92. http://dx.doi.org/10.1016/j.ijggc.2014.10.008.

MacGillivary ML, Kaczmarska I (2011) Survey of the efficacy of a short fragment of the *rbc*L gene as a supplemental DNA barcode for diatoms. J Eukaryot Microbiol 58:529–536. doi: 10.1111/j.1550-7408.2011.00585.x.

Mancinelli G, Vizzini S (2015) Assessing anthropogenic pressures on coastal marine ecosystems using stable CNS isotopes: State of the art, knowledge gaps, and community-scale perspectives. Estuar Coast Shelf Sci 156:195–204.

Marie D, Brussaard CPD, Thyrhaug R, Bratbak G, Vaulot D (1999) Enumeration of marine viruses in culture and natural samples by flow cytometry. Appl Environ Microb 65:45–52.

Mayer B, Shevalier M, Nightingale M, Kwon JS, Johnson G, Raistrick M, Hutcheon I, Perkins E (2013) Tracing the movement and the fate of injected CO_2 at the IEA GHG Weyburn-Midale CO_2 Monitoring and Storage project (Saskatchewan, Canada) using carbon isotope ratios. Int J Greenh Gas Control 16S:S177–S184. http://dx.doi.org/10.1016/j.ijggc.2013.01.035.

Mayer B, Humez P, Becker V, Dalkhaa C, Rock L, Myrttinen A, Barth JAC (2015) Assessing the usefulness of the isotopic composition of CO_2 for leakage monitoring at CO_2 storage sites: A review. Int J Greenh Gas Control 37:46–60. https://doi.org/10.1016/j.ijggc.2015.02.021.

Mehrbach C, Culberson CH, Hawley JE, Pytkowics RM (1973) Measurement of the apparent dissociation constants of carbonic acid in seawater at atmospheric pressure. Limnol Oceaneanogr 18:897–907.

Mook WG, Bommerson JC, Staverman WH (1974) Carbon isotope fractionation between dissolved bicarbonate and gaseous carbon dioxide. Earth Planet Sci Lett 22:169–176. doi:10.1016/0012-821X(74)90078-8.

Nimer NA, Iglesias-Rodriguez MD, Merrett MJ (1997) Bicarbonate utilization by marine phytoplankton species. J Phycol 33:625–631.

Noble RRP, Stalker L, Wakelin SA, Pejcic B, Leybourne MI, Hortle AL, Michael K (2012) Biological monitoring for carbon capture and storage – A review and potential future developments. Int J Greenh Gas Control 10:520–535. http://dx.doi.org/10.1016/j.ijggc.2012.07.022.

Oudot C, Gerard R, Morin P (1988) Precise shipboard determination of dissolved oxygen (Winkler procedure) for productivity studies with commercial system. Limnol Oceanogr 33:146-150. doi: 10.4319/lo.1988.33.1.0146.

Rau GH, Riebesell U, Wolf-Gladrow DA (1996) A model of photosynthetic ^{13}C fractionation by marine phytoplankton based on diffusive molecular CO_2 uptake. Mar Ecol Prog Ser 133:275–285. doi:10.3354/meps133275.

Raven JA (1991) Physiology of inorganic C acquisition and implications for resource use efficiency by marine phytoplankton: relation to increased CO_2 and temperature. Plant Cell Environ 14:779–794. doi:10.1111/j.1365-3040.1991.tb01442.x.

Riebesell U, Wolf-Gladrow DA (1995) Growth Limits on Phytoplankton. Nature. 373:28. doi:10.1038/373028b0.

Shen C, Dupont CL, Hopkinson BM (2017) The diversity of carbon dioxide-concentrating mechanisms in marine diatoms as inferred from their genetic content. J Exp Bot 68:3937–3948. doi:10.1093/jxb/erx163.

Tait K, Stahl H, Taylor P, Widdicombe S (2015) Rapid response of the active microbial community to CO_2 exposure from a controlled sub-seabed CO_2 leak in Ardmucknish Bay (Oban, Scotland). Int J Greenh Gas Control 38:171–181. http://dx.doi.org/10.1016/j.ijggc.2014.11.021.

Tamše S, Mozetič P, Francé J, Ogrinc N (2014) Stable isotopes as a tool for nitrogen source identification and cycling in the Gulf of Trieste (Northern Adriatic). Cont Shelf Res 91:145–157. http://dx.doi.org/10.1016/j.csr.2014.09.009.

Throndsen J (1978) Preservation and Storage, pp 69-74. In: Sournia, A. (Eds.), Phytoplankton Manual. Monographs on oceanographic methodology 6. UNESCO, Paris.

Uppström LR (1974) The boron/chlorinity ratio of the deep-sea water from the Pacific Ocean. Deep-Sea Res Oceanogr Abstr 21:161–162. doi: https://doi.org/10.1016/0011-7471(74)90074-6.

Warwick PD, Ruppert LF (2016) Carbon and oxygen isotopic composition of coal and carbon dioxide derived from laboratory coal combustion: A preliminary study. Int J Coal Geol 166:128–135. https://doi.org/10.1016/j.coal.2016.06.009.

Zeebe RE, Wolf-Gladrow DA (2001) CO_2 in Seawater: Equilibrium, Kinetics, Isotopes, 2nd ed. Elsevier Oceanographic Series, Amsterdam.

CHAPTER 5

Assessment of biodegradable dissolved organic matter (BDOM) and nutrients utilization in coastal seawater using a plug-flow bioreactor

Federica Relitti[1,2*], Cinzia De Vittor[1], Paola Del Negro[1]

[1] Oceanography Division, OGS (Istituto Nazionale di Oceanografia e di Geofisica Sperimentale), Trieste, Italy

[2] Department of Life Science, University of Trieste, Trieste, Italy

[*]**Corresponding author: Federica Relitti**

OGS (Istituto Nazionale di Oceanografia e di Geofisica Sperimentale), Oceanography Division

Via A. Piccard 54, 34151 Trieste, Italy

Tel.: +39 040 2249741

email: frelitti@inogs.it

In preparation for submission

Abstract

Marine dissolved organic matter (DOM) is one of the major active reservoirs of the global carbon cycle. It is a complex mixture of poorly characterized compounds of carbon (DOC), nitrogen (DON), phosphorous (DOP) and the ability of heterotrophic bacteria to use DOM defines the biodegradable fraction (BDOM). It this study a plug-flow bioreactor is used for the evaluation of DOM bioavailability in seawater, in order to confirm the effectiveness of this tool for the assessment of bioavailable DOC (BDOC), and to verify its functionality for the evaluation of DON and DOP degradation and inorganic nutrient uptake in a P-limited system (Gulf of Trieste, Northern Adriatic Sea). Bioreactor colonisation was performed using 1.0 µm filtered seawater, and after functionality tests several experiments were conducted. A first series of experiments was performed in February-March 2017 (WIN) on samples collected in the coastal station OGS-1; a second series was collected in August-September 2017 (SUM) in 4 different stations, one inside a marine protected area (C1) and the others at different distance of the diffusional zone of the sewage duct (SS-1, SS-2, SS-3). During WIN, the influence of freshwater was also tested (OGS-2 station) and in SUM a parallel series of experiments (SUM+NUT) was conducted after the addition of inorganic nutrients in order to investigate the effect on DOM microbial degradation. The results suggest a high variability in DOM composition in the area as DOM pool did not show any relationship with inorganic nutrient, and this was confirmed by the treatment of nitrate and phosphate addition (SUM+NUT). The supply of low-salinity water (OGS-2) supported the presence of differently specialised communities inside the bioreactor, as all DOM species were released because of osmotic stress, but uptake of all inorganic nutrients was clearly observed. The results confirm bioreactor as a valid tool for BDOC analysis, but further research is needed in order to define its effectiveness for the evaluation of DON and DOP bioavailability and nutrient utilisation.

Keywords

LDOM, BDOC, BDON, BDOP, Nutrients, Plug-flow bioreactor, Coastal seawater

1. Introduction

Marine dissolved organic matter (DOM) is one of the major active reservoirs of the global carbon cycle as it represents the largest pool of reduced carbon in ocean (662 PgC; Hansell et al. 2009), that is comparable to the atmospheric reservoir of inorganic carbon (Hedges 1992). DOM is a complex mixture of poorly characterized compounds of carbon (DOC), nitrogen (DON), phosphorous (DOP)

(Kujawinski et al. 2011), and has a crucial role in the functioning of marine ecosystems. In coastal areas, DOM largely derives from phytoplankton biomass, zooplankton grazing activities (e.g. sloppy feeding, dissolution of faecal pellets), viral lysis and advection of organic matter of terrestrial origin through rivers (Hansell & Carlson 2015; De Vittor et al. 2008; Dinasquet et al. 2013). An important portion of DOM is processed and consumed by heterotrophic bacteria in the microbial loop (Azam et al. 1983), thus energy and nutrients are delivered to higher trophic levels and part of DOM is remineralized back to its inorganic constituents (Hansell & Carlson 2015). About 50% or more of carbon fixed by phytoplankton is released as DOM and processed by heterotrophic bacteria, however an important fraction accumulates in surface waters and is resistant to rapid microbial degradation (Hansell & Carlson 2015). DOM is divided into three fractions in function of its lability (Hansell & Carlson 2015, and references therein): (1) a labile fraction (LDOM), with turnover time of minutes to days; (2) a semi-labile fraction (SLDOM), with turnover time of months to years; (3) a refractory fraction (RDOM), with a turnover time of centuries to millennia. The turnover of DOM depends on both biological and abiotic processes, and the ability of heterotrophic bacteria to use DOM as both a carbon source and an electron donor (Hansen & Carlson 2015) defines the biodegradable fraction of DOM (BDOM). Spatial and temporal variations in DOM production and removal affect the long-term carbon storage (Santinelli et al. 2010; Hansell 2013; Hansell & Carlson 2015), RDOM then plays a critical role in carbon sequestration and changes in its lability could influence the global carbon cycle (Hansell & Carlson 2015) and the whole marine ecosystem (Santinelli et al. 2013). The biogeochemical processes involved in the mineralisation and persistence of DOM are still not known, hence the significance of gaining insights into heterotrophic bacteria processing of DOM for better understand global carbon cycle and prevent the adverse effects of climate change (Letscher et al. 2015; Dinasquet et al. 2013). DOM production and degradation should be tightly coupled since phytoplankton-derived organic matter sustains bacterial production, however, several factors are involved in the uncoupling of these processes resulting on DOM accumulation (Malfatti et al. 2014; Larato et al. 2010). Heterotrophic prokaryotes are the only marine organisms capable of both releasing inorganic nutrients through organic matter mineralization and of using inorganic nutrients in order to balance their N and P needs (Santinelli et al. 2012), therefore nutrient limitation could severely affect DOM degradation. Indeed, according to Fajon et al. (1999), the ability of bacteria to use the C-rich substrate is limited when P is lacking and Thingstad et al. (1997) noticed that, in nutrient limited conditions, bacteria cannot consume all the degradable DOC released from the food web as fast as it is produced possibly leading to its accumulation in some marine environments (Fonda Umani et al. 2007). Therefore, the coupling of the processes related to carbon and nutrient cycling is of particular interest as they regulate the carbon sequestration in DOM pool (Malfatti et al. 2014;

Lipizer et al. 2012). Though stoichiometry drives the key role that DOM plays in marine biogeochemical cycles, currently the main improvement in knowledge is on DOC dynamics, whereas information on DON and DOP is still scarce in both the oceans and the Mediterranean Sea (Santinelli et al. 2012 and references therein).

As DOM availability to heterotrophic prokaryotes is controlled by several factors (e.g. chemical composition, inorganic nutrient, microbial community structure, and expression of enzymes (Hansell & Carlson 2015)), a direct evaluation of BDOM is difficult and different methods have been applied for an indirect estimation of its amount. Biological availability of DOC has been generally assessed by batch culture experiments, with long incubation periods of 10-30 days (Søndergaard et al. 2000; Kragh & Søndergaard 2009; Zwifel et al. 1993) or even more (Hopkinson et al. 2002; Lønborg et al. 2009; Lønborg & Søndergaard 2009; Lønborg & Álvarez-Salgado 2012 and references therein; Knudsen-Leerbeck et al. 2017; Lønborg et al. 2010), and analysis of bacteria carbon demand and bacterial growth efficiency have been frequently used as an evaluation of DOC consumption (Hansell & Carlson 2015). All these methods require long analysis period time, thus it is hard to use these approaches for the evaluation of temporal variability in the distribution of BDOM, which instead would be an important information especially in coastal systems where riverine DOM can quickly change composition of marine organic matter and favour phytoplankton bloom or microbial degradation. Faster methods have been developed (De Vittor et al. 2009 and references therein) by means of bioreactors and the use of entrapped microbial cells in order to accelerate colonisation and increase microbial abundance. De Vittor et al. (2009) demonstrated that the application of plug-flow bioreactors for the assessment of BDOC in seawater allows to get reliable BDOC results, comparable to those obtained by batch culture experiments, and significantly reducing the experimental time (a few hours instead than 20-30 days). Moreover, bioreactors capability of DOC degradation is even higher than batch culture (20% more) (Søndergaard & Worm 2001). This broad metabolic capability results from the unidirectional supply of DOM and inorganic nutrients, guaranteed by the continuous water flow that generates a longitudinal gradient of diminishing DOC quantity and quality within the reactor. Indeed, in the bioreactor the more labile molecules would be consumed first while the more recalcitrant (semilabile DOC) would be metabolised over progressively longer residence time (i.e. distance from inlet). This gradient, clearly visible by the different colour of inert support, allows the establishment of multiple niches and selects diverse communities of bacteria capable of metabolise gradually more recalcitrant compounds otherwise difficult to be degraded in batch cultures with a less diverse environment (Søndergaard & Worm 2001; De Vittor et al. 2009; Volk et al. 1997).

Bioreactors have been already used for the evaluation of DOC biovailability in different environments (Søndergaard & Worm 2001; De Vittor et al. 2009), but only in a few studies this approach has been

used for the assessment of DON and DOP degradation (Zhao & Lio 2013; Badr et al. 2008). To our knowledge, no published research exists about the evaluation of BDOC together with the biodegradable fractions of DON (BDON) and DOP (BDOP) and nutrient uptake on seawater by means of bioreactors. Inorganic nutrient uptake, indeed, together with the resistance of compounds to microbial attack, leads to DOM accumulation in marine systems. Therefore, the identification of the biodegradable fractions of DOC, DON and DOP together with information on nutrient uptake could give important insights in the understanding of DOM cycling. Following De Vittor et al. (2009) research, this study aims at the application of a plug-flow bioreactor for the evaluation of DOM bioavailability in seawater. The main purpose is to confirm the effectiveness of this tool for the assessment of BDOC, and to verify its functionality for the evaluation of DON and DOP degradation and inorganic nutrient uptake.

2. Material and methods

2.1. Study area

The Gulf of Trieste (Fig. 1) is a shallow (<25 m depth), semi-enclosed coastal zone characterised by pronounced seasonal cycles of seawater temperatures (5-26 °C) and the formation of strong salinity gradients (25-38) due to runoff and seawater exchange at the open boundary. The occurrence of persistent cooling periods in late autumn and winter causes frequent events of dense water formation (Cozzi et al. 2012). Freshwater input from the Isonzo River severely affects the surface circulation and the vertical structure of the water column; indeed together with high sea surface temperature, it enhances the annual thermal stratification occurring from spring to autumn. The hydrology of the area is also influenced by several submarine freshwater springs scattered along the eastern karstic coast. Nutrient loadings in the Gulf of Trieste depend mostly on freshwater inputs from rivers and urban and industrial sewages discharge (Cozzi et al. 2012; Fonda Umani et al. 2007; Lipizer et al. 2011). The major sewage discharges derive from the Servola disposal plant. Notwithstanding the continuous inputs, in recent years the Gulf of Trieste has evolved towards oligotrophic conditions as a result of a reduction in nutrient supply (Mozetič et al. 2010), especially in phosphorous. The area is characterised by an annual cycle of phytoplankton, with an intense late winter diatom bloom, a nutrient depleted summer and a second short-lasting fall bloom, while heterotrophic bacteria consumption reaches maximum in summer (Fonda Umani et al. 2007, 2012; De Vittor et al. 2008).
A clear seasonality is then identified in DOC concentrations (De Vittor et al. 2008, 2009). Indeed, phytoplankton bloom in late winter-early spring produces fresh DOC (Hansell 2013; De Vittor et al.

2008; Fonda Umani et al. 2012), that should be mainly composed of labile compounds, whereas in summer DOC accumulates, being mainly composed of refractory organic matter (Fonda Umani et al. 2007, 2012, De Vittor et al. 2008). Accumulation of DOM is recognised as the result of nutrient, in particular phosphorus (Thingstad & Rassoulzadegan 1995), limitation in the area, that prevents the ability of heterotrophic bacteria to degrade all DOM released from the food web as fast as it is produced (Thingstad et al. 1997).

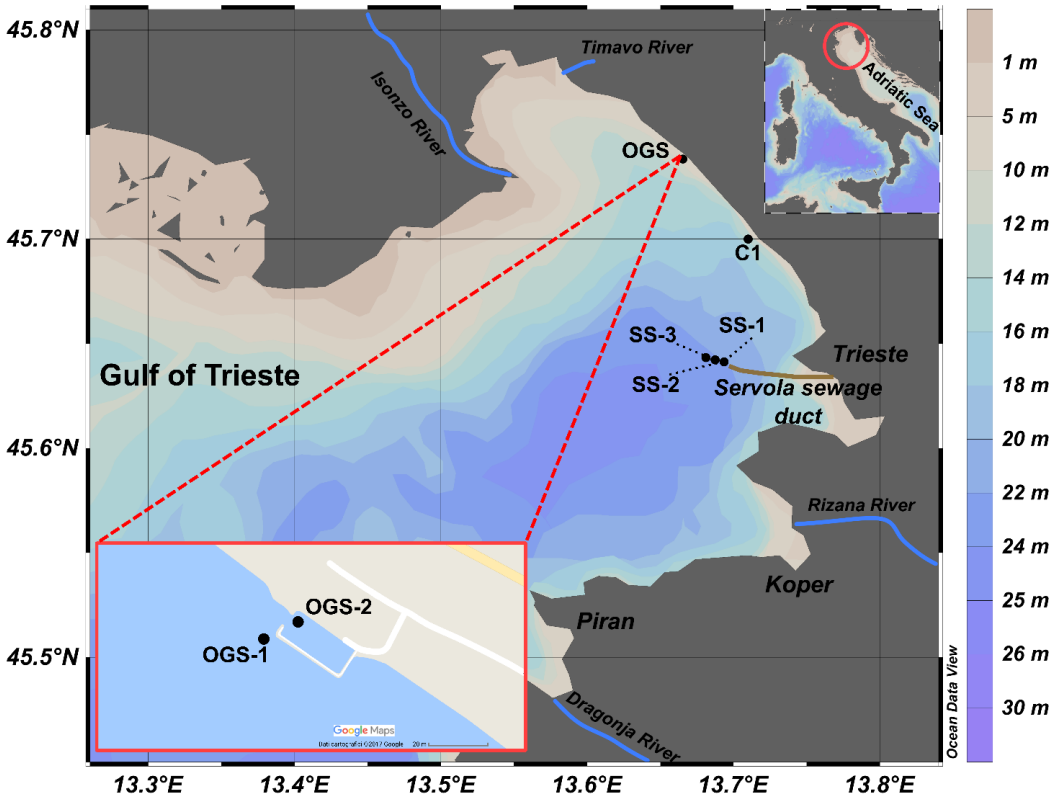

Fig. 1: Study area and sampling stations in the Gulf of Trieste (Northern Adriatic Sea). Samples for the winter experiment (WIN: February-March 2017) were collected at the coastal station OGS (OGS-1 marine salinity; OGS-2 salinity influenced by freshwater springs). Samples for the summer experiment (SUM: August-September 2017) were collected at C1 station (marine protected area) and SS stations (SS-1 at the beginning, SS-2 in the middle, SS-3 at the end of the diffusional zone of the Servola sewage duct).

2.2. Sample collection and station localisation

Several experiments were conducted in order to evaluate the biodegradable fraction of organic matter in different periods of the year, selecting the sampling periods based on DOM dynamics described above (2.1).

A first series of experiments was performed in late winter-early spring (WIN: February-March 2017) on samples collected in a coastal station (OGS) in the Gulf of Trieste (Northern Adriatic Sea), in the proximity of the Biological Laboratory of the Oceanographic section of OGS (Fig. 1). The station is

influenced by freshwater springs and is set in the proximity of a quay that favours freshwater accumulation. All samples were collected on the sea side of the quay (OGS-1; 45°44'27.4"N; 13°40'07.4"E) on 23 February (OGS-1A), 20 March (OGS-1B) and 22 March (OGS-1C). In order to investigate the effect of low salinity on DOM degradation, on 21 March seawater was collected inside the quay (OGS-2; 45°44'27.9"N 13°40'08.5"E).

The second series of experiments was conducted in summer (SUM: August-September 2017) in 4 different stations in the Gulf of Trieste (Northern Adriatic Sea). On 22 August, seawater was collected inside a marine protected area (LTER C1 station, 45°42.050' N, 13°42.600' E; Fig. 1). On 24 August and 20 September seawater for the experiments was collected in three stations placed at different distance of the diffusional zone of the Servola sewage duct (SS; Fig. 1) (Auriemma et al. 2016) in order to investigate the bioavailability of organic matter in areas subjected to different anthropogenic contamination: at the beginning of the diffusional zone of the pipe (SS-1; 45°38'28.53" N; 13°41'36.67" E; 20 September), in the middle (SS-2; 45°38'32.41"N; 13°41'14.70" E; 22 August), ad at the end (SS-3; 45°38'36.30"N; 13°40'51.70"E; 22 August). In order to investigate the effect of higher concentration of inorganic nitrogen and phosphorous on DOM microbial degradation, a parallel series of experiments (SUM+NUT) was conducted during SUM after the addition of inorganic nutrients to water samples. For each station considered for SUM, nitrate ($NaNO_3$) and phosphate ($NaH_2PO_4 \cdot H_2O$), prepared according to Andersen (2005), were added to raw water samples to reach the final concentration of 10.9 µM and 0.45 µM respectively.

2.3. Experimental design

The evaluation of the biodegradable fraction of organic matter (BDOM) was performed by means of a bioreactor, built following the design of Søndergaard & Worm (2001) modified by De Vittor et al. (2009) for the application of the method to seawater samples. The bioreactor consisted in a darkened glass chromatographic column filled with acid-washed and combusted (450 °C for 4 h) sintered glass spheres. A continuous water flux was maintained by a peristaltic pump connected to the bioreactor with Tygon tubes (Fig. 2; more technical details in De Vittor et al. 2009). The flow rate was 1 ± 0.1 mL min^{-1}, and the residence time of the bioreactor, determined measuring the variation of conductivity at the outlet after the addition of NaCl solution at the inlet, was 2.25 h. Microbial colonisation was achieved using 1.0 µm filtered seawater collected in the coastal station OGS-1 (Fig. 1). At the experimental conditions, microbial colonisation was carried out in two months, judging from the stabilisation of DOC utilisation. As microbial community cannot maintain itself (even for short periods) without a suitable supply of nutrients (De Vittor et al. 2009), the bioreactor was

maintained with the same water used for colonisation collected weekly and stored in acid-washed glass tanks (10 L) at 20±2 °C. After the colonisation and the stabilisation of the microbial community, the bioreactor degradation efficiency was tested by adding known amount of labile compounds to filtered (GF/F 0.7 µm) seawater.

DOC degradation was verified from the consumption of a solution of D(+)-Glucose (67 µM DOC added to reach final concentration 138 µM). DON and DOP degradation was separately evaluated by the consumption of a solution of AMP (adenosine 5'-monophosphate; addition of 15 µM DON and 2.8 µM DOP to reach final concentrations 21.7 µM and 2.9 µM, respectively). The bioreactor confirmed the capability to immediately react to an increase in BDOM. Indeed, the added glucose was almost completely metabolised (94.9% of C consumption), and most of AMP was also consumed, as 100% of DOP and 84% of DON were degraded. During AMP test, DOC degradation was also evaluated and 100% of carbon supplied was consumed, probably due to the lower carbon addition compared to glucose test (38 µM added to reach final concentration 106 µM).

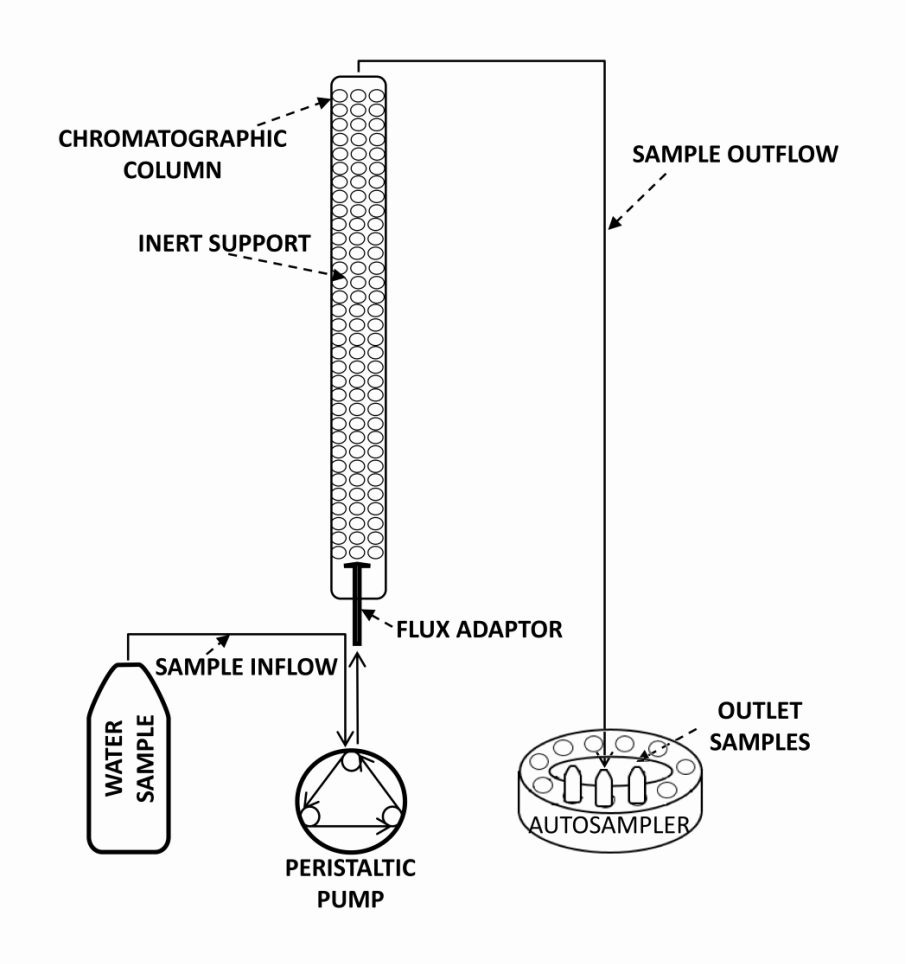

Fig. 2: Plug-flow bioreactor experimental set-up.

2.4. Analysis

Samples for DOC analyses were filtered over pre-combusted (450 °C for 4 h) Whatman GF/F filters (0.7 µm nominal pore size) in acid washed and pre-combusted (450 °C for 4 h) glass vials. Samples were stored frozen (–20 °C) until laboratory analysis. DOC analyses were performed with the HTCO (High Temperature Catalytic Oxidation) method (Sugimura & Suzuki 1988) using the Shimadzu TOC-V CSH analyser. Before the analysis, samples were acidified (automatically into instrument syringe, 2% – 2 M HCl) and purged for 7 min using high purity oxygen bubbling (150 mL min^{-1}) in order to remove inorganic carbon. After CO_2 elimination, acidified samples were combusted at 680 °C on a catalyst bed and CO_2 generated from combustion was determined in a non-dispersive infrared detector (NDIR). Analysis from a minimum of three injections showed a variation coefficient <2%. Detection limit, defined from the measurement of certificated low carbon water (Low Carbon Water CRM, University of Miami; Hansell 2005) treated as samples, was 1-2 µM. DOC results are periodically referenced against the international community of DOC analysts by using consensus reference material (Deep-Sea Water CRM, University of Miami; Hansell 2005) and the quality of the DOC measurements is also annually confirmed by the results of the inter-comparison exercises (QUASIMEME AQ14).

Samples for dissolved inorganic nutrients (nitrogenous oxides - NO_X, ammonium - NH_4, phosphate - PO_4) were filtered over pre-combusted (450 °C for 4 h) Whatman GF/F filters (0.7 µm nominal pore size) in acid washed polyethylene vials and kept frozen (–20 °C) until laboratory analysis. Inorganic nutrient concentrations were determined colorimetrically with a QuAAtro Seal Analiytical autoanalyser according to Hansen & Koroleff (1999). Detection limits reported by the analytical methods were 0.02 µM, 0.04 µM, 0.02 µM for NO_X, NH_4, and PO_4, respectively. As no certified reference material exists for the range of salinity and nutrient concentrations of area, the accuracy and precision of the analytical procedures are annually checked through the quality assurance program QUASIMEME (AQ1) and the relative coefficient of variation for five replicates was less than 5%. Internal quality control samples were used during each analysis.

Dissolved organic phosphorus (DOP) and nitrogen (DON) were calculated as the difference between TDP and PO_4 and between TDN and dissolved inorganic nitrogen (DIN= NO_X + NH_4), respectively. Total dissolved phosphorus (TDP) and nitrogen (TDN) were determined as PO_4 and NO_X, respectively, after quantitative conversion to inorganic P and N by persulfate oxidation (Hansen and Koroleff 1999). BDOC, BDON and BDOP were calculated as the difference of concentrations at the inlet and the outlet, assuming outlet concentration as refractory DOM (RDOM), since it is the pool remaining after heterotrophic bacteria activity. Samples were collected in five replicates, both at the

inlet and outlet. Given the residence time of 2.25 h, outlet samples were collected at least 2.5 h after the supply of different inlet sample, in order to allow stabilisation of outlet concentration. Results are reported as the difference between outlet and inlet concentration with analytical error of 2%.

2.5. Statistical analysis

The Spearman rank correlation test was used to investigate relationships among the different pools of DOM and inorganic nutrients using STATISTICA 7 (StatSoft, Inc., USA) and only significant data ($p < 0.05$, $p < 0.01$) are presented.

3. Results

3.1. Winter experiments (WIN)

At OGS-1A station, DOC, DON and DOP concentration at the inlet were, respectively, 90.2±2.88 µM, 2.94±0.11 µM and 0.11±0.06 µM. The biodegradable fraction of DOC (BDOC) consisted in 20.6±0.4 µM, which accounted for 22.9% of inlet consumption, whereas no significant variation at the outlet was observed for DON and DOP (Fig. 3; Tab. 1). Nitrogen oxide (NO_X) and ammonium (NH_4) concentrations at the inlet were, respectively, 17.20±0.08 µM and 0.10±0.04 µM. NO_X was slightly consumed (4.0%) whereas no significant variation was observed at the outlet for NH_4 concentration. Phosphate concentration was 0.14±0.01 µM, the highest of OGS-1 samplings, and almost half of the initial pool was consumed (49.0%) (Fig. 4; Tab. 1).

During the experiment conducted OGS-1B, DOC, DON and DOP concentration were, respectively, 86.3±1.56 µM, 6.83±0.004 µM and 0.22±0.002 µM. BDOC concentration was similar to the one detected on OGS-1A (21.3±0.4 µM), which corresponded to 24.5% consumption. Almost all initial pool of DON was consumed (91.6%), as BDON concentration was 6.26±0.13 µM, whereas a slight release of DOP was observed (0.02±0.01 µM) (Fig. 3; Tab. 1). NO_X concentration was 9.46±0.11 µM and 28.2% consumption was detected. NH_4 and PO_4 concentration were, respectively, 0.89±0.02 µM and 0.05±0.004 µM. NH_4 concentration at the outlet was almost half of the initial pool (48.9%), whereas PO_4 was released as outlet concentration was 0.09±0.002 µM higher than the inlet (Fig. 4; Tab. 1).

On the last test conducted at OGS-1 station (OGS-1C), the highest DOC concentration of the whole WIN experiment was detected (116.5±8.0 µM), whereas DON and DOP concentrations were similar to OGS-1B (respectively 7.34±0.18 µM and 0.22±0.02 µM). BDOC and BDON concentrations were,

respectively, 46.0±0.9 µM and 2.87±0.06 µM, accounting for almost 40% of the bulk pools (39.5% and 39.1%, respectively). A slight consumption of DOP seems occurring on OGS-1C experiment as BDOP concentration was 0.03±0.001 µM (Fig. 3; Tab. 1). NO_X and NH_4 concentrations were, respectively, 18.02 µM and 1.26±0.02 µM. Almost no consumption was detected for NO_X (only 1.0%), whereas NH_4 utilisation was half of the initial pool (50.2%). PO_4 concentration similar to 20 March experiment was detected (0.05±0.004 µM), and a release of 0.04±0.001 µM was measured (Fig. 4; Tab. 1).

Station OGS-2, influenced by freshwater springs (salinity of ~21 in OGS-2 versus 33-35 in OGS-1), exhibited a DOC value lower than those recorded in OGS-1, the lowest of all WIN samplings (69.2±1.6 µM), whereas DON concentration was the highest (10.57±0.06 µM) and DOP similar to February sampling. At the outlet, all organic species concentration was higher than the inlet, meaning that DOC, DON and DOP were clearly released from the bioreactor during the supply of low salinity water (respectively, values of 12.4%, 57.5% and 70.2% higher than inlet concentration were observed) (Fig. 3; Tab. 1). NO_X and PO_4 concentration were one order of magnitude higher than those of OGS-1 (112.72±0.26 µM and 1.27±0.03 µM respectively), whereas NH_4 concentration was similar to OGS-1 (0.75±0.19 µM). All inorganic nutrients were consumed in this station, in particular PO_4, whose utilisation accounted for the 82.6% of the initial pool (Fig. 4; Tab. 1).

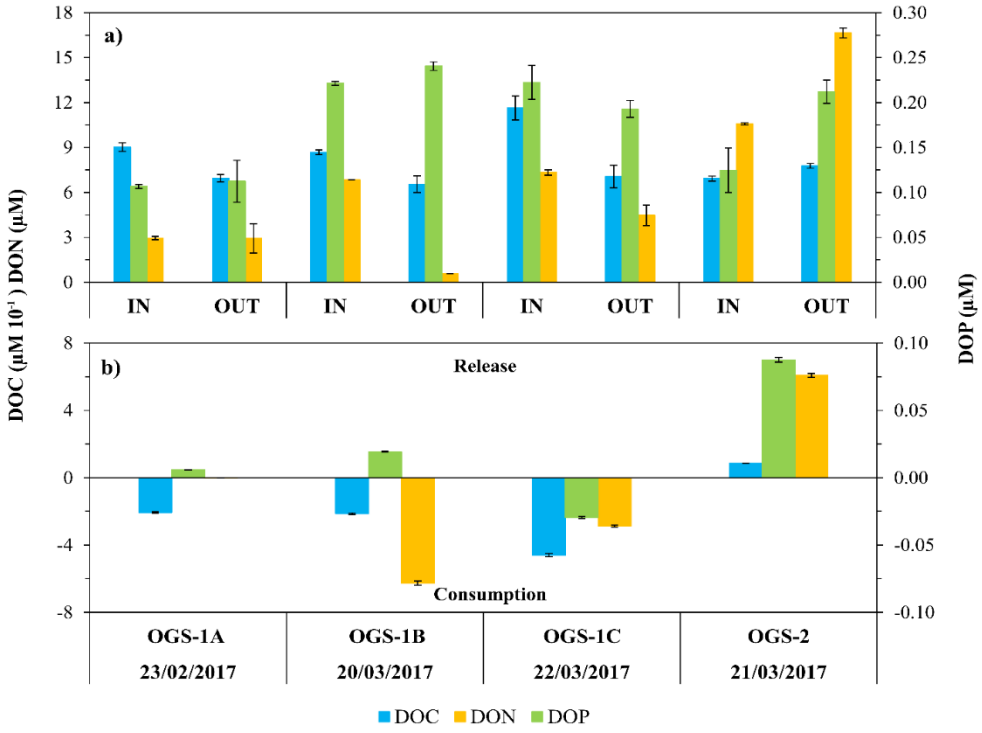

Fig. 3: Inlet and outlet concentration (A) and consumption or release (B) of dissolved organic carbon (DOC), nitrogen (DON) and phosphorus (DOP) of samples collected during the winter experiment (WIN; February-March 2017) at the coastal station OGS (OGS-1 marine salinity; OGS-2 salinity influenced by freshwater springs). DOC concentration is represented one order of magnitude lower than the real value in order to visualise it properly. DOP values are reported on the secondary vertical axis on the right.

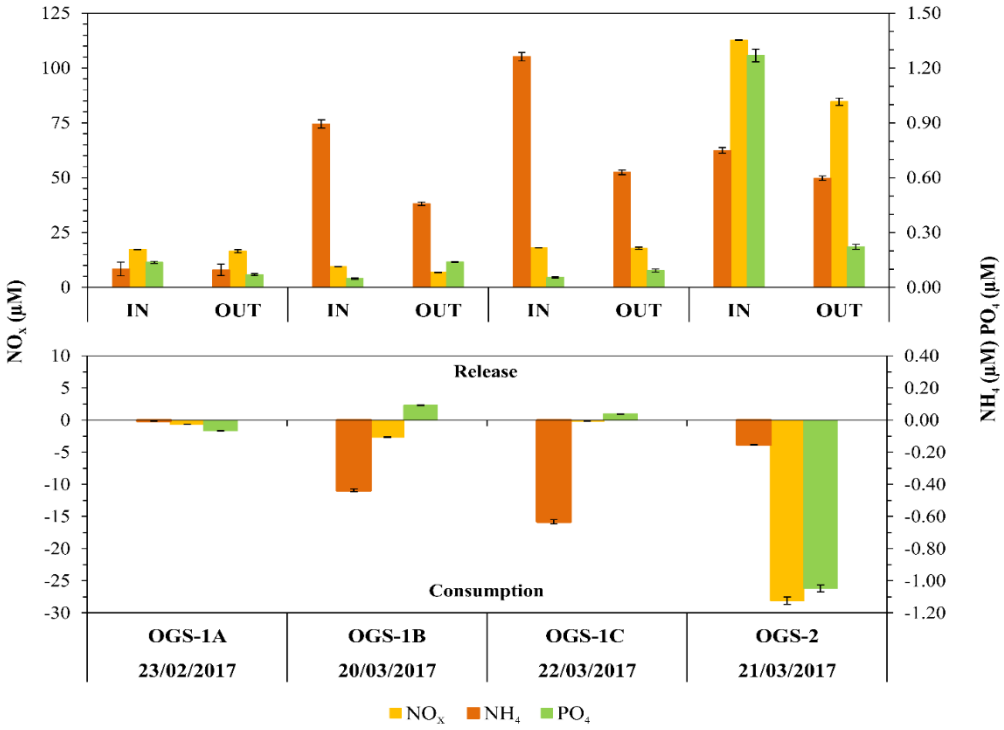

Fig. 4: Inlet and outlet concentration (A) and consumption or release (B) of inorganic nutrients (nitrogen oxides - NO_X, ammonium - NH_4, phosphate - PO_4) of samples collected during the winter experiment (WIN; February-March 2017) at the coastal station OGS (OGS-1 marine salinity; OGS-2 salinity influenced by freshwater springs). NH_4 and PO_4 values are reported on the secondary vertical axis on the right.

3.2. Summer experiments (SUM)

During the experiment conducted with water collected in C1 station (marine protected area), DOC, DON and DOP concentration at the inlet were, respectively 115.9±0.9 µM, 11.67±0.51 µM and 0.23±0.01 µM, and their bioavailable fractions accounted for 20-30% of the initial pool, with BDOC concentration of 37.5±0.7 µM, BDON 3.59±0.07 µM and BDOP 0.05±0.01 µM (Fig. 5; Tab. 1). NO_X, NH_4 and PO_4 concentrations were, respectively, 0.62±0.001 µM, 0.40±0.01 µM and 0.01±0.01 µM. 70% of inlet NH_4 was consumed (0.28±0.01 µM) and 0.10±0.002 µM of NO_X was released, whereas no significant variation of PO_4 concentration was detected at the outlet (Fig. 6; Tab. 1). After the addition of inorganic nutrients (C1+NUT), BDOC concentration remained similar to the before addition value (41.1±0.8 µM), whereas lower BDON was observed, as consumed DON was 19.5% of the initial pool (2.27±0.5 µM). No significant utilisation of DOP was detected, as the outlet concentration was 0.03±0.04 µM lower than the inlet (Fig. 5; Tab. 1). NO_X and PO_4 concentrations after nutrient addition were, respectively, 9.13±0.05 µM and 0.45±0.002 µM, whereas no change in NH_4 concentration was observed (0.40±0.02 µM). Utilisation of both NH_4 and PO_4 was higher after the addition of inorganic nutrients compared to raw water experiment, as 60% of inlet concentration

was consumed (respectively, 0.25±0.02 µM and 0.27±0.01 µM). On the contrary, NO_X outlet concentration was not significantly different from inlet (Fig. 6; Tab. 1).

In the experiment performed with water collected in SS-3, the farthest from the sewage duct, DOC and DON concentrations did not differ significantly from C1, as 115.4±2.9 µM were detected for DOC and 10.03±0.23 µM for DON. BDOC concentration too was comparable to C1 (37.3±0.7 µM, 32.3% of the inlet), whereas lower BDON was detected (2.61±0.05 µM; 26.1% of the inlet). DOP concentration was 0.07±0.01 µM and no significant consumption was identified (Fig. 5; Tab. 1). NO_X concentration was 0.78±0.03 µM, and no significant utilisation was observed (0.01 µM), whereas 0.10 µM of NH_4 were consumed (16.5%), from the inlet of 0.63±0.04 µM. Low PO_4 was detected (0.01 µM) and a release of 0.05±0.003 µM was observed (Fig. 6; Tab. 1). During the experiment of inorganic nutrient addition to SS-3 water (SS-3+NUT), the biodegradable fraction of DOC did not change significantly from the raw SS-3 experiment (34.6±0.7 µM). No significant consumption was detected for DON, whereas BDOP was 56.2% of the inlet (0.04±0.002 µM) (Fig. 5; Tab. 1). NO_X and PO_4 concentrations after nutrient addition were, respectively, 9.80±0.15 µM and 0.51±0.01 µM, whereas no change in NH_4 concentration was observed (0.67±0.03 µM). Consumption of NH_4 and PO_4 was observed, respectively 80.3% (0.54±0.01 µM) and 65.6% (0.34±0.01 µM) of inlet concentration and NO_X consumption was 1.23±0.02 µM (12.5%) (Fig. 6; Tab. 1).

During SS-2 experiment, DOC, DON and DOP concentrations were, respectively, 96.3±7.8 µM, 14.21±1.08 µM and DOP 0.27±0.02 µM. BDOC concentration was 28.6% of the inlet (27.5±0.6 µM), whereas higher consumption (40%) was observed for DON and DOP (BDON and BDOP respectively 6.20±0.12 µM and 0.11±0.02 µM) (Fig. 5; Tab. 1). High inlet NH_4 concentration was observed (3.13±0.07 µM). NO_X and PO_4 were, respectively, 0.81±0.02 µM and 0.03±0.002 µM. Almost all ammonium was consumed in the bioreactor (2.84±0.06 µM; 90.5%), whereas both NO_X and PO_4 were released (1.59±0.03 µM and 0.05±0.003 µM respectively) (Fig. 6; Tab. 1). Inorganic nutrient supply to SS-2 water, as in the previous addition experiments, did not change BDOC concentration (28.6±0.6 µM; 26.9%). BDON and BDOP concentrations were higher than that of the raw water experiment, as 51.9% of inlet DON and 60.8% of inlet DOP were used (respectively, 7.76±0.16 µM and 0.17±0.04 µM) (Fig. 5; Tab. 1). NO_X and PO_4 concentrations after nutrient addition were, respectively, 10.50±0.01 µM and 0.47±0.01 µM, and a slight decrease in NH_4 concentration was observed too (2.41±0.01 µM). After the addition of inorganic nutrients (SS-2+NUT), 87.4% (2.10±0.04 µM) of NH_4 and 61.8% (0.29±0.01 µM) of PO_4 was consumed in the bioreactor, whereas a slight release of NO_X was observed (1.20±0.02 µM) (Fig. 6; Tab. 1).

In the experiment performed with water from SS-1, the closest to the sewage duct, DOC and DOP concentration were similar to SS-3 (respectively, 101.1±2.1 µM and 0.08±0.01 µM), whereas DON

concentration was 8.76±0.24 µM. BDOC concentration accounted for 28.8±0.6 µM, representing 28.5% of inlet consumption. BDON concentration was 27.3% of inlet concentration (2.39±0.05 µM), whereas all DOP could be considered as refractory (Fig. 5; Tab. 1). NO_X and PO_4 concentrations were, respectively, 2.05±0.06 µM and 0.07±0.002 µM. NH_4 concentration was 2.23±0.12 µM and was almost completely consumed (2.16±0.04 µM; 97.1%). A lower consumption was detected for NO_X, as the outlet concentration was 26.1% (0.54±0.01 µM) lower than the inlet. No significant changes were observed at the outlet for PO_4 (0.02±0.003 µM) (Fig. 6; Tab. 1). As in the previous experiments, after the addition of inorganic nutrients (SS-1+NUT) BDOC concentration was similar to the values detected in the raw water experiment (30.0±0.6 µM; 28.9%). Lower BDON concentration was detected as 20.7% of inlet water was consumed (1.81±0.04 µM), whereas DOP was slightly released (0.04±0.01 µM) (Fig. 5; Tab. 1). NO_X and PO_4 concentrations after nutrient addition were, respectively, 14.57±0.29 µM and 0.58±0.03 µM, whereas no change in NH_4 concentration was observed (2.23±0.10 µM). 19.9% of NO_X was used, as the outlet concentration after the addition of inorganic nutrients was 2.90±0.06 µM lower than inlet. As in SS-1, almost all NH_4 was consumed (2.19±0.04 µM), whereas a high consumption of PO_4 was observed as a reduction of concentration of 0.52±0.10 µM was observed at the outlet (88.4%) (Fig. 6; Tab.1).

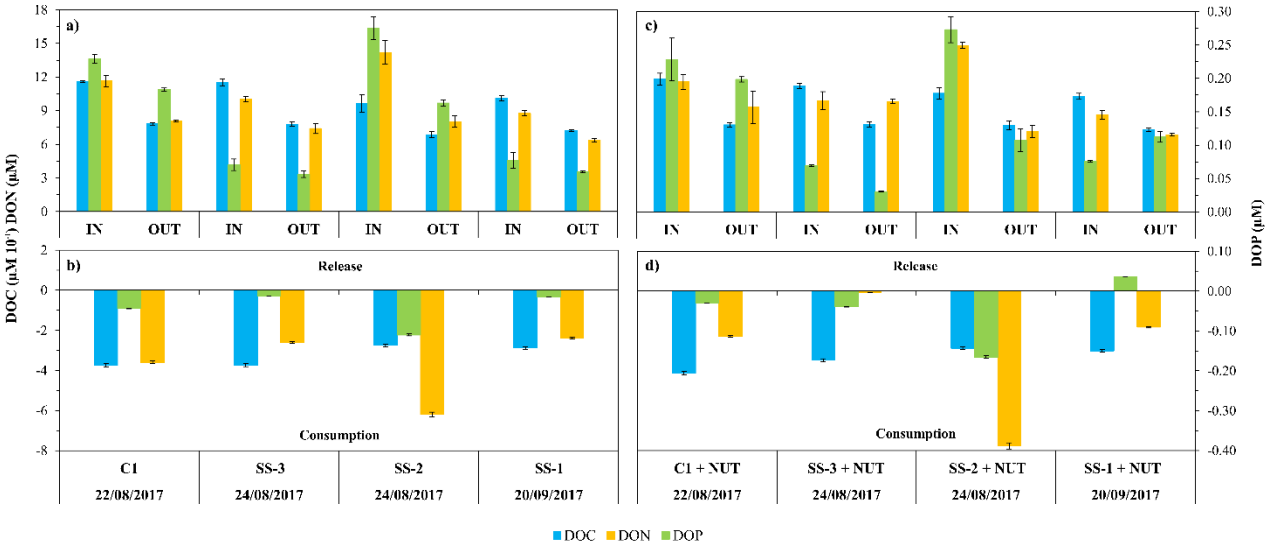

Fig. 5: Inlet and outlet concentration, before (A) and after (C) the addition of inorganic nutrients, of dissolved organic carbon (DOC), nitrogen (DON) and phosphorus (DOP) of samples collected during the summer experiment (SUM; August-September 2017) at C1 station (marine protected area) and SS stations (SS-1 at the beginning, SS-2 in the middle, SS-3 at the end of the diffusional zone of the Servola sewage duct). DOC, DON and DOP consumption or release before (B) and after (D) the addition of inorganic nutrients to water samples collected in C1 and SS stations during SUM experiment. DOC concentration is represented one order of magnitude lower than the real value in order to visualise it properly. DOP values are reported on the secondary vertical axis on the right.

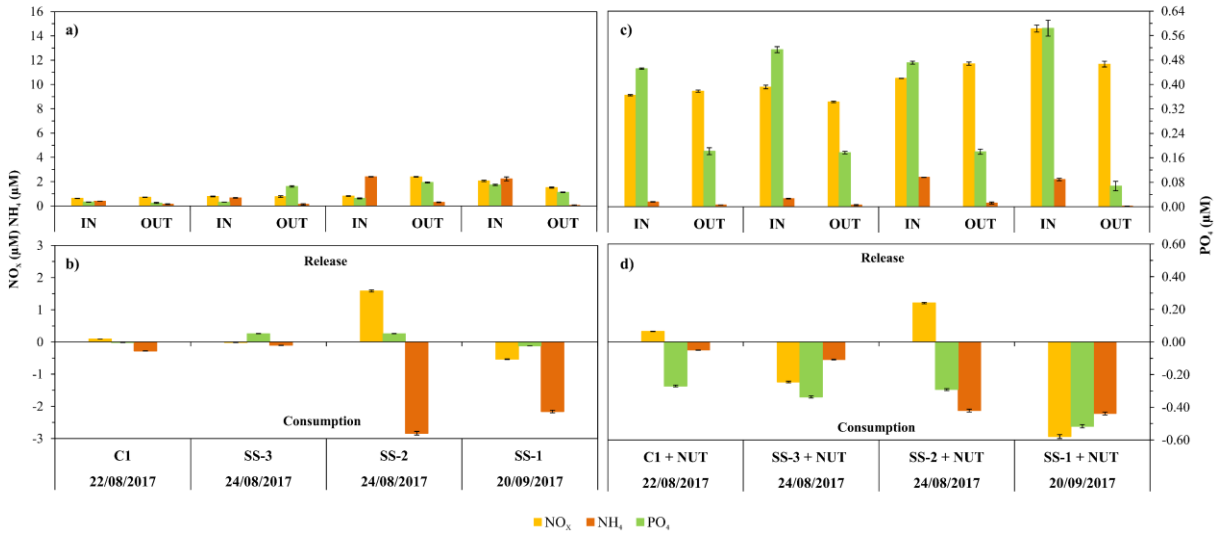

Fig. 6: Inlet and outlet concentration, before (A) and after (C) the addition of inorganic nutrients, of nitrogen oxides (NO_x), ammonium (NH_4) and phosphate (PO_4) of samples collected during the summer experiment (SUM; August-September 2017) at C1 station (marine protected area) and SS stations (SS-1 at the beginning, SS-2 in the middle, SS-3 at the end of the diffusional zone of the Servola sewage duct). NO_x, NH_4 and PO_4 consumption or release before (B) and after (D) the addition of inorganic nutrients to water samples collected in C1 and SS stations during SUM experiment. PO_4 values are reported on the secondary vertical axis on the right.

Tab. 1: Percentage of the inlet concentration consumed (negative values) or released (positive values; in grey) of dissolved organic carbon (DOC), nitrogen (DON) and phosphorus (DOP) and inorganic nutrients (nitrogen oxide-NO_x, ammonium-NH_4 and phosphate-PO_4). For each parameter, standard error was 2%. WIN: winter experiment (February-March 2017); SUM: summer experiment (August-September 2017); SUM+NUT: nitrate and phosphate addition to SUM water samples. OGS-1 stations: marine salinity; OGS-2 station: salinity influenced by freshwater springs; C1 station: marine protected area; SS stations: close to the diffusional zone of the Servola sewage duct (SS-1 at the beginning, SS-2 in the middle, SS-3 at the end).

Experiment	Date	Station	μM consumed (–) / released (+)					
			DOC	DON	DOP	NO_X	NH_4	PO_4
WIN	23/02/2017	**OGS-1A**	–20.6	–0.01	0.01	–0.69	–0.01	–0.07
WIN	20/03/2017	**OGS-1B**	–21.3	–6.26	0.02	–2.67	–0.44	0.09
WIN	22/03/2017	**OGS-1C**	–46.0	–2.87	–0.03	–0.18	–0.63	0.04
WIN	21/03/2017	**OGS-2**	8.6	6.08	0.09	–28.10	–0.15	–1.05
SUM	22/08/2017	**C1**	–37.5	–3.59	–0.05	0.10	–0.28	0.00
SUM+NUT	22/08/2017	**C1 + NUT**	–41.2	–2.27	–0.03	0.32	–0.25	–0.27
SUM	24/08/2017	**SS-3**	–37.3	–2.61	–0.01	–0.01	–0.10	0.05
SUM+NUT	24/08/2017	**SS-3 + NUT**	–34.6	–0.07	–0.04	–1.23	–0.54	–0.34
SUM	24/08/2017	**SS-2**	–27.5	–6.20	–0.11	1.59	–2.84	0.05
SUM+NUT	24/08/2017	**SS-2 + NUT**	–28.6	–7.76	–0.17	1.20	–2.10	–0.29
SUM	20/09/2017	**SS-1**	–28.8	–2.39	–0.02	–0.54	–2.16	–0.02
SUM+NUT	20/09/2017	**SS-1 + NUT**	–30.0	–1.81	0.04	–2.90	–2.19	–0.52

4. Discussion

In order to evaluate BDOM and nutrient uptake in natural conditions, the experiments performed will be first discussed considering only the typical marine conditions (OGS-1 and SUM experiments). The effect of low salinity (OGS-2 experiment) and of the increase in inorganic nutrient content (SUM+NUT experiments) will be then discussed.

The biodegradable fraction of DOC ranged from 20.6±0.4 µM (OGS-1A) to 46.0±0.9 µM (OGS-1C), and is similar to BDOC concentration measured by De Vittor et al. (2009) in the Gulf of Trieste using a plug-flow bioreactor. However, De Vittor et al. (2009) found lower winter concentrations (on February) than those detected in OGS-1 experiments. Indeed, in the present work, BDOC highest concentration was found in OGS-1C, and accounted for 39% of degradation of the inlet DOC concentration (116.5±8.0 µM). On the other OGS-1 experiments, BDOC accounted for about 22-25% of the initial pool. During SUM experiments, the biodegradable fraction of DOC increased, as a higher percentage of inlet pool was consumed, ranging between 28.5% and 32.3%, and BDOC concentration ranged between 27.5±0.6 µM (SS-2) and 37.5±0.7 µM (C1). As in other biodegradability studies (Lønborg et al. 2009; Lønborg et al. 2010; De Vittor et al. 2009), a positive linear relationship is found between BDOC and DOC concentrations ($p < 0.01$), therefore the bulk DOC pool directly depends on BDOC concentration. The slope of the linear regression of 1.30 indicates that the seasonal variation of DOC depends on BDOC, as previously suggested (Lønborg et al. 2009), and the intercept indicates the residual DOC concentration (i.e. the refractory portion in the experimental design). Refractory DOC derived by linear regression is 62.5 µM and is comparable to the experimental RDOC detected at the outlet of bioreactor (71.9±4.8 µM). Both experimental and calculated RDOC values are higher than deep-sea DOC concentration (35-45 µM; Hansell & Carslon 1998) which is generally considered resistant to bacterial degradation. The higher value of calculated RDOC compared to deep-sea concentration could imply that the experimental approach is not able to degrade the whole pool of labile and semi-labile organic carbon. Indeed, in natural systems, during the transport of coastal DOM to the deep-sea, other processes that affect its degradation have to be considered, e.g. the degradation of the semi-labile pool, the dilution in the ocean and photo-degradation of DOM (Lønborg & Søndeergard 2009). RDOC value observed in the experiments performed, is however similar to Lønborg et al. (2009, 2010) after long incubation experiments (70 days maximum in Lønborg et al. (2010) and 150 days in Lønborg et al. (2009)), confirming the bioreactor approach as a suitable tool for rapid evaluation of BDOC, as the time required for its estimation is about 4h.

BDON concentration ranged between 2.39±0.05 µM (SS-1) and 6.26±0.13 µM (OGS-1B), and is similar to values detected by Lønborg et al. (2009) after 150-day incubation experiment in a temperate Scottish fjord. The degradation values obtained fall within the BDON range reviewed by Lønborg and Álvarez-Salgado (2012) in coastal oceans, nevertheless, a high variability in DON degradation was observed. In OGS-1A experiment, DON can be considered as completely refractory, as no significant difference was detected at the outlet, while in the other samplings degradation ranged from 26.1% (SS-3) and 91.6% (OGS-1B). This broad variation does not directly depend on the bulk DON pool. Differently to Lønborg et al. (2009), no relationship exists between inlet concentrations and the bioavailable fractions, but a strong correlation ($p < 0.01$) was observed between inlet DON and the residual DON concentration detected at the outlet, assumed as refractory DON. At the experimental conditions, except for the lowest value detected in OGS-1B (0.58±0.01 µM), RDON concentration was always higher than the deep-sea DON (<3 µM; Bronk 2002), especially in SUM experiments, when also higher DON inlet concentrations were detected. This could imply that the increase in the bulk DON pool is mainly due to a higher concentration of less bioavailable compounds, and other factors than the total DON amount affect its bioavailability. DOM consumption by bacteria depends on numerous factors, including temperature, nutrient availability, bacterial community composition, DOM chemical composition, and length of the experiments (Wiegner et al. 2006). During the experiments performed, bioreactor temperature did not change, the same initial bacterial community was always maintained, the bioreactor was kept in the dark, and test duration was similar among the different experiments, thus the variability of DON consumption has to be addressed to some nutrient limiting and/or different chemical composition of the bioavailable DOM. No correlation was found between DON pools and inorganic nutrients, thus consumption of DON is affected by its chemical composition, and not by inorganic nutrient availability. Polimene et al. (2017) demonstrated that a substantial fraction (60%) of diatom derived DON is resistant to degradation. Polimene et al. (2017) study, however, was only focussed on degradation by a single bacterial cell line (*Alteromonas* sp.), while inside bioreactors, similar to the one used in the experiment described, different species of the bacterial community operate in succession and synergy (Søndeergard & Worm 2001), and DOM degradation could be higher than that operated by a single species. In the Gulf of Trieste, however, diatoms represent the major contributors to primary production (Fonda Umani et al. 2007, 2012), and the high degradation range could depend mostly on the different chemical composition of compounds released by phytoplankton. Moreover, it should be also taken into account that not all available DON could have been consumed, as bioreactor DON degradation efficiency, assessed by AMP consumption, was 84%.

Concerning inorganic nitrogen species, independently to inlet concentration, ammonium uptake seemed to be preferred to NO_X, as it is the inorganic nitrogen species always consumed. NH_4 uptake is generally recognised as an important source of inorganic nitrogen for heterotrophic bacteria. Indeed, NO_X uptake is energetically demanding, requiring intracellular reduction to NH_4 prior to assimilation. Heterotrophic bacteria have very efficient systems for ammonium uptake, and the proportion of total uptake tends to increase at decreasing NH_4 concentrations (Church 2008 and references therein). DON degradation should be connected to inorganic nitrogen regeneration; however, NO_X released was coupled with DON degradation only in SS-2. The absence of the expected correlation between DON and DIN may depend on a continuous flux of uptake and regeneration inside the bioreactor, directly related to the chemical composition of DOM. As already described above, inside the bioreactor different niches and communities are selected in a longitudinal gradient of gradually more recalcitrant organic matter (Søndergaard & Worm 2001). Nutrients regenerated by the first communities of the bioreactor might be immediately consumed by following species, especially if most of DON available is difficult to degrade.

Similarly as BDON, DOP bioavailability exhibited a high variability. BDOP ranged between 0.03±0.01 µM (SS-1) and 0.11±0.02 µM (SS-2), and, as for BDOC and BDON, this range is consistent with values observed by Lønborg et al. (2009). However, all DOP seemed to be refractory on OGS-1A, SS-3 and SS-1, while a slight release was observed at OGS-1B. On the other hand, a variable consumption from 13.3% (OGS-1C) to 40.9% (SS-2) was observed in the other experiments. As for BDON, neither BDOP broad variation directly depends on the bulk DOM pool, as no relationship exists between inlet concentrations and the bioavailable fractions. Moreover, in other studies DOP is generally ≥80% degraded (Lønborg et al. 2009, 2010; Hopkinson et al. 2002; Lønborg & Álvarez-Salgado 2012), as it represents the DOM pool that is preferentially consumed over DON and DOC, whereas in the present study DOP seems less available. Indeed, residual DOP concentration, which ranged from 0.06±0.001 µM (SS-1) to 0.24±0.005 µM (OGS-1B), was higher than the deep-sea DOP value (0.02 µM; Karl & Björkman 2002) and also than residual DOP found in other studies (Lønborg et al. 2009, 2010; Hopkinson et al. 2002). In addition, contrary to what generally observed (Karl & Björkman 2015), no overall relationship exists with inorganic nutrients, especially between consumed DOP and released PO_4, which is strange as the area is P-limited (Thingstad & Rassoulzadegan 1995). On the other hand, focusing on each experiment, some connections between BDOP and PO_4 exist, e.g. in OGS-1C and SS-2 DOP consumption was associated to PO_4 release, and in OGS-1A all DOP was refractory and half of PO_4 pool was used. Degradation and release, however, vary independently to inlet concentrations. This complex patter of DOP and PO_4 consumption might depend on a different chemical composition of organic matter,

considering that the bioreactor demonstrated the capability to completely degrade labile DOP, as in AMP test 100% of inlet DOP was consumed. The absence of the expected correlation between DOP consumed and PO_4 released may depend, as already described for DON, on a continuous flux of uptake and regeneration inside the bioreactor. Microbial community colonising the inert support is typical of the P-limited area, therefore should have evolved several mechanisms for a more efficient P uptake. In the case of high concentrations of less labile inlet DOP, all PO_4 released by remineralisation from the first bacterial community in the bioreactor would be preferentially consumed by the following communities before DOP degradation. In addition, large DOP compounds need to be enzymatically hydrolysed for the assimilation of the released inorganic phosphorus (Karl & Björkman 2015). Moreover, DOP production by healthy microorganisms has been recognised as a wide phenomenon, and may be released by heterotrophic bacteria colonising bioreactor.

The presence of differently specialised communities inside the bioreactor could also be inferred by the low salinity experiment (OGS-2). When bioreactor was supplied with low-salinity water (~21), all DOM species were released because of osmotic stress. On the other hand, uptake of all inorganic nutrient was clearly observed, especially PO_4 (82.6% of the inlet pool). Osmotic stress might have caused the lysis of non-resistant species resulting in DOM release, and thus only the activity of species resistant to salinity changes is detectable. Moreover, a higher concentration of inorganic nutrients was available, while DOM could have been more refractory as OGS-2 station is strongly influenced by freshwater springs. Hence, when low salinity water was supplied, only more resistant heterotrophic bacteria communities could have survived to osmotic stress, and they preferentially utilised inorganic nutrients due to the highest availability. Furthermore, eventual DOM consumption could have been hidden by the high release of DOM after cellular lysis.

Several studies have found that bacterial growth and DOM bioavailability can be limited by inorganic nutrients (Church 2008 and references therein; Pinhassi et al. 2006; Lønborg & Søndergaard 2009). However, none of DOM pool show any relationship with inorganic nutrient, and this was also confirmed by the treatment of nitrate and phosphate addition done on SUM experiments (SUM+NUT). Indeed, DOC consumption was not affected by the higher availability of nutrients, whereas differences were found in DON and DOP degradation, but no common variation pattern could be identified. The addition of phosphate resulted in increased uptake by heterotrophic bacteria in the bioreactor. PO_4 consumption was higher than in the raw water samples for all stations, even in those where a release was observed, confirming phosphate uptake as an important substrate (Karl & Björkman 2015) for microbial community of the area. No relationship, however, seems to exist with DOP. Indeed, in SS-3+NUT and SS-2+NUT DOP degradation increased, while in C1+NUT lower

BDOP values were detected and in SS-1+NUT a slight release of DOP was observed. Concerning nitrogen species, no homogeneous patter could be identified for NO_X. In C1+NUT and SS-1+NUT no significant changes were detected comparing to the raw water samples, NO_X consumption increased in SS-3+NUT, and a lower production was measured in SS-2+NUT. NH_4 consumption did not change significantly, except for SS-3+NUT where NH_4 utilisation increased to 80%. Similarly to inorganic nitrogen, DON did not exhibit a homogenous trend after nutrient addition. As for DOP, DON degradation in C1+NUT decreased, whereas in SS-2+NUT DON bioavailability increased. In SS-3+NUT almost no DON was consumed, while SS-1+NUT BDON concentration did not change from the raw value. The insignificant effect of inorganic nutrient addition on biodegradable DOC amounts suggests that DOC degradation in the experiments was not limited by inorganic nitrogen or phosphorus availability. This is in contrast to a commonly observed stimulation of heterotrophic DOC utilization by addition of inorganic nutrients (e.g. Kuparinen & Heinänen 1993; Zweifel et al. 1995), but is consistent with Asmala et al. (2013) experiments in Baltic Sea. However, the different patterns found for DON and DOP suggest a high variability in DOM composition in the area. Indeed, no common DOM degradation trend was identified even in samplings performed on the same day in SS stations. Nutrient limitation can, indeed, affect quantity and quality of DOM produced, and especially P-limitation has resulted in several experiments to produce refractory DOM (Carlson & Hansell 2015 and references therein).

Concluding, overall, BDOM ranged from 20.6 µM to 46.0 µM for C, from 2.39 µM to 6.26 µM for N and from 0.02 µM to 0.11 µM for P, and represented 30±6% of DOC, 43±25% of DON and 25±14% of DOP. Bioavailability seemed highest for DON, followed by DOC and DOP. However, the high variability of DON and DOP consumption among the experiments performed makes difficult to establish a clear pattern of preferential consumption of DOM components, despite the general consensus that DON and DOP are selectively mineralised with respect to DOC (Aminot & Kérouel 2004; Lønborg et al. 2009; Lønborg et al. 2010; Knudsen-Leerbeck et al. 2017). Focussing on each single experiment performed, DOC is the easiest to degrade component of DOM in OGS-1A, OGS-1C, C1, SS-1 and SS-3, whereas in OGS-1B and SS-2 DON is the preferred DOM consumed fraction. Nutrient addition does not change C1 and SS-1 selectivity, but in SS-3 and SS-2 DOP becomes DOM fraction preferentially degraded.

5. Conclusions and experimental set-up criticism

The plug-flow bioreactor tested confirmed its functionality for BDOC evaluation in the Gulf of Trieste, as values similar to previous studies were obtained. However, the experimental approach applied seemed to be not effective for DON and DOP degradation and for nutrient uptake evaluation, as it was not possible to identify any specific relationship between DOM bioavailability and other factors. Nevertheless, to our knowledge, this work represents the first attempt for the simultaneous evaluation of all DOM components degradation and nutrient uptake in seawater by means of a plug-flow bioreactor, and further research is needed. In this study, no batch experiment was conducted for comparing bioreactor performance in DON and DOP degradation and nutrient uptake. AMP test showed good performance for both DON and DOP degradation, however, a parallel test would be useful in order to confirm these results, especially for evaluating if the lower DON degradation efficiency (84%) has to be addressed to the experimental set-up or to the composition of DOM tested. De Vittor et al. (2009) verified that no interaction with inert support affected DOC degradation in seawater condition, but no abiotic test has been previously conducted to verify possible physical DON and DOP release/retention, neither is it known the effect of any physical disturbance by biofilm. Indeed, Zhao & Liu (2013), in a study on estuarine environment, hypothesized that refractory DOP (as phytic acid) might have displaced PO_4 on biofilm surface, resulting in phosphate release. Considering that the Gulf of Trieste is a P-limited environment, the interference of RDOP with PO_4 might have hidden inorganic phosphorus uptake. Moreover, in the same study, Zhao & Liu (2013) found that 30%-38% of glucose-6-phosphate was hydrolysed in abiotic conditions, resulting in PO_4 release from the bioreactor. More research is needed to verify Zhao & Liu (2013) results focusing on marine water; however, if their findings were confirmed bioreactor would not be a useful tool in P-limited systems. In addition, considering the low P concentration in both organic and inorganic compartment, it is difficult to verify the significance of small variations between inlet and outlet.

Abiotic and biofilm interferences should also be verified for DON. Badr et al. (2008) tested a plug-flow bioreactor performance for estuarine waters, but they did not perform any test to verify abiotic interaction, assuming it to be minor on the basis of previous works focussed on DOC (e.g. Kaplan & Newbold 1995). However, considering that DON mineralisation involves several complex processes, it should be useful to perform abiotic tests and parallel batch cultures in order to verify the effectiveness of bioreactors approach for BDON evaluation.

The experiments performed have highlighted the relevance of the establishment of specialised communities inside the bioreactor for the degradation of gradually more recalcitrant organic matter. For this reason, other studies should deal with the identification of the different communities forming

the longitudinal gradient in order to gain insights on DOM dynamics inside the bioreactor. The identification of heterotrophic bacteria should also be combined with the evaluation of virus activity, as viral lysis is one of the main causes of DOM release (Hansell & Carlson 2015).

Acknowledgments

We are thankful to Fondo Trieste for having financially supported this PhD research project. We would like to thank Lidia Urbini and Martina Kralj for nutrient analysis, and Sergio Predonzani for the help provided in the bioreactor set-up.

References

Aminot A, Kérouel R (2004) Dissolved organic carbon, nitrogen and phosphorus in the N-E Atlantic and the N-W Mediterranean with particular reference to non-refractory fractions and degradation. Deep Sea Res I 51:1975–1999. doi:10.1016/j.dsr.2004.07.016.

Andersen RA (2005) Algal Culturing Techniques, 1st ed. Elsevier Academic Press, Burlington, Mass.

Asmala E, Autio R, Kaartokallio H, Pitkänen, Stedmon CA, Thomas DN (2013) Bioavailability of riverine dissolved organic matter in three Baltic Sea estuaries and the effect of catchment land use. Biogeosciences 10:6969–6986. doi:10.5194/bg-10-6969-2013.

Auriemma R, Nasi F, Del Negro P (2016) The macrozoobenthic fauna of the bottoms nearby the underwater swage duct of Trieste (Northern Adriatic Sea). Biol Mar Mediterr 23: 90–93.

Azam F, Fenchel T, Field JG, Gray JS, Meyerreil LA, Thingstad F (1983) The ecological role of water column microbes in the Sea. Mar Ecol Prog Ser 10: 257–263.

Badr E-SA, Tappin AD, Achterberg EP (2008) Distribution and seasonal variability of dissolved organic nitrogen in two estuaries in SW England. Mar Chem 110:153–164.

Bronk DA (2002) Dynamics of dissolved organic nitrogen. In: Hansell DA, Carlson CA (Eds.), Biogeochemistry of Marine Dissolved Organic Matter. 1st Ed. Academic Press, USA, pp. 153–247.

Church MJ (2008) Resource control of bacterial dynamics in the sea. In Kirchman DL (Eds), Microbial ecology of the oceans. 2nd Ed. Jhon Wiley & Sons, Inc.

Cozzi S, Falconi C, Comici C, Cermelj B, Kovac N, Turk V, Giani M (2012) Recent evolution of river discharges in the Gulf of Trieste and their potential response to climate changes and anthropogenic pressure. Estuar Coast Shelf Sci 115:14–24. doi:10.1016/j.ecss.2012.03.005.

De Vittor C, Paoli A, Fonda Umani S (2008) Dissolved organic carbon variability in a shallow coastal marine system (Gulf of Trieste, northern Adriatic Sea). Estuar Coast Shelf Sci 78:280–290

De Vittor C, Larato C, Fonda Umani S (2009) The application of a plug-flow reactor to measure the biodegradable dissolved organic carbon (BDOC) in seawater. Bioresour Technol 100:5721–5728.

Dinasquet J, Kragh T, Schrøter ML, Søndergaard M, Riemann L (2013) Functional and compositional succession of bacterioplankton in response to a gradient in bioavailable dissolved organic carbon. Environ Microbiol 15:2616–2628. doi:10.1111/1462-2920.12178

Fajon C, Cauwet G, Lebaron P, Terzic S, Ahel M, Malej A, Mozetič P, Turk V (1999) The accumulation and release of polysaccharides by planktonic cells and the subsequent bacterial response during a controlled experiment. FEMS Microbiol Ecol 29:351–363.

Fonda Umani S, Del Negro P, Larato C, De Vittor C, Cabrini M, Celio M, Falconi C, Tamberlich F, Azam F (2007) Major inter-annual variations in microbial dynamics in the Gulf of Trieste (northern Adriatic Sea) and their ecosystem implications. Aquat Microb Ecol 46:163–175.

Fonda Umani S, Malfatti F, Del Negro P (2012) Carbon fluxes in the pelagic ecosystem of the Gulf of Trieste (Northern Adriatic Sea). Estuar Coast Shelf Sci 115:170–185.

Hansell DA, Carlson CA (1998) Deep-ocean gradients in the concentration of dissolved organic carbon. Nature 395:263–266.

Hansell DA (2005) Dissolved organic carbon reference material program. Eos Trans AGU 86:318.

Hansell DA, Carlson CA, Repeta DJ, Schlitzer R (2009) Dissolved organic matter in the ocean: a controversy stimulates new insights. Oceanography 22:202–211.

Hansell DA (2013) Recalcitrant Dissolved Organic Carbon Fractions. Annu Rev Mar Sci 5:421–45. doi:10.1146/annurev-marine-120710-100757

Hansell DA, Carlson CA (2015) Biogeochemistry of marine dissolved organic matter. 2nd Ed. Elsevier Science, USA.

Hansen HP, Koroleff F (1999) Determination of nutrients. In: Grasshoff K, Kremling K, Ehrhardt M (Eds.), Methods of seawater analysis, 3rd ed. Wiley-VCH, Weinheim.

Hedges JI (1992) Global biogeochemical cycles: progress and problems. Mar Chem 39:67–93.

Hopkinson Jr CS, Vallino JJ, Nolin A (2002) Decomposition of dissolved organic matter from the continental margin. Deep Sea Res II 49:4461–4478.

Kaplan LA, Newbold JD (1995) Measurement of streamwater biodegradable dissolved organic carbon with a plug-flow bioreactor. Water Res 29:2696–2706.

Karl DM, Björkmann K (2015) Dynamics of dissolved organic phosphorus. In Hansell DA, Carlson CA, 2015. Biogeochemistry of marine dissolved organic matter. 2nd Ed. Elsevier Science, USA.

Knudsen-Leerbeck H, Mantikci M, Bentzon-Tilia M, Traving SJ, Riemann L, Hansen JLS, Markager S (2017) Seasonal dynamics and bioavailability of dissolved organic matter in two contrasting temperate estuaries. Biogeochemistry 134:217–236. doi:10.1007/s10533-017-0357-2.

Kragh T, Søndergaard M (2009) Production and decomposition of new DOC by marine plankton communities: carbohydrates, refractory components and nutrient limitation. Biogeochemistry 96:177–187.

Kujawinski EB (2011) The impact of microbial metabolism on marine dissolved organic matter. Annu Rev Mar Sci 3:567–99. doi:10.1146/annurev-marine-120308-081003.

Kuparinen J and Heinänen A (1993) Inorganic nutrient and carbon controlled bacterioplankton growth in the Baltic Sea. Estuar Coast Shelf Sci 37:271–285.

Larato C, Celussi M, Virgilio D, Karuza A, Falconi C, De Vittor C, Del Negro P, Fonda Umani S (2010) Production and utilization of organic matter in different P-availability conditions: A mesocosm experiment in the Northern Adriatic Sea. J Exp Mar Biol Ecol 391:131–142.

Letscher RT, Knapp AN, James AK, Carlson CA, Santoro AE, Hansell DA (2015) Microbial community composition and nitrogen availability influence DOC remineralization in the South Pacific Gyre. Mar Chem 177: 325–334.

Lipizer M, Cossarini G, Falconi C, Solidoro C, Fonda Umani S (2011) Impact of different forcing factors on N:P balance in a semi-enclosed bay: The Gulf of Trieste (North Adriatic Sea). Cont Shelf Res 31:1651–1662. doi:10.1016/j.csr.2011.06.004

Lipizer M, De Vittor C, Falconi C, Comici C, Tamberlich F, Giani M (2012) Effects of intense physical and biological forcing factors on CNP pools in coastal waters (Gulf of Trieste, Northern Adriatic Sea). Estuar Coast Shelf Sci 115:40–50. doi:10.1016/j.ecss.2012.03.024.

Lønborg C, Álvarez-Salgado XA (2012) Recycling versus export of bioavailable dissolved organic matter in the coastal ocean and efficiency of the continental shelf pump. Global Biogeochem Cycles 26:Gb3018. doi:10.1029/2012gb004353.

Lønborg C, Davidson K, Álvarez-Salgado XA, Miller AEJ (2009) Bioavailability and bacterial degradation rates of dissolved organic matter in a temperate coastal area during an annual cycle. Mar Chem 133:219–226. doi:10.1016/j.marchem.2009.02.003

Lønborg C, Søndeergard M (2009) Microbial availability and degradation of dissolved organic carbon and nitrogen in two coastal areas. Estuar Coast Shelf Sci 81:513–520.

Lønborg C, Álvarez-Salgado XA, Martínez-Garcia S, Miller AEJ, Teira E (2010) Stoichiometry of dissolved organic matter and the kinetics of its microbial degradation in a coastal upwelling system. Aquat Microb Ecol 58:117–126. doi:10.3354/ame01364.

Malfatti F, Turk V, Tinta T, Mozetič P, Manganelli M, Samo TJ, Ugalde JA, Kovač N, Stefanelli M, Antonioli M, Fonda Umani S, Del Negro P, Cataletto B, Hozić A, Ivošević De Nardis N, Žutić V, Svetličić V, Mišić Radić T, Radić T, Fuks D, Azam F (2014) Microbial mechanisms coupling carbon and phosphorus cycles in phosphorus-limited northern Adriatic Sea. Sci Total Environ 470–471:1173–1183. doi:10.1016/j.scitotenv.2013.10.040

Mozetič P, Solidoro C, Cossarini G, Socal G, Precali R, Francé J, Bianchi F, De Vittor C, Smodlaka N, Fonda Umani S (2010) Recent trends towards oligotrophication of the Northern Adriatic: evidence from chlorophyll *a* time series. Estuar Coasts 33:362–375. doi:10.1007/s12237-009-9191-7.

Pinhassi J, Gomez-Consarnau L, Alonso-Saez L, Sala MM, Vidal M, Pedros-Alio C, Gasol JM (2006) Seasonal changes in bacterioplankton nutrient limitation and their effects on bacterial community composition in the NW Mediterranean Sea. Aquat Microb Ecol 44:241–252.

Polimene L, Clark D, Kimmance S, McCormack P (2017) A substantial fraction of phytoplankton-derived DON is resistant to degradation by a metabolically versatile, widely distributed marine bacterium. PLOS ONE 12:e0171391. doi:10.1371/journal.pone.0171391.

Santinelli C, Nannicini L, Seritti A (2010) DOC dynamics in the meso and bathy pelagic layers of the Mediterranean Sea. Deep Sea Res II 57:1446–1459. doi:10.1016/j.dsr2.2010.02.014

Santinelli C, Ibello V, Lavezza R, Civitarese G, Seritti A (2012) New insights into C, N and P stoichiometry in the Mediterranean Sea: The Adriatic Sea case. Cont Shelf Res 44:83–93.

Santinelli C, Hansell DA, d'Alcalà MR (2013) Influence of stratification on marine dissolved organic carbon (DOC) dynamics: The Mediterranean Sea case. Prog Oceanogr 119:68–77. doi:10.1016/j.pocean.2013.06.001.

Søndergaard M, Borch NH, Riemann B (2000) Dynamics of biodegradable DOC produced by freshwater plankton communities. Aquat Microb Ecol 10:69–85.

Søndergaard M, Worm J (2001) Measurement of biodegradable dissolved organic carbon (BDOC) in lake water with a bioreactor. Water Res 35:2505–2513.

Sugimura Y, Suzuki Y (1988) A high temperature catalytic oxidation method for the determination of non-volatile dissolved organic carbon in seawater by direct injection of liquid sample. Mar Chem 24:105–131.

Thingstad TF, Hagström Å, Rassoulzadegan F (1997) Accumulation of degradable DOC in surface waters: is it caused by a malfunctioning microbial loop? Limnol Oceanogr 42:398–404.

Thingstad TF, Rassoulzadegan F (1995) Nutrient limitations, microbial food webs, and 'biological C-pumps': suggested interactions in a P-limited Mediterranean. Mar Ecol Prog Ser 117:299–306.

Volk CJ, Volk CB, Kaplan LA (1997) Chemical composition of biodegradable dissolved organic matter in streamwater. Limnol Oceanogr 42:39–44.

Wiegner TN, Seitzinger SP, GlibertPM, Bronk DA (2006). Bioavailability of dissolved organic nitrogen and carbon from nine rivers in the eastern United States. Aquat Microb Ecol 43:277–287.

Zhao J, Liu X (2013) Organic and inorganic phosphorous uptake by bacteria in a plug-flow microcosm. Front Environ Sci Eng 7:173–184.

Zweifel UL, Norrman B, Hagström A (1993) Consumption of dissolved organic carbon by marine bacteria and demand for inorganic nutrients. Mar Ecol Prog Ser 101:23–32.

Zweifel UL, Wikner J, Hagström Å, Lundberg E, Norrman B (1995) Dynamics of dissolved organic carbon in a coastal ecosystem. Limnol Oceanogr 40:299–305.

Acknowledgments

I wish to express all my gratitude to my supervisors, Dr. Paola Del Negro and Dr. Cinzia De Vittor, for the confidence they showed in me, for the great support provided and for the always interesting and challenging opportunities they have given me.

I also want to thank Dr. Michele Giani for the fundamental scientific help and for the stimulating professional chances provided during these years.

Special thanks goes to Nives Ogrinc for the valuable support during experiments and field activities, and for having hosted me in Ljubljana to help me writing the paper. I also want to thank all the students and technicians of the Jožef Stefan Institute for their kind hospitality and for the analysis performed.

I am thankful to Dr. Daniela Berto and Dr. Christian Millo for their availability to review this thesis and for their suggestions that have really helped me in improving the manuscript.

I really want to thank all my past and present colleagues of OGS for their support and encouragement and principally for making the time spent in the institute always pleasant. Thanks in particular to my "chemical brothers" for unloading me from laboratory activities, especially during the last period of thesis writing, even if they always have a lot to do.

I wish to thank "Fondo Trieste" for having financially supported this PhD research project.